2006

Investigation of the performance of articular cartilage and synthetic biomaterials in multi-directional sliding motion as in orthopedic implants

Christian John Schwartz
Iowa State University

Investigation of the performance of articular cartilage and synthetic biomaterials in multi-directional sliding motion as in orthopedic implants

by

Christian John Schwartz

A dissertation submitted to the graduate faculty

in partial fulfillment of the requirements for the degree of

DOCTOR OF PHILOSOPHY

Major: Mechanical Engineering

Program of Study Committee:
Shyam Bahadur, Major Professor
Abhijit Chandra
Surya Mallapragada
Steve Martin
Palaniappa Molian

Iowa State University

Ames, Iowa

2006

Graduate College
Iowa State University

This is to certify that the doctoral dissertation of

Christian John Schwartz

has met the dissertation requirements of Iowa State University

Signature was redacted for privacy.

Major Professor

Signature was redacted for privacy.

For the Major Program

TABLE OF CONTENTS

CHAPTER 1
GENERAL INTRODUCTION

1.1 Introduction

The use of artificial joints is commonplace for the treatment of joint pain and lost functionality due to the loss of articular cartilage from injury or arthritis. These implants completely replace the ailing joints including the hips, knees, shoulder, elbow, and knuckles, with synthetic materials. The most common design of artificial joint consists of a polished metallic surface articulating against a component made from ultra-high molecular weight polyethylene (UHMWPE). This design has been used for several decades because of the extremely low wear rate of UHMWPE and it relative stability *in vivo*. However, the pain-free lifetime of these implanted joints is typically limited to approximately 15 to 20 years in ideal conditions. In reality, many artificial joints must be removed long before this time. The fundamental problem that leads to degradation of comfort and functionality is tissue inflammation and loss of periprosthetic bone resulting from the immune response to UHMWPE wear particulate. This process, known as osteolysis, disrupts the process of bone modeling that occurs continually *in vivo*. The presence of UHMWPE wear particulate suppresses cells that deposit bone (osteoblasts), while not hindering the activity of bone-resorption cells (osteoclasts). This eventually leads to bone loss and slippage at the interface between bone and implant.

The two most direct methods to increase the pain-free lifetime of artificial joints are to reduce the wear of UHMWPE, or to use an alternative material whose wear particulate does not incite as strong of an osteolytic response. This study focused on these two objectives. As a means of studying candidate biomaterials for joint applications, a wear testing machine

was designed and fabricated, thus allowing simple pin geometry samples to be used for wear testing. An investigation was made into the most suitable settings for this device to produce wear amounts and mechanisms similar to what have been found in artificial joints retrieved after *in vivo* use. Compliant polyurethane (PUR) elastomers were studied to determine their wear behavior compared to UHMWPE, as well as the performance of bovine articular cartilage. Filling UHMWPE with Pt-Zr quasicrystals was investigated as a means of reducing the wear of UHMWPE while providing improved mechanical properties. To further investigate wear reduction methods, mild crosslinking of UHMWPE was also studied in terms of its wear resistance, dynamic mechanical properties, and oxidation resistance. Finally, an attempt was made to combine the low wear of UHMWPE with the beneficial compliance of elastomers by investigating blends of UHMWPE and PUR. The results of this work show that there is a great potential both for treatments to UHMWPE to reduce its wear, and for alternative materials that have significantly different mechanical properties than UHMWPE.

1.2 Dissertation Organization

This dissertation is organized in the form of five papers. Each paper includes an abstract, introduction, details of materials and methods, results and discussion, and conclusions, followed by the references, tables and figures. Near the end are complied general conclusions made from the investigations, and acknowledgements. The first part of the work details the design and workings of the Dual-Axis Wear Simulator (DAWS), a wear testing machine designed to expose candidate biomaterials to the environment and wear conditions found in a synovial joint. This device was used to quantify the wear of UHMWPE,

polytetrafluoroethylene (PTFE), polyoxymethylene (POM), and a compliant PUR elastomer. The second part of this dissertation details work on the wear behavior and viscoelastic properties of bovine articular cartilage as a model of how complaint and porous materials perform *in vivo*. The third part focuses on the use of Pt-Zr quasicrystals as separate-phase fillers in UHMWPE and their effect on wear resistance, viscoelastic properties, and impact resistance as compared to the crosslinked polymer. The fourth part details the use of mildly crosslinked UHMWPE without subsequent stabilization. This technique was proposed in order to avoid the large degradation in mechanical properties and oxidation resistance found in highly crosslinked UHMWPE. The fifth part of this dissertation reports the results of using lessons learned in the earlier portions of this work to produce a novel biomaterial with high wear resistance and mechanical properties, namely a blend of PUR and UHMWPE. UHMWPE particles were used as fillers in elastomeric PUR, and these materials were examined for their morphology, viscoelastic properties, and wear behavior.

CHAPTER 2
DEVELOPMENT AND TESTING OF A NOVEL JOINT WEAR SIMULATOR AND INVESTIGATION OF THE VIABILITY OF AN ELASTOMERIC POLYURETHANE FOR TOTAL-JOINT ARTHROPLASTY DEVICES

A paper accepted for publication in *Wear*

Christian J. Schwartz and Shyam Bahadur

2.1 Abstract

The use of artificial joints for the treatment of degenerative diseases of the hip and knee is becoming more widespread as life expectancy increases. Because of the latter, there is also the need for joint replacement components of higher durability than the commonly used artificial joints with ultra-high molecular weight polyethylene (UHMWPE) articulating against a metallic counterface. This requires the use and testing of novel materials. Relatively inexpensive and effective screening devices that would allow investigators to rapidly characterize the wear behavior of such materials are thus needed. This paper reports the design and development of a Dual Axis Wear Simulator (DAWS) to screen materials for wear behavior in a simulated *in vivo* environment. The machine allows for direct control of the applied normal load and the two-dimensional wear path shape of the pin against a cylindrical counterface. With this new machine, the effects of wear path shape and applied load were investigated. A 39 N load coupled with a 6.4-mm square wear path was shown to produce wear amounts comparable to those from other screening devices and also from artificial hips retrieved after *in vivo* use. The results further showed the importance of multidirectional sliding motion and a trend for higher wear rates as the aspect ratio of the wear path was increased. The wear rate of polytetrafluoroethylene was found to be orders of

magnitude higher than that of UHMWPE, while that of polyacetal was somewhat lower. The development and use of compliant materials that simulate the mechanical properties of natural articular cartilage will likely lengthen the pain-free lifetimes of artificial joints. In view of this, the elastomeric polyurethane Pellethane™ 2363-80A, which is currently used in non-orthopedic biomedical applications, was tested for wear and its wear rate was found to be much lower than that of UHMWPE, likely due to its ability to conform to the counterface and thus reduce the contact pressure. This investigation showed the DAWS to be an effective wear simulator for the screening of new biomaterials for use in artificial joints and will be useful in the development of such joints.

2.2 Introduction

With the increase in human life expectancy, the demand for the use of biomedical arthroplasty devices such as hip and knee replacements has increased. 193,000 total-hip replacements and 318,000 total-knee replacements were performed in the United States in 2002 [1]. Although such devices are common, they are not without limitations on their pain-free lifetimes after implantation. In the most common design of artificial hip, the femoral head is a polished metallic alloy that articulates against an ultrahigh molecular weight polyethylene (UHMWPE) acetabular cup. Even though UHMWPE is biocompatible in its bulk form, polymer wear debris has been reported to initiate osteolysis in surrounding tissues [2], leading to implant loosening and eventual revision surgery for replacement of the implant. It has been shown that the wear rate of the UHMWPE acetabular component has a large effect on the initiation of osteolysis and the ultimate lifetime of the implanted device, with osteolysis rarely occurring with a wear rate less than 0.1 mm^3 per year. Based on this

evidence, the two basic approaches to extending the lifetime of such devices are: a) reducing the wear rate of the UHMWPE acetabular component through material or surface treatment, or b) using an alternative material that either has a lower wear rate *in vivo* or produces wear debris that does not induce osteolysis.

UHMWPE as an articulating surface in a joint system has been studied extensively. Researchers have explored various crosslinking methods for UHMWPE [3-5], which have been found to be beneficial in terms of the improved life of the joint. The main limitation of UHMWPE is that it is a fairly rigid material that does not mimic the viscoelastic properties of native articular cartilage found in hip and knee joints. Furthermore, the wear surface of UHMWPE joint does not benefit from synovial fluid lubrication as well as a more compliant material would. Investigators have been forced to begin looking at alternative materials that have mechanical properties similar to articular cartilage.

With the above in mind, analytical and numerical modeling studies of compliant joints have been pursued [6-8], while experimental investigations have examined the use of compliant polyurethanes *in vitro* [9, 10]. Approaches using laminated polyurethane layers to produce a gradient of mechanical properties, similar to cartilage, have shown promise [6]. Based on the mechanical properties, degradation resistance, and fabrication issues of candidate biomaterials, investigators have recommended optimal compliant materials for the acetabular component of a hip joint [11]. One of these materials is the elastomeric polyurethane Pellethane™ 2363-80A. Elastomeric polyurethanes, which have been widely used for biomedical implants such as pacemaker leads and heart valves, are a class of materials that can presumably be made with compliance similar to cartilage. Since no work has been done to validate the performance of Pellethane 2363-80A in a wear environment

similar to *in vivo* conditions, this was undertaken as a part of this work and the results are reported.

The ultimate determination of an implant's performance can be made only by the retrieval of devices from *in vivo* use after revision surgery or death of the recipient. This option is available only for approved devices that use thoroughly investigated materials such as UHMWPE. One step short of *in vivo* implantation is *in vitro* testing of a full-scale implant in a wear simulator that is either custom designed or commercially available and duplicates the motions and loading found in the joint of interest. However, a variety of compliant, porous, and even fluid-bearing materials have been proposed as potential replacements for UHMWPE in artificial joints. These materials present a host of fabrication challenges for producing a full-scale joint component for *in vitro* testing. It would be advantageous for the materials developer to determine their wear behavior before an effort is made to fabricate them into final forms such as acetabular cup liners. Therefore, screening devices are needed that can test easily fabricated samples such as cylindrical wear pins in an environment that simulates *in vivo* wear mechanisms.

The minimum performance requirement for a screening device, as per the ASTM standard *F 732-00* [12], is that it must produce wear amounts for standard materials UHMWPE, polytetrafluoroethylene (PTFE), and polyacetal (same as polyoxymethylene, POM, but referred to as PA in the ASTM standard) that rank appropriately with respect to each other (PTFE > PA $\geq$ UHMWPE). In addition, the wear rates should be comparable to the rates observed in retrieved implants from *in vivo* application. Furthermore, wear mechanisms must bear resemblance to the mechanisms observed in harvested implants from *in vivo* use. Finally, any new screening device should produce wear results that agree with

those for UHMWPE from previous work. A testing device that is able to fulfill all of the preceding requirements should have the potential to serve as a reliable screening tool once the testing parameters of the device are established. Testing devices based on simpler motions than those found in full-scale simulators have been developed in the past. Such approaches have included pin-on-disk designs (with translation of the pin in addition to disk rotation) for use in hip simulation [13]. The fundamental requirement for a viable testing device is that it incorporates multidirectional motions [14-16]. However one drawback to pin-on-disk devices, such as the OrthoPOD™ (Advanced Medical Technology, Inc.), is that the counterface is planar while artificial hip and knee devices use a convex metallic counterface which articulates against the UHMWPE component. In light of issues such as the lubrication condition at the wear interface, a cylindrical counterface has the potential to produce a more realistic wear environment.

In view of the above requirements, the authors developed a novel wear testing device with the capability to screen materials by subjecting them to a wear environment that is directly controllable and can simulate an *in vivo* joint. The design of the device, called the Dual Axis Wear Simulator (DAWS), is presented in this paper. In addition, the experimental results are reported on the effects of wear path shape and applied normal load on wear. These are needed to identify the optimal settings that would produce wear somewhat representative of *in vivo* conditions. Using the newly developed wear testing device and the established conditions of wear path shape and normal load, wear investigation of the elastomeric Pellethane 2363-80A was carried out and the results are reported in this paper.

2.3 Materials and Methods

2.3.1 Design of the joint wear simulator

The DAWS device was designed and constructed to allow the user direct control of the wear parameters. A schematic of one of the test stations of the device is shown in Figure 2.1a, while a photograph of three test stations is shown in Figure 2.1b. There are six such stations for wear testing and two soak-control stations. Each test station consists of a pressure-regulated pneumatic cylinder and a sample holder for holding a planar-faced pin of the material of interest and generating a normal load between the pin and the counterface. The counterface is a 12.7 mm diameter shaft of 316LS surgical stainless steel (BioDur® 316LS, Carpenter Technology Corporation). This arrangement provides a flat-on-cylinder wear interface configuration. The six sample holders are integrated into a carriage that moves laterally on linear bearings in a direction parallel to the axis of the counterface shaft. The soak-control sample holders are stationary. The samples and counterface are immersed in liquid in the respective immersion chambers and the liquid temperature is regulated by a heater. The lateral movement of the sample holders is accomplished through the use of a computer-controlled servomotor connected to the carriage through a rack-and-pinion connection. The motion of the counterface shaft is provided by a direct connection with another computer-controlled servomotor. In this way, the lateral movement of the sample holder carriage can be directly coordinated with the rotation of the counterface shaft to accomplish various wear path geometries. The device provides the capability to test experimental materials against a round counterface with wear paths of any two-dimensional geometry such as rectangles of varying aspect ratio, circles, or ellipses. In addition to wear

path, the loads and sliding speeds can also be varied based on the intended wear environment.

2.3.2 Materials

The materials tested for wear in this study were UHMWPE, POM, PTFE, and elastomeric polyurethane (PUR). UHMWPE was implant grade GUR 1050 supplied by Perplas Medical. PTFE and POM were Teflon® and Delrin®, respectively, from Dupont. These three materials were in the form of extruded rods and were tested for wear to determine the validity of the newly designed joint wear simulator in terms of the ASTM Standard F 732-00, and the wear mechanisms as compared to results reported for the OrthoPOD™ [16] multidirectional wear tester and retrieved Charnley implants [17].

The fourth material was Pellethane 2363-80A from Dow Chemical, an elastomeric polyurethane. In was in the form of resin and so was molded to produce specimens. This material has been recommended for the acetabular component of a hip joint [11] based on its mechanical properties and biocompatibility in light of *in vivo* conditions within the hip. Table 2.1 lists the mechanical properties of the materials tested as reported by suppliers. While there may be some small variance in these values due to material processing history, their relative magnitudes are useful for comparison to each other.

2.3.3 Investigation of loading and wear path geometry

To determine the test parameters that would produce representative wear rates and failure modes with respect to *in vitro* and retrieved *in vivo* joint implants, a two-factor screening study was performed involving the applied static load on the pins and the geometry of the wear path on the counterface. UHMWPE pins were machined from an extruded rod and immediately stored in a desiccator. The pins were 6.4 mm in diameter, 9.5 mm in length, and

had a planar wear surface that was finished in flowing water to a surface roughness of 0.15 μm Ra using abrasive disks on an automated polishing station. The stainless steel counterface was finished with abrasive paper and diamond paste to a surface roughness of 0.10 μm Ra on an engine lathe prior to assembly of the DAWS.

Two levels of applied static load were chosen for the experiment: a) 39 N and b) 78 N. The load was applied by setting the pressure regulator that controlled the pneumatic cylinders. Because of the flat-on-cylinder configuration the interface pressure varied during initial part of the test but soon reached a fairly constant value. The worn area on the pins was measured at the end of the test to determine the average normal pressure. The calculated average pressures were 3.1 MPa and 6.2 MPa for the low and high load settings, respectively. They are comparable to the average pressures found in the hip joint and also those used by ASTM [12] and other investigators [5]. Three wear path geometries were chosen for the study: a) a square with dimensions of 6.4 mm parallel to the counterface shaft axis (referred to as the lateral direction) and 6.4 mm perpendicular to the axis (referred to as the circumferential direction), b) a rectangle with dimensions of 9.5 mm lateral and 3.2 mm circumferential, and c) a linear reciprocating path of 12.7 mm lateral only. Each path traversed a total distance of 25.4 mm per cycle. The wear cycles were traversed at approximately 0.82 Hz, producing a sliding velocity of 21 mm/s. The initial test was performed for a total of 500,000 wear cycles, with one interruption for wear measurement at 250,000 cycles. Subsequent tests were done for 250,000 cycles because it was found that the wear volume for a quarter-million cycles was of sufficient magnitude to be accurately measured, and wear was exactly half of that for a half-million cycles.

The lubricant used was a 25% solution of bovine calf serum (HyClone) diluted with purified, de-ionized water (18 MΩ resistance), with the addition of 20 mM EDTA, and 2% penicillin-streptomycin-neomycin solution (Sigma-Aldrich Cat. No. P3664) to inhibit microbial degradation. The lubricant solution had a protein concentration of approximately 18 mg/mL as calculated from the serum specifications and dilution factor. During presoaking and wear testing, the temperature of the lubricant was maintained at 37 ± 3°C. Prior to each wear test, eight pins (six for wear plus two for soak control) were soaked for 24 hours in the lubricant solution maintained at 37°C. The mass of the pins was measured prior to the soak, after the soak, and after the completion of 250,000 cycles in the wear test. The microbalance used had a readout resolution of 10^{-5} g and measurement precision with a standard deviation of 1.02×10^{-5} g. The mass loss due to wear was corrected for fluid absorption by accounting for the change in mass of the soak specimens. Using the measured density of UHMWPE, the mass loss was converted to volumetric wear loss. Analysis of variance (ANOVA) was performed to identify whether any test parameter, such as load, wear path geometry, or the interaction between these two had a statistically significant effect on wear.

In order to determine which load and wear path geometry combination contributed to wear mechanisms that resembled those reported in the literature for UHMWPE, the worn tips were examined by scanning electron microscopy (SEM). For this purpose, the worn tip was sliced to produce a disk approximately 3 mm thick. The disk was bonded to a sample mount and sputter coated with gold. SEM images were taken and compared to the images and descriptions reported in the literature for *in vitro* and *in vivo* wear. To provide further evidence of the wear mechanism, the wear debris from each test lubricant was retrieved using

the digestion and separation method described by Biggs *et al.* [18] for UHMWPE. Following the Biggs method, sodium hydroxide was added to the used lubricant to eliminate any protein solids in the fluid. UHMWPE wear particles were then suspended at the interface between hexane and a water-ethyl alcohol mixture in a separatory funnel. A pipette was used to extract the particles from the interface, the particles were washed and placed in hexane, and an aliquot of the particles was placed on a membrane filter to hold the particles while the hexane evaporated. 0.1 μm pore size membrane filters (Isopore™, Millipore Corporation) covered with retrieved wear debris were vacuum desiccated, gold sputter coated, and imaged by SEM.

Once the load and wear path geometry had been selected for the DAWS based on the above work, the wear behavior of PTFE and POM were investigated. PTFE and POM pins were prepared, tested, and analyzed as described above. Papain digestion was used to collect wear particles, because the densities of the debris were inappropriate for funnel separation. Papain was added to the used lubricant and heated to 37°C for 5 hours. An aliquot of the fluid was then placed on a membrane filter for drying. The filters were subsequently sputter coated and imaged by SEM. Student-t tests were performed to compare the wear rates of UHMWPE, PTFE, and POM in order to determine if their wear rates fell in the order reported in the literature [15, 19].

2.3.4 Investigation of Pellethane 2363-80A

Pellethane resin was dried in an oven at 93°C for six hours to remove absorbed moisture, due to its hygroscopic nature. The dried resin was placed in a mold under approximately 138 MPa of pressure in a heated press. The mold was heated to 215 °C and held at that temperature for ten minutes. The heat was then lowered and pressure was maintained on the

resin until the mold cooled to room temperature. This produced 6.4 mm diameter rods with a length of approximately 38 mm. These polyurethane rods were cut to 9.5 mm long pins and the planar faces were finished on an automated polishing station to a surface roughness of 0.15 μm Ra. It is widely believed that the compliance of elastomeric polyurethanes is advantageous in artificial hips because it supports the development of hydrostatic and hydrodynamic lubrication conditions unlike rigid UHMWPE. This lubrication effect is enhanced by using a wear interface where the pin surface is made with a curvature that conforms to the counterface curvature, as in the hip joint. In order to make a very conservative observation of the potential benefits of using compliant polyurethanes, the pins were produced with planar wear surfaces and tested in the same manner as UHMWPE.

The finished pins were placed in a 93°C oven for 72 hours to completely remove moisture. The pins were placed in the lubricant solution for 24 hours at 37°C prior to testing. The pins were tested under 39 N loading with a square wear path for 250,000 cycles. Following testing, the pins were again dried in the 93°C oven for 72 hours to eliminate any absorbed fluid. Pins were then weighed and wear was calculated.

To retrieve the debris from the Pellethane wear testing, the used lubricant fluid was collected and digested with sodium hydroxide for 72 hours. The digested fluid was agitated in a vortex mixer and a 5-mL aliquot was removed with a pipette and placed in a 15-mL centrifuge tube. 5 mL of ethanol was added and the tube was again placed in the vortex mixer. The tube was centrifuged and then most of the liquid phase was removed. This was followed by the addition of 5 mL hexanes, mixing, and centrifugation. A small Pasteur pipette was then used to extract some of the particle-rich fluid from the bottom of the tube.

The debris was then placed on a membrane filter, desiccated, and gold coated for SEM examination.

2.4 Results and Discussion

2.4.1 Loading and wear path effects

The mean and standard deviation of volumetric wear for different combinations of load and wear path geometry are presented in Table 2.2. The mean wear values reported were calculated from the wear of six pins for 250,000 cycles. Because of the level of measurement error of the microbalance, wear amounts less than approximately 0.029 mm^3 (for UHMWPE) are not statistically different from zero wear at 95% confidence. The linear paths had wear amounts so small as to fall below the minimum detection threshold of the gravimetric wear measurement procedure.

Analysis of variance revealed that both load ($p=0.0034$) and path ($p<0.0001$) had a significant statistical effect on the wear amounts. Wear path appeared to have the greatest effect. There was an indication of some interaction between load and path ($p=0.0467$) but this accounted for very little of the variation in the wear data. Student-t testing showed that wear with 78 N was greater than with 39 N at a 95% confidence level. Furthermore, square and rectangular wear paths produced significantly greater amounts of wear than the linear paths. Based on the above wear data, it was concluded that the wear amounts for UHMWPE on square and rectangular wear paths were very much in line with what has been reported for other screening devices. If the results are extrapolated to one million cycles by multiplying by a factor of four, the data agree exceptionally well with that reported by Wang *et al.* [20] for UHMWPE in a ring-on-flat device. The wear rates reported by these workers were from

0.225 to 0.652 mm^3 per million cycles for samples that were shown to have ductility, while wear rates were an order of magnitude higher for samples that did not exhibit ductility during tensile testing. They reported a maximum Hertzian contact pressure of approximately 20 MPa. This closely matches the initial Hertzian pressure of 19.6 MPa attained when a 39 N load was used in our work. The calculated wear coefficient for the 39 N, square path test in our work is 1.64×10^{-6} mm^3/Nm, This is very close to the value of approximately 2.2×10^{-6} mm^3/Nm reported for a 5 mm x 5 mm square-path test performed on an OrthoPOD™ multidirectional wear tester [16]. Furthermore, the wear coefficient of 1.64×10^{-6} mm^3/Nm from our tests is close to the reported wear coefficient of 1.86×10^{-6} mm^3/Nm for a 31.4 mm circular path on another multidirectional wear machine [21]. Perhaps most importantly, our wear coefficient agrees well with the reported mean wear coefficient of 2.1×10^{-6} mm^3/Nm, obtained from the measurement of wear on 129 retrieved acetabular cups from Charnley hip implants [17].

Figures 2.2a through 2.2d show SEM images of the worn surfaces and debris of selected UHMWPE pins. The linear path (Fig. 2.2a) clearly shows material displacement from surface deformation in the sliding direction but there is no indication of wear. Contrast this with the surface resulting from a square wear path (Fig. 2.2b). The square path shows surface scales with a periodic spacing of 4 to 5 μm. This suggests a wear mechanism involving the deformation of asperities on the UHMWPE surface undergoing successive cyclic strain until failure. It may be that the asperities are extruded under initial loading and stretched in the direction of motion until a limit of extension is reached. Upon motion reversal, the extruded asperities are stretched in the opposite direction until a limiting strain is reached. Each motion cycle imparts a strain history that on successive loading cycles will

lead to the eventual fatigue failure of asperities in the form of extruded sheets. The linear path wear surface shows no such features as observed for multidirectional motion. With reciprocating linear motion, the polymer chains are oriented in the direction of sliding and are able to deform to a great extent without failure, thus leading to an extremely low wear rate. However, the changing wear direction of the square path does not allow such long-range chain orientation and thus material fails after a relatively small amount of extension. The idea that UHMWPE material is removed in sheets under multidirectional motion is supported by Figures 2.2c and d, showing the wear debris collected from the used serum solution from square path testing. The figure shows that most particles were in the size range of 1 to 2 μm and possessed a jagged, crumpled appearance as if they are formed from a thin sheet. The crumpling of the particles presumably results after separation from the pin due to a high level of residual stresses imparted in the sheet particulate during back and forth stretching. In summary, the 39 N, square path produces a wear surface that resembles those found in UHMWPE tested in other screening devices [20]. Other investigators [22] have examined the wear mechanisms of UHMWPE under multidirectional motion and have proposed wear mechanisms similar to that described here.

The testing done with square or rectangular paths produced varying amounts of surface protuberances in addition to the scaling features described above. The protuberances have a markedly different texture than the scaled portions, and have been observed by other investigators [23, 24]. With the higher load of 78 N, the protuberances produced were more extensive. Figure 2.3 shows the scaling mechanism overlapped by a protuberance of much smoother texture. The protuberance appears to rise above the plane of the scaling wear, and has a smooth rippled appearance. This suggests that the protuberance does not undergo

material removal due to fatigue as does the rest of the wear surface. Rather, the ripples appear to be due to plastic deformation. Other investigators have suggested that protuberances are caused by insufficient protein concentration in the lubricant solution [24], and have attributed them to slower-wearing regions of the wear surface that exhibit recovery once the loading is removed [23]. It may be that the protuberances are nucleated on the pin surface when loading pressures are severe, but no clear mechanism for their formation has been investigated.

Although the wear amounts from square and rectangular paths were not different statistically in this investigation, observation of the data suggests that the rectangular path does produce slightly less wear. This suggests a trend, as other investigators have reported, that wear decreases as the aspect ratio of the wear path is increased from one (square or circular motion) to infinity (linear reciprocating motion). The trend observed here, drastic wear reduction with increased aspect ratio, is further evidence that the DAWS subjects the specimens to a wear environment that is very similar to more complex and costly screening devices, and is suggestive of the conditions found *in vivo*.

2.4.2 Comparison of UHMWPE, POM, and PTFE wear

Wear data for polytetrafluoroethylene (PTFE) and polyacetal (POM) along with UHMWPE for 39 N loading and the square wear path (6.4 mm x 6.4 mm) are presented in Table 2.3 for the sake of comparison. Using Student-t tests, the wear of PTFE was found to be significantly greater than that of UHMWPE or POM with 95% confidence. This is also obvious from direct observation of the data. PTFE wear was so excessive that the fluid in the immersion chambers was clouded because of the suspension of wear particles, and debris

was piled visibly on the chamber bottoms. This was not witnessed with the other materials. It was further determined that the wear of POM was statistically less than that of UHMWPE.

Figure 2.4a shows the PTFE wear surface. Deformation zones were observed here similar to that found in UHMWPE, but of much larger size. This would be expected because of the much lower shear strength of PTFE than that of UHMWPE (see Table 2.1). Figure 2.4b shows PTFE wear debris collected from the used serum solution. The shape of the debris is similar to that of UHMWPE (Figure 2.2d) but the debris size is more than two orders of magnitude higher than that of UHMWPE, which would account for its much higher wear. Although PTFE was investigated by Charnley as the original material for acetabular cups [25], it was quickly realized that wear rates were too high and tissue reaction too severe for the material to be of practical use. Thus, one method of investigating the performance of a screening device is to measure the wear of PTFE. The extremely large amount of PTFE wear agrees well with previous investigations.

The wear surface of POM was smooth and featureless and so is not being presented here. The smooth surface is indicative of the removal of fairly small wear debris as shown in Figure 2.5. The debris size was similar to that of UHMWPE, and they share a similar crumpled sheet appearance. There is more lubricant residue present in the POM micrograph due to the papain digestion, which did not allow for as thorough of a cleaning of wear particles as in UHMWPE. The history of POM wear testing has shown mixed results based on the particular polymer type being used. Delrin®, as used in this study, has shown promising results for hip implants with tissue effects similar to that of UHMWPE. But to complicate matters, a different formulation of POM (Ertacetal®) has been shown to have wear rates much greater than UHMWPE based on *in vivo* results [19]. The vast differences

in wear behavior between POM formulations may have played a role in the limited study of this class of materials for articulating joints. Furthermore, these differences in performance suggest that testing standards, such as the ASTM standard mentioned above, should reference a particular grade of POM to be used in validation of screening devices.

2.4.3 Wear Studies on Pellethane 2363-80A

Quigley *et al.* [11] ranked selected compliant materials as an alternative to UHMWPE in view of the mechanical properties and the loading and environmental requirements at the articulating surface of an artificial hip. Of these, the elastomeric polyurethane Pellethane 2363-80A was among the three highest ranking materials. Pellethane has tensile strength comparable to that of UHMWPE (Table 2.1) and good biocompatibility, as evidenced by its use in artificial heart valves. Being an elastomer, it resists shear failure which is involved in wear failure. It was decided to test this material for wear in order to determine the potential for using Pellethane 2363-80A in future joint implants.

Table 2.4 shows that the mean wear of Pellethane pins under 39 N load and square wear path was less than that of UHMWPE pins tested under the same conditions. A Student-t test showed that the statistical likelihood that Pellethane wear is less than UHMWPE wear is quite likely ($p=0.0617$). Due to the surface irregularities observed on worn surfaces, four Pellethane pins were used to calculate the mean, rather than six. The large standard deviation in the wear data for Pellethane may be indicative of the uncertainty introduced by the drying method of the pins before and after testing. Elastomeric polyurethanes tend to be more absorbent than the rigid polymers, so the cleaning and drying procedure used with the other materials was not practical with Pellethane. It must be noted that the use of compliant polyurethanes such as Pellethane in an artificial hip would involve two articulating surfaces

with conformal curvature, as opposed to the plane-on-cylinder configuration tested here. However, conformal curvature would enhance the possibility of better interfacial lubrication and thus it is likely that greater reductions in wear versus UHMWPE would be found in such a configuration.

The surface of the Pellethane pins showed that a greater surface area was exposed to wear due to the compliant nature of the elastomer. This, in turn, led to reduced contact pressures and a less severe wear environment than what would have been experienced by the rigid polymers tested previously. To the naked eye, the worn surface of the Pellethane pins had a highly reflective, burnished appearance as did the worn surfaces of UHMWPE and POM. Figure 6 shows the Pellethane wear surface at high magnification. Although it does not have the systematic deformation patterns as was observed on the worn UHMWPE surfaces, the Pellethane surface does show parallel tears with a characteristic spacing of 2 to 3 microns. Judging by the characteristics of the wear debris, shown in Figure 2.7, it appears that material was removed due to the growth of accumulated fatigue cracks developed in response to the cyclic shear stresses during wear. The wear particles appeared to be gouged from the surface, and their characteristics suggest that while the polymer was able to be elastically stretched during the wear process, it was not able to undergo significant plastic deformation before fracture. This is likely due to the fact that elastomeric polyurethanes have an inherent degree of crosslinking not found in the UHMWPE tested.

The experimental wear results reported above show that the DAWS is an effective screening device. It provides results consistent with other screening devices and similar to those from harvested *in vivo* implants. With the ability to control the loading, wear path geometry, and specimen surface configuration (i.e. planar or curved), the parameters of

particular anatomical joints can be simulated in the machine based on the implant type. Thus, it may be discovered that certain settings of the DAWS work better for the screening of hip joint materials versus knee or knuckle materials. The machine also has the potential for screening more delicate materials such as harvested articular cartilage and tissue engineered cartilage. It is likely that, in the future, artificial joints will incorporate more exotic materials than UHMWPE to increase both the comfort and pain-free lifetime of the implants, and the use of a testing machine such as the DAWS will be advantageous.

The wear results of Pellethane 2363-80A indicated that this material is more wear resistant than UHMWPE. The material is biocompatible and has good resilience similar to that of cartilage in a natural joint. These attributes warrant further evaluation of this material in a full-scale wear simulator for potential use in artificial joints.

2.5 Conclusions

1. The DAWS device showed credible results in the investigation of potential biomedical wear materials. It thus serves as a useful screening device for initial testing of candidate materials before the investment of time and resources is devoted to developing such materials into full-scale implant components for further testing.
2. The aspect ratio of the wear path geometry was extremely important in the amount of wear produced using the DAWS device, with a square path (aspect ratio = 1) producing wear amounts representative of *in vitro* and *in vivo* results. Reciprocating linear motion (aspect ratio = ∞) produced wear of such low magnitude as to not be a reliable simulation of anatomical joint conditions.

3. Load applied to the specimens during the test also had an effect on the amount of wear produced by UHMWPE during testing. 39 N loading produced a wear surface similar to that produced in other screening devices, however 78 N loading produced an extensive amount of surface protuberances. It was determined that 39 N loading coupled with the square wear path produced a reasonable simulation of *in vivo* hip or knee wear conditions based on comparison with results from other testing devices and from retrieved acetabular cups.
4. PTFE wear was orders of magnitude higher than that of UHMWPE or POM and thus is not a suitable material for orthopedic joint implants.
5. POM showed lower wear than UHMWPE and so it may be reasonable to examine this material further as a candidate material for biomedical wear situations.
6. Pellethane 2363-80A had a smaller amount of wear than UHMWPE. This was concluded to be due to its ability to conform to the counterface curvature, which resulted in reduced contact pressure.

2.6 References

1. C.J. DeFrances, M.J. Hall, 2002 National Hospital Discharge Survey. Adv Data, 2004(342): p. 1-29.
2. J.H. Dumbleton, M.T. Manley, A.A. Edidin, A literature review of the association between wear rate and osteolysis in total hip arthroplasty. J Arthroplasty, 2002. 17(5): p. 649-661.

3. H. Oonishi, Y. Kadoya, S. Masuda, Gamma-irradiated cross-linked polyethylene in total hip replacements--analysis of retrieved sockets after long-term implantation. J Biomed Mater Res, 2001. 58(2): p. 167-171.

4. O.K. Muratoglu, D.O. O'Connor, C.R. Bragdon, J. Delaney, M. Jasty, W.H. Harris, E. Merrill, P. Venugopalan, Gradient crosslinking of UHMWPE using irradiation in molten state for total joint arthroplasty. Biomaterials, 2002. 23(3): p. 717-724.

5. O.K. Muratoglu, C.R. Bragdon, D.O. O'Connor, M. Jasty, W.H. Harris, R. Gul, F. McGarry, Unified wear model for highly crosslinked ultra-high molecular weight polyethylenes (UHMWPE). Biomaterials, 1999. 20(16): p. 1463-1470.

6. T. Stewart, Z.M. Jin, J. Fisher, Analysis of contact mechanics for composite cushion knee joint replacements. Proc Inst Mech Eng [H], 1998. 212(1): p. 1-10.

7. A.N. Suciu, T. Iwatsubo, M. Matsuda, Theoretical investigation of an artificial joint with micro-pocket-covered component and biphasic cartilage on the opposite articulating surface. J Biomech Eng, 2003. 125(4): p. 425-433.

8. M.T. Raimondi, C. Santambrogio, R. Pietrabissa, F. Raffelini, L. Molfetta, Improved mathematical model of the wear of the cup articular surface in hip joint prostheses and comparison with retrieved components. Proc Inst Mech Eng [H], 2001. 215(4): p. 377-391.

9. S.L. Smith, H.E. Ash, A. Unsworth, A tribological study of UHMWPE acetabular cups and polyurethane compliant layer acetabular cups. J Biomed Mater Res, 2000. 53(6): p. 710-716.

10. T. Stewart, Z.M. Jin, J. Fisher, Friction of composite cushion bearings for total knee joint replacements under adverse lubrication conditions. Proc Inst Mech Eng [H], 1997. 211(6): p. 451-465.

11. F.P. Quigley, M. Buggy, C. Birkinshaw, Selection of elastomeric materials for compliant-layered total hip arthroplasty. Proc Inst Mech Eng [H], 2002. 216(1): p. 77-83.

12. ASTM F 732-00, Wear test method for wear testing of polymeric materials used in total joint prostheses. Annual Book of ASTM Standards. 2000: ASTM International.

13. V. Saikko, A multidirectional motion pin-on-disk wear test method for prosthetic joint materials. J Biomed Mater Res, 1998. 41(1): p. 58-64.

14. C.R. Bragdon, D.O. O'Connor, J.D. Lowenstein, M. Jasty, W.D. Syniuta, The importance of multidirectional motion on the wear of polyethylene. Proc Inst Mech Eng [H], 1996. 210(3): p. 157-165.

15. ASTM F 732-00, Wear test method for wear testing of polymeric materials used in total joint prostheses. Annual Book of ASTM Standards: ASTM International.

16. M. Turell, A. Wang, A. Bellare, Quantification of the effect of cross-path motion on the wear rate of ultra-high molecular weight polyethylene. Wear, 2003. 255(2): p. 1034-1039.

17. R.M. Hall, A. Unsworth, P. Siney, B.M. Wroblewski, Wear in retrieved Charnley acetabular sockets. Proc Inst Mech Eng [H], 1996. 210(3): p. 197-207.

18. S.A. Biggs, C.R. Bragdon, K. Garas, O.K. Muratoglu, P.J. Caruso, W.H. Harris. Qualitative analysis of polyethylene particles extracted from bovine serum used in a

hip simulator. in 11th Conference of the European Society of Biomechanics. 1998. Toulouse, France.

19. H.A. McKellop, I.C. Clarke, Evolution and evaluation of materials-screening machines and joint simulators in predicting in vivo wear phenomena, in Functional Behavior of Orthopedic Biomaterials, P. Ducheyne, G.W. Hastings, Editors. 1984, CRC Press, Inc.: Boca Raton, FL. p. 51-85.
20. A. Wang, Sun D.C., Stark, C., Dumbleton, J.H., Wear mechanisms of UHMWPE in total joint replacements. Wear, 1995. 181(1): p. 241-249.
21. V. Saikko, O. Calonius, J. Keranen, Effect of slide track shape on the wear of ultra-high molecular weight polyethylene in a pin-on-disk wear simulation of total hip prosthesis. J Biomed Mater Res B Appl Biomater, 2004. 69(2): p. 141-148.
22. S. Sambasivan, D.A. Fischer, M.C. Shen, S.M. Hsu, Molecular orientation of ultrahigh molecular weight polyethylene induced by various sliding motions. J Biomed Mater Res, 2004. 70B(2): p. 278-285.
23. V. Saikko, T. Ahlroos, Type of motion and lubricant in wear simulation of polyethylene acetabular cup. Proc Inst Mech Eng [H], 1999. 213(4): p. 301-310.
24. V. Saikko, Effect of Lubricant Protein Concentration on the Wear of Ultra-High Molecular Weight Polyethylene Sliding Against a CoCr Counterface. 2003.
25. J. Charnley, Factors in the design of an artificial hip joint. Proc Inst Mech Eng, 1966. 181(3J): p. 104.

Table 2.1 Mechanical properties of the materials tested for wear as reported by suppliers. The average normal pressures encountered during wear testing were 3.1 and 6.2 MPa for the low and high load settings, respectively.

Material	Tensile Strength (MPa)	Tensile Modulus (MPa)	Shear Strength (MPa)	Elongation (%)
UHMWPE	52	620	24	325
PTFE (Teflon)	23	480	5	210
POM (Delrin)	69	3100	66	60
Pellethane 2363-80A	36	4 to 12	not reported	550

Table 2.2 Wear amounts for UHMWPE tested for 250,000 cycles under various loading and path aspect ratios.

Load	Wear Path	Mean wear (mm^3)	Standard deviation (mm^3)
39 N	square	0.408	0.070
	rectangular	0.354	0.070
	linear	Below Detection	-
78 N	square	0.642	0.233
	rectangular	0.485	0.052
	linear	Below Detection	-

Table 2.3 Wear comparison among materials with 39 N loading and square wear path.

Material	Mean wear (mm^3)	Standard deviation (mm^3)
UHMWPE	0.408 (6 pins)	0.070
PTFE	14.7 (6 pins)	2.38
POM	0.062 (4 pins)	0.062

Table 2.4 Wear comparison between UHMWPE and Pellethane (39 N load, square wear path).

Material	Mean wear (mm^3)	Standard deviation (mm^3)
UHMWPE	0.408 (6 pins)	0.070
Pellethane	0.200 (4 pins)	0.197

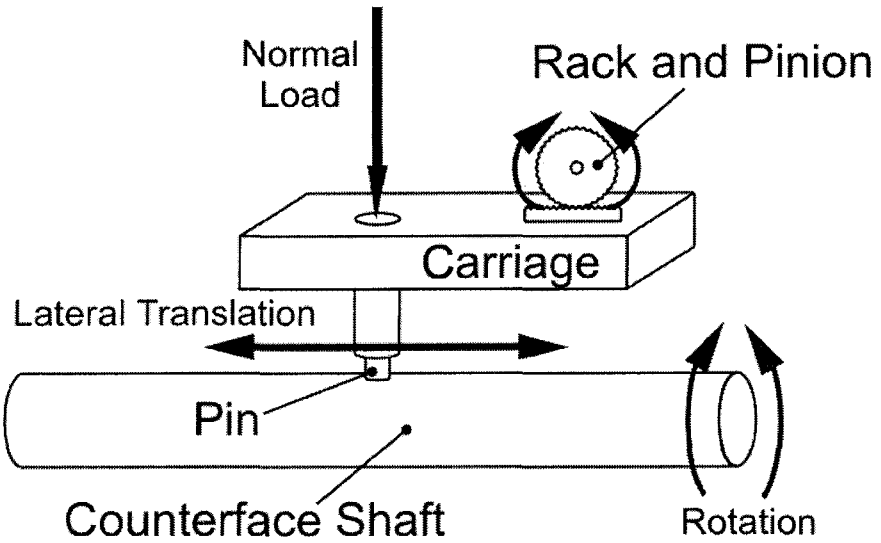

Figure 2.1 a) Details of a test station of the DAWS. The carriage is driven to produce lateral motion, while the counterface shaft produces rotation. The shaft and pin are immersed in bovine serum solution.

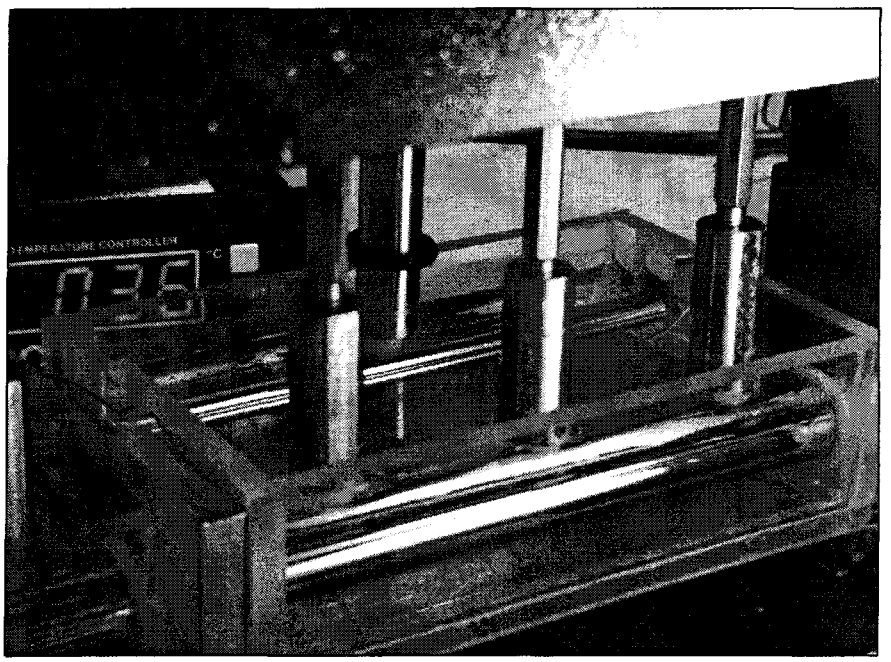

Figure 2.1 b) Photograph of three test stations and a soak station in the DAWS. The chamber cover has been removed.

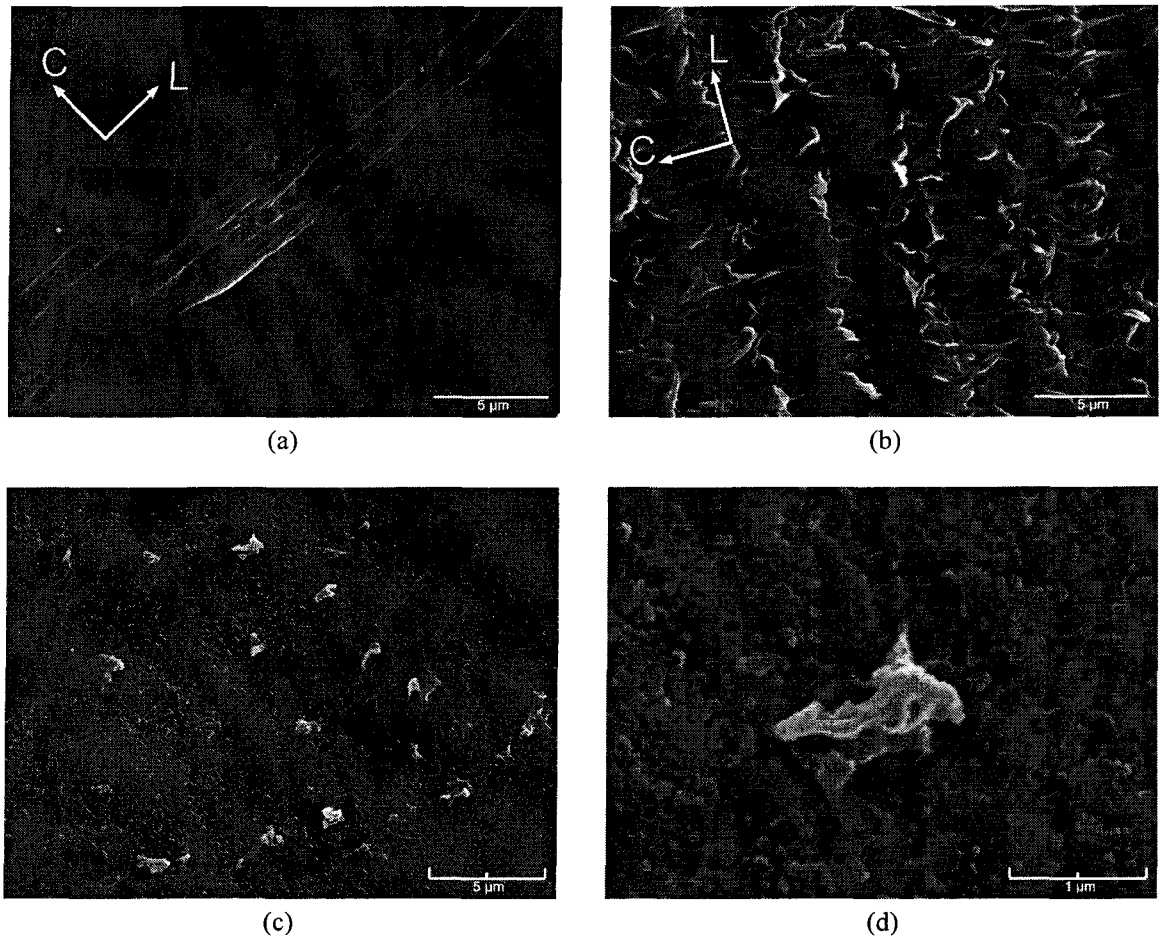

Figure 2.2 SEM micrographs of wear surfaces for sliding conditions: (a) 39 N, linear path; (b) 39 N, square path; and wear debris for sliding conditions of 39 N, square path: (c) at low magnification; and (d) at higher magnification.

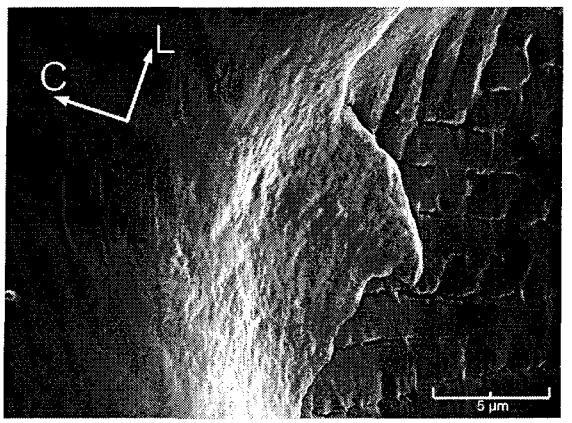

Figure 2.3 SEM micrograph of UHMWPE wear surface for 78 N, rectangular path test. The smooth textured area on the left is the edge of a protuberance on the surface adjoining the scaled region on the right.

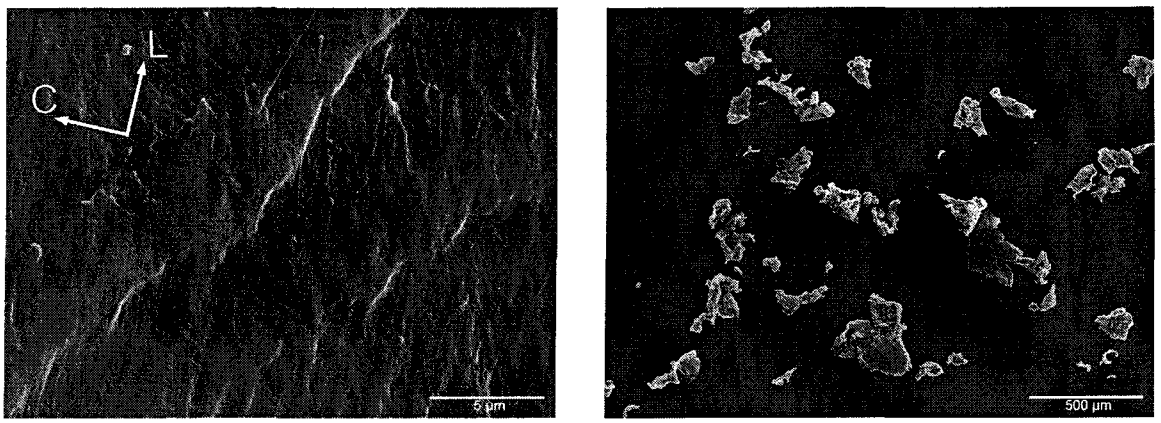

(a) (b)

Figure 2.4 SEM micrographs of (a) PTFE wear surface showing very rough topography, and (b) PTFE wear debris size distribution. 39N load, square path.

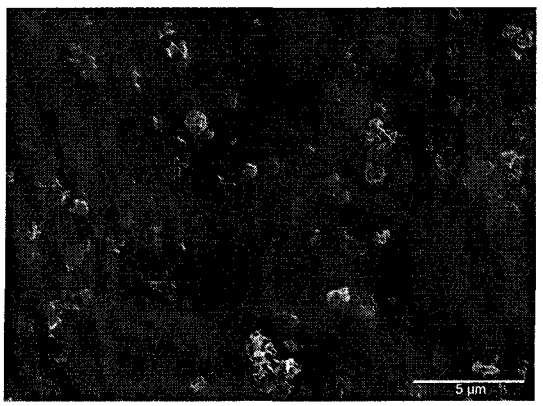

Figure 2.5 SEM micrograph of POM wear debris.

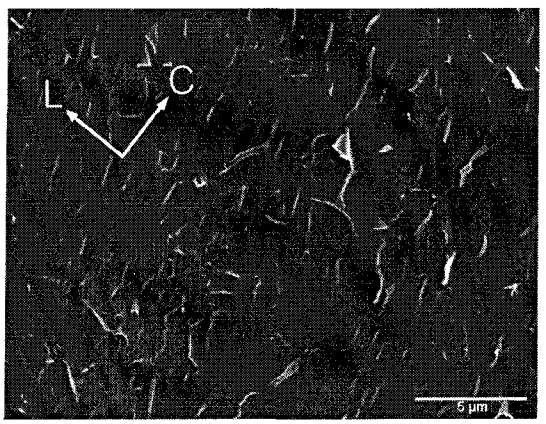

Figure 2.6 SEM micrograph of worn Pellethane surface.

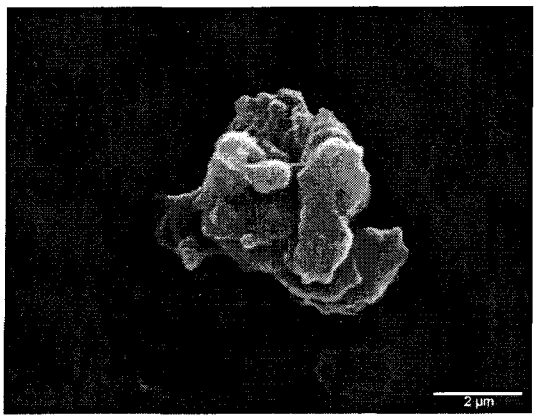

Figure 2.7 SEM micrograph of Pellethane wear particle.

CHAPTER 3
INVESTIGATION OF ARTICULAR CARTILAGE FAILURE IN MULTI-DIRECTIONAL SLIDING AS IN ORTHOPEDIC IMPLANTS

A paper submitted to *Wear*

Christian J. Schwartz and Shyam Bahadur

3.1 Abstract

As the use of total-joint replacement devices has become widespread, debris-induced osteolysis from ultra-high molecular weight polyethylene (UHMWPE) is still the primary challenge to lengthening the pain-free lifetime of these implants. Investigators have long suspected that the natural cartilage-on-cartilage interface found in synovial joints is an optimal system, but technology has not advanced to the point of producing such an implant for use in total-joint replacement. The authors have investigated the performance of such a joint by developing an *in vitro* model of a cartilage-on-cartilage system. Bovine articular cartilage was fabricated into pins and subjected to multi-directional sliding in the Dual Axis Wear Simulator (DAWS), a machine developed by the authors to simulate conditions in an *in vivo* joint. The pins were worn against a rigid stainless steel counterface, similar to that found in conventional total-joint implants, and these results were compared to wear against a compliant polymeric counterface. The rigid counterface produced cartilage wear amounts with a mean of 25.65 mg after 100,000 cycles of 39 N loading and a 6.4-mm square wear path. However, use of the compliant counterface yielded a mean wear value of 9.97 mg for the same testing conditions. It is likely that the mechanism responsible for this wear involves the generation and subsequent depletion of a fluid layer at the interface between the cartilage

pin and the counterface such that the majority of material removal occurred during the fluid deficient portions of the wear cycle. This difference in wear amounts was attributed to the substantial difference in contact pressures between the rigid and compliant counterfaces. To estimate the contact pressures in each case, the storage and loss moduli were measured for cartilage samples through dynamic mechanical analysis (DMA). It was found that over a frequency range from 0.1 to 10 Hz, the storage modulus ranged from 470 to 1010 kPa, while the loss modulus increased more modestly, from 176 to 249 kPa. The results of wear testing and the measurement of the viscoelastic properties of articular cartilage suggest the possibility of successful cartilage-on-metal implant systems where the contact pressures are kept low through joint geometry or the use of a biocompatible compliant surface on the metallic component.

3.2 Introduction

The need for total-joint replacement surgery has steadily grown as life expectancy has increased. The most widely used artificial hip, with a rigid metallic femoral head articulating against a rigid acetabular cup of crosslinked ultra-high molecular weight polyethylene (UHMWPE), produces extremely low wear of the polymer and a low friction coefficient. However, the lifetime of the implanted hip is limited by the osteolytic effect of submicron-sized UHMWPE wear debris [1] leading to the requirement for eventual revision surgery. Therefore, investigators have begun to search for alternative materials to crosslinked UHMWPE that produce debris that does not induce an osteolytic response in the body.

Consideration of the lubrication conditions found in synovial joints has guided the search in the direction of compliant materials with mechanical properties similar to articular

cartilage. The authors have shown in previous work that the elastomer Pellethane® 2363-80A produces wear rates lower than UHMWPE in a simulated *in vivo* wear environment [2]. They observed that much of the reason for lower wear was the compliance of the elastomer and its ability to reduce contact pressure by conforming to the geometry of the cylindrical counterface. In order to follow up on this work, it would be prudent for investigators to know if the reason for low wear rates in healthy articular joints is the compliance of the articulating cartilage surfaces.

The best possible total-joint implant would likely involve cartilage-on-cartilage articulation, as found in a healthy joint. Such joints would have mating compliant surfaces that have the appropriate combination of elastic and viscous properties to support static loads while dampening impacts and minimizing creep. Previous work has involved the investigation of cartilage on a rigid counterface, such as done by Lipshitz *et al.* [3-5], using bovine articular cartilage pins sliding on stainless steel disks. More recent work has been performed by Berrien *et al.*[6] and Steika *et al.* [7] using human articular cartilage pins obtained from biopsies. However in none of the work reported, have investigators subjected cartilage to aggressive multi-directional sliding as has been shown with polymeric biomaterials to produce wear amounts comparable to harvested joints [8]. Nor have researchers looked at an *in vitro* model for a cartilage-on-cartilage articular joint, by manipulating the compliance of the counterface and observing its effects on wear.

In an effort to connect the characteristics of articular cartilage with its wear behavior against rigid and compliant counterfaces, some measure of the mechanical properties of articular cartilage is warranted. Due to its biphasic nature and its high fluid content, such mechanical properties can be difficult to obtain for cartilage. However, being a compliant

material it is natural that viscoelastic properties should be measured and an attempt should be made to estimate contact pressures within articular joints.

In view of the wear systems involving cartilage-on-metal mentioned above and the lack of investigation of cartilage in a realistic kinematic wear environment, the authors investigated the wear behavior of bovine articular cartilage in multi-directional sliding motion against both rigid and compliant counterfaces. This was accomplished in the Dual Axis Wear Simulator (DAWS), a machine developed by the authors and described in an earlier paper [2]. An attempt was made to determine wear mechanisms, and calculate contact pressures between pin and counterface for this testing. Along with the wear results, the viscoelastic properties of cartilage as measured by dynamic mechanical analysis (DMA) tests are discussed.

3.3 Materials and Methods

3.3.1 Fabrication of wear specimens

Healthy bovine hip joints were obtained from a meat packing firm (courtesy Amend Packing Company, Des Moines, Iowa). Immediately following slaughter, the joints were cut from the animal and frozen. Prior to preparation, the joint was thawed in isotonic saline solution and the femoral head was retrieved. The head was placed in a fixture on a drill press while cores were being extracted. Using a flowing saline solution as coolant, a plug-cutting drill bit (McMaster-Carr No. 2806A11) was fed, while rotating at slow speed, perpendicular to the surface of the joint. This produced a core with a diameter of 6.4 mm by 9.5 mm long. The core consisted of the cartilage still bonded to the underlying subchondral bone. The

cores were immediately placed in refrigerated isotonic saline solution until ready for testing as pins in multi-directional sliding.

Because of the high fluid content of articular cartilage and the partial dissolution of wear particulate in the test lubricant, a direct gravimetric measurement of cartilage wear by changes in pin weight was not possible. As such, another approach was adopted for wear estimation. Since the amino acid hydroxyproline is found almost exclusively in cartilage, its measurement in the used test fluid was used to calculate the amount of cartilage loss during wear. This is possible because the hydroxyproline content of articular cartilage is nearly constant throughout its depth [3]. In order to measure the hydroxyproline content of the cartilage specimens, small coupons of articular cartilage were removed from the joints with a scalpel at sites adjacent to core removal. The coupons were then dehydrated in sequential ethanol solutions, and dried in vacuum for 48 hours. The dried coupons were weighed in a precision balance to determine their mass. An assay [7] was performed on the coupons to determine the mass fraction of hydroxyproline in the cartilage. This procedure involved digestion of the dry cartilage in hydrochloric acid at elevated temperatures; neutralization with sodium hydroxide solution; oxidation of the hydroxyproline with a combination of copper sulfate, sodium hydroxide, and hydrogen peroxide; addition of p-dimethylaminobenzaldehyde solution; and the measurement of absorption of the fluid at 540 nm on a spectrophotometer. The absorption was then compared with that of several standards of selected concentrations prepared from trans-4-hydroxy-L-proline powder (Acros Organics) dissolved in water. Several batches of cartilage coupons were assayed to ensure that hydroxyproline content was the same for all cartilage pins used in this investigation.

3.3.2 Wear testing of cartilage specimens

The bovine cartilage pins were subjected to multi-directional sliding wear in the DAWS device [2]. The DAWS subjects pins to loading against a 12.7-mm diameter surgical stainless steel counterface shaft (BioDur® 316LS, Carpenter Technology Corporation) while immersed in bovine serum solution (18 mg/mL protein concentration) maintained at 37°C. To achieve multi-directional wear, the pins are held by a carriage that undergoes oscillating translation in a direction parallel to the shaft axis. The shaft itself undergoes rotary oscillation. Both motions are governed by servomotors controlled by a computer based on the wear path geometry desired. A normal load is applied to the pins by the use of pneumatic cylinders controlled by an air pressure regulator. The pins were kept in the DAWS under 39 N loading in 37°C serum solution for 24 hours prior to testing. Based on our earlier work with UHMWPE [2], a 6.4-mm square wear path was chosen with a cycle frequency of 0.82 Hz. A normal load of 39 N was applied to each pin during testing. The pins were tested for 100,000 cycles, at which time it was observed that the cartilage was nearly worn through to the subchondral bone. Two groups of tests were run. One group of tests subjected cartilage pins to wear against the rigid stainless steel counterface of the DAWS. For the second group of tests, a compliant counterface was used. To achieve this compliance, lengths of vinyl laboratory tubing (Tygon® R-3606, 55 Shore A durometer hardness) were stretched tightly over the stainless steel shaft of the DAWS causing a slight increase in counterface diameter of approximately 2.5 mm.

At the end of the wear tests, the used fluid from each pin was carefully collected and put into separate sealed containers. As each pin was removed from the DAWS, it was rinsed with water into the container containing the used fluid from the particular pin. This was done

to ensure that no wear particulate had adhered to the pin. The total volume of fluid from the chamber of each tested pin was measured, and a 20-mL aliquot of each pin's testing fluid was placed in a 50-mL capacity centrifuge tube. The tubes were then lyophilized in preparation for hydroxyproline assay. Due to the complicating factors of serum proteins on the assay used above, the method developed by Woessner [9] was used to determine hydroxyproline content in the used testing fluids. The Woessner method follows the same general procedure as that described above, and it includes steps that involve the extraction of serum proteins during the spectrophotometric absorption measurement to eliminate their effects on the measurement. The method also uses light at 557 nm for measurement rather than 540 nm. A sample of unused bovine serum solution was also assayed to ensure that there was no hydroxyproline in the fluid before testing.

Immediately following the wear tests, each pin was prepared for examination in a scanning electron microscope (SEM). The pins were fixed in a solution of 45% ethanol, 45% water, 5% formaldehyde, and 5% acetic acid for 24 hours. They were then placed in a solution of 70% ethanol for 1 hour, 90% ethanol for 1 hour, and finally 100% ethanol for 12 hours before drying in a vacuum. Some of the fixed and dried pins were then placed in liquid nitrogen and cryo-fractured along their axis to expose their cross section. While warming to room temperature, they were maintained in a dry nitrogen atmosphere to prevent condensation of water on their surfaces. Each prepared sample was then sputter coated in gold and examined in the SEM.

3.3.3 Dynamic mechanical analysis

To produce samples for use in dynamic mechanical analysis, untested cartilage pins were used. A scalpel was used to carefully cut the thin cartilage layer from the underlying

subchondral bone. Each cartilage disk was then placed in bovine serum solution until the time for measurement in the dynamic mechanical analyzer (DMA). A cup and plate configuration was used to apply loading to the cartilage disk. The plate had a diameter of 3.0 mm, while the cup diameter was approximately 8.0 mm. A single cartilage disk was placed in the DMA cup, which was filled with bovine serum solution of the same composition used in the wear tests. After temperature and load calibration of the DMA, the loading plate was lowered onto the cartilage disk and the initial thickness was measured. The temperature of the sample was maintained at 37°C during testing. A frequency sweep program was executed on the DMA from 0.1 to 10 Hz with a static load of 100 mN and a dynamic load of 100 mN. The data from the DMA test was stored on a personal computer and was used to calculate the storage and loss moduli as a function of frequency. Multiple cartilage disks were tested to ensure that the data was repeatable.

3.4 Results and Discussion

3.4.1 Hydroxyproline concentration in bovine articular cartilage

The hydroxyproline concentration of the cartilage was measured at five locations on the hip joint used for producing wear pins. It was determined that the hydroxyproline concentration in the cartilage had a mean value of 7.87% by weight, with a standard deviation of 0.70%. This agrees very well with the concentration values in the range of 7.4 to 8.2% in the top 1.000 mm of bovine articular cartilage, reported by Lipshitz *et al.* [3]. 7.87% was used in the analysis of the wear test fluids, below, to determine the mass of cartilage lost during the wear process.

3.4.2 Cartilage wear and failure mechanisms

The wear results for the six pins tested against the stainless steel counterface are given in Table 3.1. With a mean value of 25.65 mg, the wear of the cartilage is significantly higher than that reported by Lipshitz from pin-on-disk tests. For testing durations similar to the work done here, Lipshitz reported wear values less than 2.0 mg [4]. The reasons for this difference may be threefold. Firstly, Lipshitz cites the amount of time the specimens were subjected to wear in the pin-on-disk setup, but does not mention the sliding speeds involved. It is possible that the actual distance traversed by the pins is vastly different between these two investigations. Secondly, our investigation involved a plane-on-cylinder wear interface which would produce much higher contact pressures than those in a pin-on-disk configuration. Higher contact pressures typically lead to increased wear. Thirdly, there is considerable difference in wear rates between unidirectional and multi-directional sliding, as has been reported earlier [8]. In polymers, the bulk of the wear occurs during the cross-shear portion of the wear cycle in a multi-directional test. The results of the current investigation are representative of what would be expected in a cartilage-on-metal implant with the cylinder-on-plane or ball-on-plane configurations that approximate the configuration of a knee joint. Hip and shoulder configurations are ball-in-socket joints which would be subjected to lower contact pressures. Our results indicate that a successful design for a cartilage-on-metal joint with high contact pressures such as a knee hemiarthroplasty would be very challenging.

Contrast the above results with those of the cartilage pins tested against the compliant counterface, as given in Table 3.2. The mean wear of 9.97 mg is markedly lower than that of the rigid counterface. It is likely that the primary factor in the wear decrease is the

significantly lower contact pressures between pin and compliant counterface. A further analysis of these pressures is discussed in a later section of this paper. These wear results suggest the possibility that implants retaining one of the native cartilage surfaces, such as hip or shoulder hemiarthroplasties where a metallic ball articulates against the native cartilage acetabulum, may benefit from making the implant articulating surface more compliant. By lowering the contact pressures between ball and cup, wear may potentially be reduced and implant lifetime increased if a suitable compliant biomaterial were used.

Figure 3.1 shows a cross sectional view of a wear pin after testing. It is clear from the image that the center of the pin, where contact pressures against the counterface shaft were highest, retains very little cartilage compared to the edges. Material removal appears to be the cause for the thin cartilage layer at the center upon viewing the pin at low magnifications. However at higher magnifications, it can be seen that the cartilage has been deformed away from the center as shown in Figure 3.2. Therefore, the thickness change is due mostly to material removal, but there is also creep of the tissue away from the maximum stress region. This creep behavior is expected in compliant materials such as cartilage, and reduces the maximum contact pressure on the pin surface.

Figures 3.3a and 3.3b show the wear surface of a cartilage pin after testing against the stainless steel counterface. Though the amount of wear of the cartilage was drastically higher than in polymers such as UHMWPE [2], the characteristics of the worn surfaces share similarities. As shown in Figure 3.3b, the worn cartilage surface shows striations as does UHMWPE worn in the DAWS. Figure 3.4 is a schematic of the relative motions of the pin against the counterface during each wear cycle. Initially, the pin is translated parallel to the shaft axis in what the authors have called lateral sliding. At the onset of this step and step 3,

lubricant is likely present at the interface between the pin and counterface. However as the lateral motion continues, the lubricant layer is depleted and the two surfaces come into closer contact until the end of the step. Subsequent to the lateral steps, the shaft rotates under the pin producing what the authors have termed circumferential sliding. Because of the viscous adhesion of the fluid to the shaft, fluid is likely entrapped at the wear interface and provides some hydrostatic lubrication during steps 2 and 4, respectively. Through this cycle of regeneration and depletion of the lubricant layer, the cartilage surface is exposed to the most severe stresses during the lateral motions. This hypothesis is supported by the orientation of the wear striations in Figure 3b that show surface separation in a direction normal to the shear and tensile stresses induced during lateral motion. This method of material removal is likely unique to multi-directional sliding, and thus may explain the much higher wear rates than found in unidirectional motion.

Upon completion of wear tests against the compliant counterface, no evidence was found of wear damage to the compliant overlays. Figure 3.5 shows the wear surface of a pin worn against the compliant counterface. The figure shows the presence of striations normal to the lateral sliding direction, much like those found after testing against the rigid counterface. The fact that striation orientation is the same for both cases suggests that the wear mechanisms are similar, however, the magnitude of material removal differs as discussed above.

3.4.3 Cartilage viscoelasticity

The role of cartilage in synovial joints includes resisting wear, and also cushioning impact and maintaining separation of the underlying bone surfaces under static and dynamic loads. The presence of both elastic and viscous components allows articular cartilage to

remain stiff enough to support static loading of the joints, while offering sufficient damping of dynamic forces during walking. This compliance of cartilage is beneficial for maintaining fluid-layer lubrication within the joint and thus providing extremely low coefficients of friction. The characterization of this viscoelasticity not only helped to determine the mechanical behavior of articular cartilage under load, but also enabled the calculation of contact pressures between pin and counterface during the wear testing in this investigation.

Figure 3.6 is a plot of storage and loss moduli measured for the bovine articular cartilage tested in bovine serum solution at 37°C. The plot shows that over all frequencies the material has both elastic and viscous components. There is a considerable increase in elastic behavior as frequency is increased, from a storage modulus of approximately 470 kPa to a maximum value of 1010 kPa at higher loading frequencies. The viscous component remains more constant over the range of frequencies investigated, with a range from 176 to 249 kPa. This amount of viscous behavior helps to explain the mechanism of creep away from maximum contact pressure as observed above in the worn pins.

As mentioned above, it is likely that the lower wear rates of cartilage pins against the compliant counterface are due to lower contact pressures. To support this idea, the measurement of the storage modulus of cartilage from the DMA investigation can be used to estimate contact pressures. This is accomplished by calculation of the Hertzian stress between the pin and each counterface using the following three relations:

$$\frac{1}{R} = \frac{1}{R_1} + \frac{1}{R_2} \tag{3.1}$$

In relation (3.1), R is termed the effective curvature of the interface, where R_1 is the counterface radius, and R_2 is the pin face radius, it is infinite for plane contact. For the stainless steel counterface, the effective curvature was calculated to be 6.35 mm. The compliant sleeve added slightly to the diameter of the counterface shaft, producing an effective curvature of 7.62 mm. The contact modulus, E*, is calculated from the relation:

$$\frac{1}{E^*} = \frac{1-\nu_1^2}{E_1} + \frac{1-\nu_2^2}{E_2} \tag{3.2}$$

where ν_1 and ν_2 are the Poisson's ratios of the counterface and cartilage, respectively, and E_1 and E_2 are the elastic moduli of the counterface and cartilage, respectively. Using values reported by the suppliers, the elastic modulus of the stainless steel counterface was 193 GPa, while the vinyl tubing had a modulus of approximately 4.5 MPa at 100% extension. Both materials were assumed to have Poisson's ratios of 0.3, for the purposes of this comparison. The storage modulus of the cartilage at 1.0 Hz was measured to be 840 kPa. These values yielded contact moduli of 923 kPa and 778 kPa for the rigid and compliant counterfaces, respectively. Finally, the maximum contact pressure, P_0, is given by:

$$P_0 = \sqrt{\frac{P'E^*}{\pi R}} \tag{3.3}$$

where P' is the force per unit length on the wear interface. Using the 39 N load and the pin diameter of 6.4 mm, this value was calculated to be 6.09 kN/m. In the case of the stainless

steel counterface, the maximum contact stress was calculated to be 533 kPa, while the compliant counterface contact stress was calculated to be 447 kPa. This was a considerable difference in the pin contact pressures generated between rigid and compliant counterfaces. Furthermore, it suggests that lower wear rates may be accomplished in a cartilage-on-metal implant by covering the rigid metal side of the implant with a biocompatible compliant material with suitable viscoelastic properties.

3.5 Conclusions

1. The wear of bovine articular cartilage in the DAWS was significantly reduced with the use of a compliant counterface. This was due to the lower contact pressures generated at the wear interface using a compliant overlay versus a rigid stainless steel surface.
2. The lubrication conditions at the wear interface had a substantial effect on the wear mechanism of articular cartilage in multi-directional sliding. With a square wear path, the circumferential segments generated a fluid layer at the interface protecting the cartilage from extensive wear, while the lateral segments led to depletion of the fluid layer and considerable material removal.
3. Bovine articular cartilage exhibited a considerable amount of viscoelastic behavior over the loading frequencies investigated. It had sufficient elastic stiffness to support loading during wear testing, yet it possessed a significant amount of viscous behavior to allow for small-scale flow of material away from highly stressed regions within the wear interface.

3.6 References

1. J.H. Dumbleton, M.T. Manley, A.A. Edidin, A literature review of the association between wear rate and osteolysis in total hip arthroplasty. J Arthroplasty, 2002. 17(5): p. 649-661.
2. C.J. Schwartz, S. Bahadur, Development and testing of a novel joint wear simulator and investigation of the viability of an elastomeric polyurethane for total-joint arthroplasty devices. Submitted to Wear, 2005.
3. H. Lipshitz, R. Etheredge, 3rd, M.J. Glimcher, In vitro wear of articular cartilage. J Bone Joint Surg Am, 1975. 57(4): p. 527-534.
4. H. Lipshitz, R. Etheredge, 3rd, M.J. Glimcher, In vitro studies of the wear of articular cartilage--III. The wear characteristics of chemical modified articular cartilage when worn against a highly polished characterized stainless steel surface. J Biomech, 1980. 13(5): p. 423-436.
5. H. Lipshitz, M.J. Glimcher, A technique for the preparation of plugs of articular cartilage and subchondral bone. J Biomech, 1974. 7(3): p. 293-294.
6. L.S. Berrien, M.J. Furey, H.P. Veit, Tribological study of joint pathology. Crit Rev Biomed Eng, 2000. 28(1-2): p. 103-108.
7. N.A. Steika, *A Comparison of the Wear Resistance of Normal, Degenerate, and Repaired Human Articular Cartilage*, in *Mechanical Engineering*. 2004, Virginia Polytechnic Institute and State University: Blacksburg, VA. p. 78.

8. M. Turell, A. Wang, A. Bellare, Quantification of the effect of cross-path motion on the wear rate of ultra-high molecular weight polyethylene. Wear, 2003. 255(2): p. 1034-1039.

9. J.F. Woessner, The determination of hydroxyproline in tissue and protein samples containing small proportions of this imino acid. Arc. Biochem. Biophys., 1961. 93: p. 440-447.

Table 3.1 Individual wear results for bovine articular cartilage pins tested in the DAWS under 39 N loading and a 6.4-mm square wear path.

Sample identification	Cartilage wear (mg)
Pin A	23.86
Pin B	31.36
Pin C	23.50
Pin D	22.74
Pin E	25.85
Pin F	26.59
mean	25.65
standard deviation	3.16

Table 3.2 Individual wear results for cartilage pins tested against a compliant counterface under 39 N loading and a 6.4-mm square wear path.

Sample identification	Cartilage wear (mg)
Pin G	8.37
Pin H	12.02
Pin I	11.60
Pin J	9.29
Pin K	10.03
Pin L	8.52
mean	9.97
standard deviation	1.55

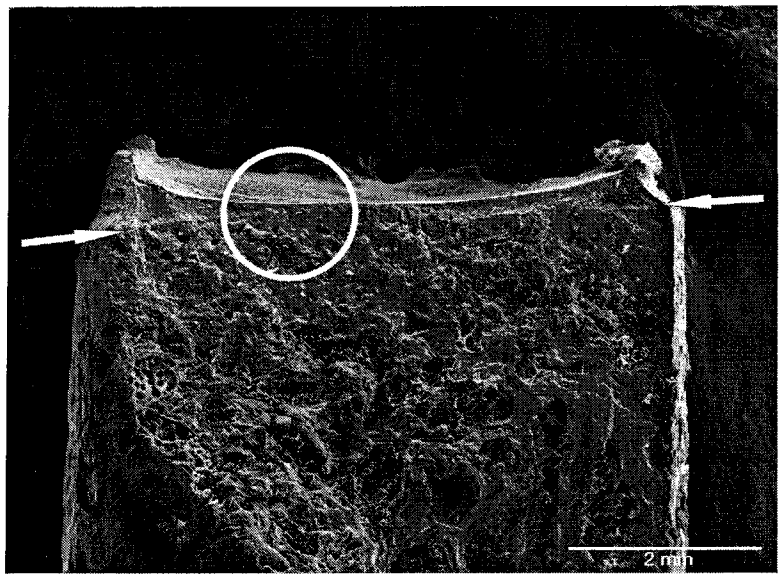

Figure 3.1 Cross section of Pin B showing the cartilage layer and subchondral bone. Circle indicates area magnified in Fig. 2. Arrows indicate transition from subchondral bone to cartilage layer.

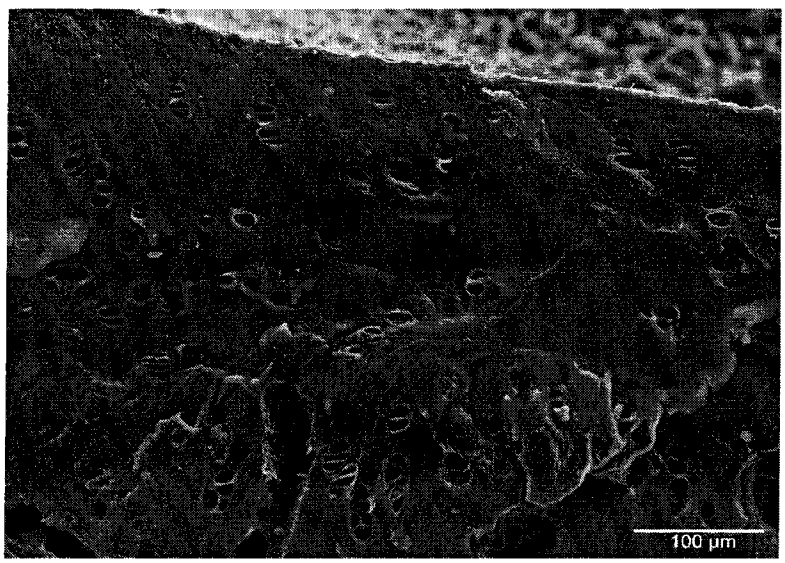

Figure 3.2 High magnification of Pin B cross section showing the oblique deformation of the cartilage tissue away from the pin center.

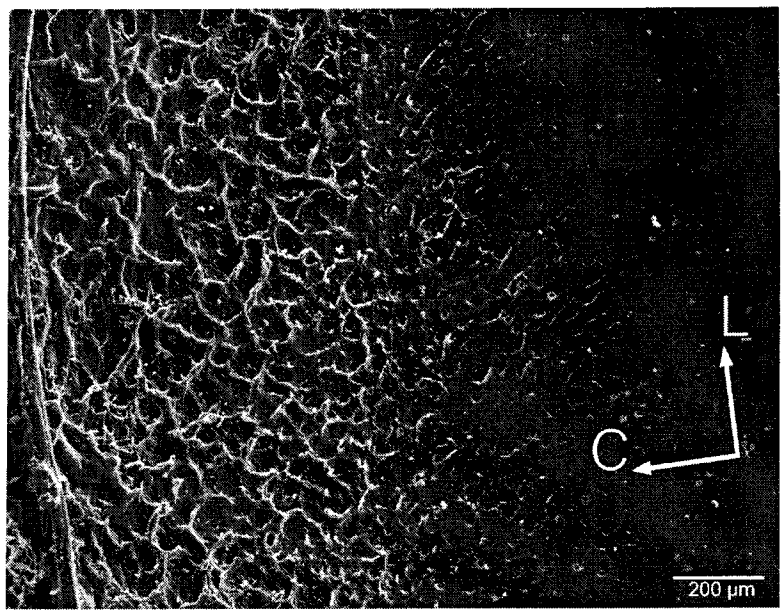

(a)

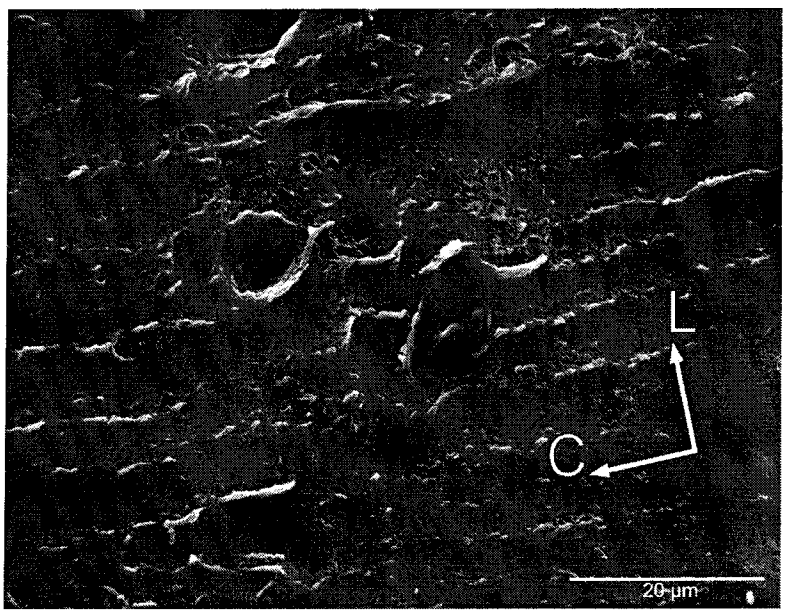

(b)

Figure 3.3 Micrographs of worn Pin D surface (a) at low magnification at the transition between unworn (left) and worn (right) regions and, (b) higher magnification showing striations of material removed.

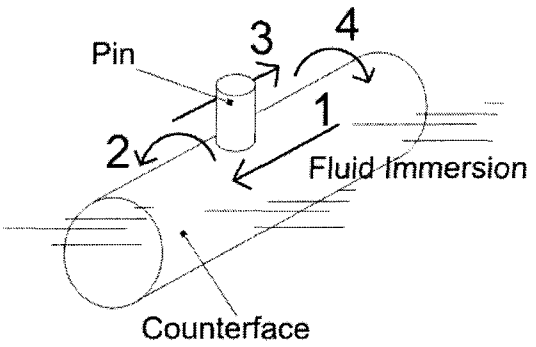

Figure 3.4 Diagram of relative motions of cartilage pin against the counterface for a square wear path. Motions 1 and 3 are lateral, 2 and 4 are circumferential. The total sliding distance is 25.4 mm per cycle.

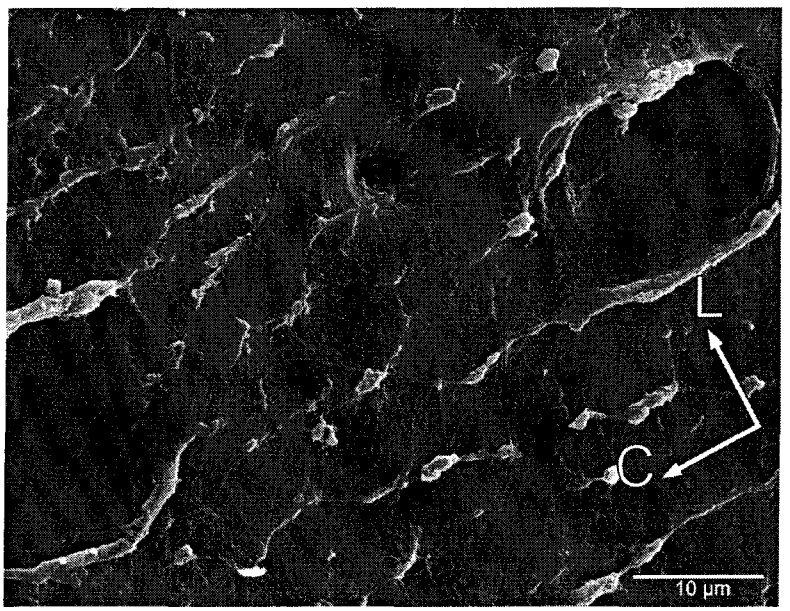

Figure 3.5 Micrograph of the wear surface of Pin G tested on the compliant counterface. Striations are visible in a direction normal to lateral sliding.

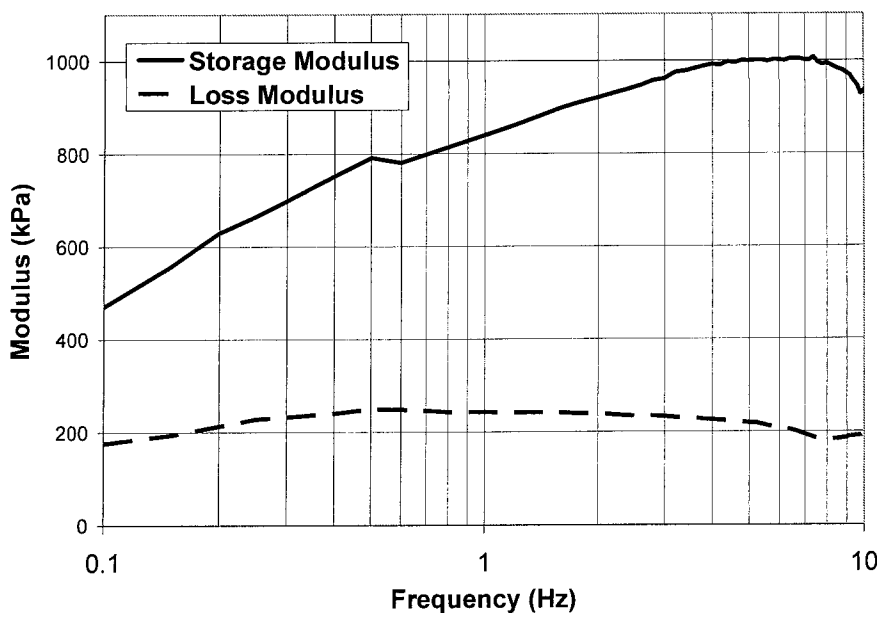

Figure 3.6 Storage and loss moduli of bovine articular cartilage tested in 37°C bovine serum solution from 0.1 to 10 Hz.

CHAPTER 4
EFFECT OF CROSSLINKING AND PT-ZR QUASICRYSTAL FILLERS ON THE MECHANICAL PROPERTIES AND WEAR RESISTANCE OF UHMWPE FOR USE IN ARTIFICIAL JOINTS

A paper submitted to the 16th International Conference on Wear of Materials, Montreal

Christian J. Schwartz, Shyam Bahadur, and Surya K. Mallapragada

4.1 Abstract

The use of artificial joints is common for restoration of comfort and functionality in joints that have been afflicted with cartilage loss due to disease or injury. These implants incorporate an articulating interface of ultra-high molecular weight polyethylene (UHMWPE) sliding against a polished metallic counterface such as 316L stainless steel. While the design of these joints has been refined over several decades, there are still significant limitations to their pain-free lifetime due to osteolysis induced by UHMWPE particulate. Crosslinking has been used recently to increase the wear resistance of the polymer, but there are significant tradeoffs involving reduced elastic modulus and impact toughness. The authors have proposed using Pt-Zr quasicrystals (QC) as fillers in UHMWPE as a method of increasing the wear resistance of the polymer while avoiding significant losses in mechanical properties. UHMWPE samples that had been irradiation crosslinked, filled with 20 wt.% Pt-Zr quasicrystals, or both, were tested in a dynamic mechanical analyzer to determine their viscoelastic properties. Furthermore, Charpy impact tests were performed on these materials, as well as multi-directional sliding wear tests in the Dual Axis Wear Simulator (DAWS), a machine designed to simulate *in vivo* joint wear conditions. It was found that while crosslinking reduced elastic modulus of UHMWPE over 30%, the use

of QC fillers led to a slight increase. Additionally, the reduction in impact toughness when using QC fillers was not as great as with crosslinking. Finally, it was found that both QC fillers and crosslinking provided the same significant reduction in wear amounts over untreated UHMWPE. The reduction in wear is explained in terms of the wear mechanisms. This involves inhibition of polymer chain orientation in the case of crosslinking, and shear load shielding effects of quasicrystals in the case of QC-filled polymer. These results suggest that Pt-Zr quasicrystal filler may be a desirable alternative to crosslinking when attempting to increase the wear resistance of UHMWPE for biomedical applications.

4.2 Introduction

The use of artificial implants for replacement of the hip, knee, and other articular joints has become very commonplace in light of increasing life expectancies and improvement of implant designs [1]. Total-joint arthroplasty restores functionality to joints that have experienced considerable cartilage degradation due to arthritis or injury. The typical artificial joint includes a polished metallic surface made from cobalt-chromium or surgical stainless steel alloy that articulates against an ultra-high molecular weight polyethylene (UHMWPE) component. In the hip, the metallic component has a long stem which is cemented within a deep bore drilled into the femur. This system is the result of decades of development in biomaterials and implant design, and exhibits very low wear rates [2]. However, such implants have a limited pain-free lifetime due to the results of UHMWPE wear particulate being deposited in tissues surrounding the joint. The anatomical reaction to this particulate is termed osteolysis, which results in gradual loss of the bone tissue surrounding the stem of the implant eventually leading to implant loosening [3]. To reduce

the incidence of osteolysis, and thus extend implant lifetimes, the most direct approach appears to be reducing the wear rate of the UHMWPE components. Two methods of wear reduction that show the most potential are crosslinking of the polymer, and the use of reinforcing filler particles in the polymer to enhance its durability.

Crosslinking of UHMWPE, a commonly used method to reduce wear, is done commercially through the use of either electron beam or gamma irradiation. The ionizing radiation creates free radicals, through removal of hydrogen and chain breaking, which recombine to produce the crosslinked structure. It has long been known that the UHMWPE surface of the artificial hip undergoes multidirectional sliding against the femoral ball during the walking cycle. This results in constant reorientation of the polymer chains in the directions of shear stress, thus producing a weakened polymer when sliding perpendicular to the chain orientation direction [4]. Crosslinking produces a more wear resistant material than the untreated polymer by limiting polymer chain orientation from shear stresses [5]. The disadvantage of crosslinking is that it reduces fracture toughness of the polymer and other mechanical properties [6]. An additional drawback of crosslinking is that the free radicals generated in crosslinking the polymer vulnerable to oxidative damage as it is exposed to the environment. Oxidation of the polymer, whether during storage or *in vivo* use, leads to embrittlement and loss of wear resistance. Thermal stabilization methods to inhibit oxidation after irradiation are typically used to avoid this; however, this is not a desirable approach because it adversely affects the mechanical properties of UHMWPE such as fatigue strength [7]. In addition to this, even with a thorough stabilization protocol, UHMWPE acetabular cups have shown oxidative damage after storage in vacuum packaging or *in vivo* use [8]. While crosslinking of UHMWPE shows tremendous benefits in lowering wear, the tradeoffs

encountered with its use suggest that investigation is warranted into the use of alternative approaches to wear reduction.

An alternative to crosslinking may be found in the reinforcement of UHMWPE with filler particles. In order to improve some mechanical properties, polymers are often filled with separate-phase inorganic filler particles. The improvement in wear resistance with the use of fillers in various polymers has been widely reported [9-11]. The most direct advantage of using filler particles over crosslinking is the avoidance of free radical generation and accelerated oxidation. However, it remains to be seen how much of a wear reduction is possible with the use of fillers in UHMWPE, and whether they degrade impact properties in the polymer as much as crosslinking does. An immense challenge in using fillers in a biomedical implant is the toxicological effects that the filler may have on the body. Therefore, care must be taken in the selection of these fillers.

Previous work has looked at the performance of a novel class of metallic alloys called quasicrystals (QC). Discovered in the 1980s, quasicrystals are produced by the rapid solidification of molten metallic solutions through processes such as melt spinning [12] or gas atomization [13]. Because of the rapid cooling rate involved in this technique, quasicrystals do not develop typical crystallographic rotational symmetry. Rather, they possess five- or ten-fold symmetry. Quasicrystals possess unique properties not found in other alloys such as high hardness and low friction coefficient [14]. Investigators have shown that epoxy composites made with quasicrystal fillers exhibit high wear resistance [15]. Furthermore, Al-Cu-Fe quasicrystals have been shown to significantly reduce wear in UHMWPE when sliding against a stainless steel counterface as found in an artificial joint [16]. However, there is concern that the elemental components of the Al-Cu-Fe material may

pose a toxicological hazard *in vivo*. In order to probe into the practicality of using quasicrystals as fillers in a biomedical application, the authors have investigated the properties of UHMWPE filled with platinum-zirconium quasicrystals. Platinum and zirconium, as pure metals, have been shown to be fairly biocompatible, and thus Pt-Zr quasicrystals offer the potential for significant wear reduction with minimal toxicological concern.

In this work, the authors have focused on the characterization of Pt-Zr quasicrystal-filled UHMWPE as compared to the crosslinked polymer in artificial joints. In order to study the behavior of these materials in response to the stresses and strains as experienced in an artificial joint, dynamic mechanical analysis (DMA) has been performed. In addition, the wear performance of these materials was investigated by testing in a joint wear simulator. Wear mechanisms were identified for comparison among untreated, filled, and crosslinked UHMWPE. In addition, the impact strength of the materials was studied in view of the fact that these joints are subjected to impact loading because of their functionality.

4.3 Materials and Methods

4.3.1 Dynamic mechanical analysis

The polymeric articulating component of an artificial joint must be stiff enough to support static loading, but also have some damping capability to absorb impact loads. The most direct way to assess these properties is with dynamical mechanical analysis. DMA data can be used to determine two fundamental properties, storage and loss moduli. Storage modulus indicates the amount of elastic deformation of the material when a static load is applied, as would be experienced by an artificial joint while an artificial joint recipient is

standing still. On the other hand, loss modulus indicates the amount of damping offered by the material during dynamic and impact loading as would occur during walking, jogging, or stair climbing. In view of these considerations, the viscoelastic behavior of UHMWPE and its modifications was characterized using a dynamic mechanical analyzer (Perkin Elmer DMA 7e) in a three-point bend configuration.

In order to produce samples for the DMA work, UHMWPE powder (Sigma Aldrich, Inc.) was compression molded in a cylindrical mold on a heated press with an applied pressure of 250 MPa at a temperature of 200°C. The mold produced rods of solid UHMWPE of 6.4-mm diameter and approximately 40-mm length. These rods were subsequently cut using a sharp blade to pins of 9.5-mm length. Filled UHMWPE pins were prepared in the same manner, with a 20% proportion of the Pt-Zr quasicrystals ($Zr_{80}Pt_{20}$) by weight. This proportion was used because it was shown to be nearly optimal when Al-Cu-Fe quasicrystals were used as fillers in UHMWPE [16]. The Pt-Zr quasicrystals were approximately spherical with a distribution of diameters between 5 and 60 μm, but with the vast majority between 45 and 55 μm. They were produced prior to this work (courtesy Daniel Sordelet, Ames Laboratory, U.S. Dept. of Energy), and are shown in Figure 4.1. Four groups of pins in terms of their treatment were produced for DMA and wear testing: unfilled, non-crosslinked UHMWPE; QC-filled, non-crosslinked UHMWPE; unfilled, crosslinked UHMWPE; and QC-filled, crosslinked UHMWPE.

The pins were vacuum packed and stored in a dark, cool area until crosslinking. Crosslinking was performed by exposing the samples to a dose of 50 kGy of electron-beam radiation in a linear accelerating facility. Packages of the irradiated pins were kept in an air-circulating oven at 120°C for 10 hours for thermal stabilization of the free radicals. A sledge

microtome was used to slice thin sections parallel to the pin axis for three-point bend testing in the DMA equipment. The size of the specimens obtained was 9.5 mm long by 5.5 mm wide with a thickness of 0.24 mm. The specimens were supported on a fixture with a span between the supports of 5.0 mm, and loading was applied at the midpoint of the specimen span. A static loading of 110 mN was applied concurrently with a dynamic loading of 100 mN, producing a sinusoidal loading profile. Storage and loss moduli were measured at loading frequencies ranging from 0.5 to 5.0 Hz.

4.3.2 Impact toughness

An important property of an artificial joint component is its resistance to brittle fracture upon impact, as would be encountered during catastrophic loading events. This is one of the primary reasons why polymer-on-metal hip designs are more widely used than ceramic-on-ceramic designs. Since crosslinking is reported to degrade the impact toughness of UHMWPE [17], the extent of degradation by crosslinking as well as by quasicrystal fillers was studied by Charpy impact tests. In order to produce samples for Charpy tests, a special mold was fabricated and the samples were molded under a pressure of 20 MPa and a temperature of 200°C. The molded specimens were 10-mm by 10-mm square bars with a length of 55 mm and a V-notch in the center. For crosslinking, the specimens were vacuum packed and irradiated with a dosage of 50 kGy in the linear accelerator and later thermally stabilized for 10 hours at 120°C. Three types of Charpy specimens were produced: unfilled, non-crosslinked UHMWPE; filled, non-crosslinked UHMWPE; and unfilled, crosslinked UHMWPE. Because of fabrication defects found after irradiation, the UHMWPE specimens that had been both filled and crosslinked were not examined in impact. All specimens were numbered and their testing order was randomized.

The impact energy of the specimens was measured using a pendulum-style impact tester (Ametek, Inc.) with a 66.7-N hammer and a drop height of 0.61 m. Prior to testing, all of the Charpy specimens were placed in a water bath at 37°C for one hour. Each specimen was tested in order by placing it in the impact tester, then raising and releasing the pendulum to strike and break the specimen. The energy loss incurred in breaking the specimen was recorded on a calibrated dial incorporated into the tester. At least seven specimens from each treatment group were tested in order to produce a reliable statistical representation of the impact data.

4.3.3 Wear testing

As an articulating component of an artificial joint, the wear behavior of a biomaterial is of vital importance and hence needs to be determined by wear tests. The cylindrical pins used for the wear tests had a diameter of 6.4 mm, and a length of 9.5 mm. The surface of the pins subjected to wear was finished by abrasion to a surface roughness of 0.15 μm Ra. The pins were subsequently cleaned and vacuum packaged prior to crosslinking.

The wear behavior of pins as affected by fillers and crosslinking was studied in the Dual Axis Wear Simulator (DAWS), a joint wear simulation device that was designed for screening of candidate wear materials and has been described elsewhere [18]. The cylindrical counterface of 316L stainless steel was finished to a surface roughness of 0.10 μm Ra in the axial direction by spinning the shaft in a lathe while abrasive diamond paste was applied. The DAWS was programmed to produce a 6.4-mm by 6.4-mm square wear path with the pins sliding against the counterface under a load of 39 N producing a nominal contact pressure of approximately 3.1 MPa. This resulted in a plane-on-cylinder wear configuration. The pins were cleaned and weighed and then subjected to 250,000 wear

cycles while immersed in a bovine serum solution at 37°C. The pins traversed the square wear path (total distance 25.6 mm) every 1.22 seconds. Prior to wear testing, each pin was given an identification number and randomly assigned to a particular test run and testing station in the DAWS. Two stations on the DAWS were used as soak controls, where the pins were subjected to loading but not sliding, in order to determine the amount of fluid uptake during the test. After the completion of wear tests, the pins were again cleaned, dried, and weighed to a precision of 10^{-5} g to determine the loss of mass due to wear. This value was corrected based on the fluid uptake of the control pins, and the density of the pin material was used to calculate volumetric wear. Analysis of variance (ANOVA) methods were used to compare the mean wear of the four treatment groups to determine if there were statistically significant differences in the wear amounts.

The wear surfaces from representative worn pins from each treatment group were removed from the pins and gold coated to allow for examination by scanning electron microscopy (SEM). The purpose of this examination was to identify the wear mechanisms. In order to determine whether the filler particles supported normal load directly during sliding, stereo-electron microscopy was used to quantify the observed height differences between features on the worn pin surfaces.

The bovine serum solution used during each wear test was retrieved immediately following the test and digested with sodium hydroxide for 3 days. The digested solutions were poured in a separatory funnel with hexane and an ethanol-water mixture and agitated to allow for retrieval of the wear particles. The wear particles were deposited on a polycarbonate filter with a pore size of 0.1 μm. The particles were then dried in a vacuum

desiccator, as described by Biggs et al. [19]. The filter disks were coated with gold to allow the wear particles to be examined in the SEM.

4.4 Results and Discussion

4.4.1 Dynamic mechanical properties

Figure 4.2 shows the results of dynamic mechanical analysis of the four treatment groups in three-point bending. The plots show significant changes in storage moduli with the addition of fillers and with crosslinking. The first observation is that the crosslinked sample had significantly lower storage modulus than that of the non-crosslinked sample at any frequency, reducing the value by more than 30%. This indicates that crosslinked UHMWPE components in a joint would tend to deform to a greater extent under static loading. This result may seem paradoxical at first, until one considers the fact that the degree of crystallinity of the polymer typically controls its elastic stiffness. In non-crosslinked UHMWPE, polymer chains have sufficient mobility during molding to develop a certain amount of crystallinity. Chains that have formed crystalline regions within the bulk show a higher resistance to deformation than amorphous regions. During crosslinking, some of the crystallinity imparted during compression molding is destroyed. The resulting increase in amorphous microstructure in the polymer leads to a bulk with lower stiffness. This phenomenon has been reported by other researchers [20, 21] as well.

With QC fillers in UHMWPE, a slight increase in storage modulus of approximately 5% over that of the unfilled polymer is observed. This may be explained in direct mechanical terms by reinforcement models that predict an increase in elastic modulus when there is reasonable bonding between the polymer and the filler [22]. Such models suggest ways to

increase storage modulus even further by modifying the size or shape of the quasicrystals, or using bonding agents to ensure strong adhesion between the polymer and the filler. When UHMWPE is both crosslinked and filled with quasicrystals, the storage modulus at any frequency is higher than that of the crosslinked polymer but lower than that of the filled polymer. This obviously shows that the presence of quasicrystals increases the elastic modulus of the crosslinked polymer for the reasons cited above.

An examination of loss moduli of the various treatment groups suggests that there are no significant differences in the damping behavior of the polymers. As expected, all treatments had high loss moduli at lower frequencies and the moduli decreased as the frequency was increased and the materials behaved more elastically. This indicates that a) crosslinking did not measurably degrade damping capability of the polymer, and b) that damping capability of QC-filled UHMWPE did not suffer even as storage modulus benefited from the use of filler. Therefore, Pt-Zr quasicrystals appear to enhance the viscoelastic properties in such a way as to produce a stiffer joint component that retains the damping capability of UHMWPE.

4.4.2 Impact toughness

The effect of fillers and crosslinking on the impact toughness of UHMWPE is shown in Figure 4.3. The untreated UHMWPE has the highest impact energy. Crosslinking significantly reduces the impact toughness. This is so because polymer chains have less mobility when crosslinked and so are not able to absorb the energy during impact as well as before crosslinking. This is an undesirable tradeoff that is made in producing more wear-resistant UHMWPE for use in artificial joints. The QC-filled UHMWPE also shows some reduction in impact toughness but much less than with crosslinking. This suggests that the

non-crosslinked polymer chains have a significant amount of energy absorption capability even in the presence of fillers.

4.4.3 Wear behavior

The results from wear tests for 250,000 cycles on the four treatment groups are shown in Figure 4.4. Clearly, the wear of UHMWPE is significantly reduced with either the use of quasicrystal fillers or crosslinking. Interestingly, there is no statistically significant difference (Tukey's HSD, $\alpha = 0.05$) among the wear rates of UHMWPE that had been filled, crosslinked, or both. This indicates that the use of fillers provides wear reduction comparable to that produced by 50 kGy irradiation. However, it also indicates that once the initial benefit on wear is realized by using either fillers or crosslinking, no further benefit appears to be gained by combining the two treatments. Currently, crosslinking is the primary method used to increase wear resistance of UHMWPE in artificial joints, but it decreases the elastic modulus as shown above. These results are significant because they indicate that, unlike crosslinking, quasicrystal fillers may be used to increase wear resistance without any detrimental effect on the elastic modulus.

Figure 4.5 shows SEM micrographs of the wear surfaces of the specimens from the four groups tested. The characteristics of each wear surface suggest that the wear mechanism involved asperities on the worn pin surfaces accumulating strain due to cyclic shear loading, with the eventual separation of particles from the bulk. However, there were clear differences between the crosslinked and non-crosslinked specimens in terms of the amount of stretching that the surface asperities could undergo before fracture. The untreated UHMWPE wear surface in (a) shows ridges of raised and frayed polymer that are highly directional and evenly spaced. Removal of material appears to be due to the accumulation of strain cycles

that lead to the separation of a strained fibril from the pin surface. It appears that most material was removed during lateral movement of the pin, which is the direction parallel to the counterface shaft axis. The surface of the quasicrystal-filled specimen in (b) shows a similar mechanism though wear was substantially lower than in the untreated UHMWPE. Note that no quasicrystals are present in the region shown. It is likely that three key factors are responsible for this wear behavior: polymer molecule orientation, the directionality of counterface surface roughness, and lubricant depletion from the scraping action of the polymer pin. Each of these effects is discussed in the context of wear behavior separately below.

Because of the square wear path traversed by the pin, the latter experienced four changes in shear stress direction during each wear cycle. During the sliding motion, the polymer chains oriented themselves in the direction of applied shear stress. This led to higher mechanical properties and wear resistance in the direction of orientation. However, it also led to reduced wear resistance along a vector perpendicular to the orientation direction. Thus, each change in direction during the wear cycle exposed the pins to sliding in a direction of degraded wear resistance. Therefore multidirectional sliding, as encountered in this study, does not allow the polymer to develop chain orientation that resists wear. Rather it continually exposes the pin surface to a situation of degraded wear resistance. This is what causes much higher wear rates to be observed in multidirectional sliding versus linear or linear-reciprocating sliding. It has been shown that multidirectional sliding is a much better indicator of wear rates and mechanisms found in harvested artificial joints.

The next factor responsible for material removal is dependent on the surface characteristics of the counterface shaft used in the DAWS machine. In order to finish the

metallic counterface to an appropriate surface roughness, the cylindrical counterface was rotated about its axis while it was abraded. This polishing action produced finish marks with asperities oriented laterally ("L" direction). As the pin slid laterally, the wear surface was subjected to the aggressive action of these asperities which produced greater damage. Thus the loss of material from the pin surface while sliding in the lateral direction was greater than in the circumferential direction.

Finally, the lubricant also played a role in the wear behavior of the specimens tested. Because of the plane-on-cylinder configuration in the DAWS, lubricant was drawn into the wear interface between pin and shaft during shaft rotation (circumferential legs of the wear path). In contrast to this, during lateral pin movement when the shaft was stationary, the lubricant layer between pin and counterface was depleted because of the scraping action of the pin. Thus there was more intimate contact between the sliding surfaces when the pin slid on the counterface in the lateral direction than in the circumferential direction. This difference in the nature of contact governed the wear behavior.

The micrograph of the worn surface of crosslinked UHMWPE in Figure 4.5 (c) shows the same wear features as described above but the ridges are of shorter lengths. The latter is presumably due to the crosslinking effect because the crosslinks reduce the deformation ability of the material. The wear surface for crosslinked and filled polymer in Figure 4.5 (d) exhibits similar features but these are somewhat subdued. Both of these observations suggest a reduction in the long-range chain orientation effects as found in Figure 4.5 (a) and (b). The factors related to surface roughness and lubricant depletion were still present. Thus the reduction in chain reorientation, and consequently less frayed material, likely led to reduced

wear in these cases. However, the mechanisms of material removal were the same in all the cases.

The SEM examination of wear particles was carried out to shed further light on the wear mechanisms involved. For both the filled and unfilled UHMWPE, wear particles in Figure 4.6 show the considerable stretching that would occur in the orientation process discussed above. When the stretched fragment is separated from the bulk polymer it curls up to relieve stresses. In the case of the crosslinked UHMWPE (both filled and unfilled), the wear particles do not show much stretching and curling as observed for the non-crosslinked polymer. As stated earlier, crosslinking reduces the extent of deformation and hence the amount of stretching before fracture. Thus the findings for the worn surfaces are in agreement with those on the wear particles.

To better understand the wear mechanism responsible for the increased wear resistance of the specimens filled with quasicrystals, stereomicroscopy was performed using the SEM. This allowed for height differences to be measured between features on the wear surfaces. Figure 4.7 shows a region on the wear surface of a QC-filled specimen that contained a quasicrystal. The micrograph shows that the quasicrystal has a flattened surface that was in contact with the counterface during wear. The absence of wear marks on the quasicrystal indicates that this flattening is due more to deformation than material removal. This suggests the capability of the quasicrystals to deform plastically under loading. However, there are no mechanical property data available for Pt-Zr quasicrystals. The ability of the quasicrystal to undergo this deformation indicates that the filler particles deformed and supported a significant portion of the normal load applied to the pin during sliding. Therefore, the surrounding UHMWPE matrix was subjected to lower shear stresses during the wear process.

This is illustrated in Figure 4.8 which shows in (a) that the UHMWPE surface with a quasicrystal filler particle in it is ready to contact the counterface. Note that initially the undeformed filler particle protrudes from the surface of the polymer. As the pin is loaded on the counterface, the filler particle deforms plastically, thus supporting a substantial amount of the normal load. Therefore, the polymer supports less normal load than it would in the absence of filler, and thus less shear stress during sliding if a direct relationship between normal load and shear stress is assumed. The reduced shear stress would result in lower wear. Upon removal of the normal load on the pin, both the filler and the polymer undergo elastic recovery. However, because the polymer is less stiff than the filler, it undergoes a greater amount of recovery. The result is a difference in heights between the flattened quasicrystal surface and the surrounding polymer, shown as Δa in the figure. Confirmation of such a height difference would help to confirm the hypothesis of the filler particles shielding the surrounding polymer from high shear loading. Stereomicroscopy measurements on the wear surfaces of the quasicrystal-filled specimens showed that the flattened surfaces of the quasicrystals had a mean height difference of 1.52 μm from the surrounding UHMWPE surface. This evidence of elastic recovery of the filler and polymer surfaces suggests that the wear mechanism hypothesis of load shielding as proposed is valid.

These wear results show that Pt-Zr quasicrystals compare very favorably to crosslinking in regards to increasing the wear resistance of UHMWPE. Furthermore, when their beneficial effects on storage modulus and their relatively modest reduction in impact toughness are taken into account with the wear data, there appears to be great potential in the use of Pt-Zr quasicrystals as fillers in UHMWPE for use in biomedical applications.

4.5 Conclusions

The following conclusions have been made based on the results of this work:

1. With the addition of 20 wt.% Pt-Zr quasicrystal fillers, the storage modulus of UHMWPE increased over a range of frequencies from 0.5 to 5.0 Hz. On the other hand, electron-beam irradiation crosslinking followed by thermal stabilization significantly reduced the storage modulus of UHMWPE.
2. Impact toughness of UHMWPE decreased with the use of fillers as well as crosslinking, however the decrease with fillers was less than that found with crosslinking.
3. Pt-Zr quasicrystal fillers increased the wear resistance of UHMWPE in multi-directional sliding by an amount statistically similar to that by irradiation crosslinking the polymer.
4. The mechanism of wear with a 6.4-mm by 6.4-mm square path involved stretching and polymer chain orientation resulting in the formation of ridges of raised and frayed polymer. The ridges were aligned perpendicular to the axial direction of the cylindrical counterface.
5. Crosslinking reduced the wear of UHMWPE by hindering polymer chain orientation during the sliding process.
6. Pt-Zr quasicrystal filler particles underwent plastic deformation under load and thus supported a significant amount of the contact stresses during sliding. This behavior reduced the effective shear stress on the surrounding polymer and thus led to the reduction in wear.

7. The wear particles retrieved from the non-crosslinked UHMWPE specimens showed evidence of extensive stretching before removal from the bulk. However, wear debris from the crosslinked pins showed much less stretching.
8. QC-filled UHMWPE has a great potential for use as an articulating component of artificial joints because of its combined attributes of high wear resistance and high elastic modulus.

4.6 References

1. C.J. DeFrances, M.J. Hall, 2002 National Hospital Discharge Survey. Adv Data, 2004(342): p. 1-29.
2. E.D. Rentfrow, S.P. James, G.P. Beauregard, K.R. Lee, J.R. McLaughlin, Comparison of the in vivo wear rates of 43 surgically retrieved direct compression molded and ram extruded ultra high molecular weight polyethylene acetabular components. Biomed Sci Instrum, 1996. 32: p. 135-141.
3. D. Sacomen, R.L. Smith, Y. Song, V. Fornasier, S.B. Goodman, Effects of polyethylene particles on tissue surrounding knee arthroplasties in rabbits. J Biomed Mater Res, 1998. 43(2): p. 123-130.
4. M. Turell, A. Wang, A. Bellare, Quantification of the effect of cross-path motion on the wear rate of ultra-high molecular weight polyethylene. Wear, 2003. 255(2): p. 1034-1039.
5. O.K. Muratoglu, C.R. Bragdon, D.O. O'Connor, M. Jasty, W.H. Harris, R. Gul, F. McGarry, Unified wear model for highly crosslinked ultra-high molecular weight polyethylenes (UHMWPE). Biomaterials, 1999. 20(16): p. 1463-1470.

6. S.J. Gencur, C.M. Rimnac, S.M. Kurtz, Failure micromechanisms during uniaxial tensile fracture of conventional and highly crosslinked ultra-high molecular weight polyethylenes used in total joint replacements. Biomaterials, 2003. 24(22): p. 3947-3954.

7. E. Oral, K.K. Wannomae, N. Hawkins, W.H. Harris, O.K. Muratoglu, Alpha-tocopherol-doped irradiated UHMWPE for high fatigue resistance and low wear. Biomaterials, 2004. 25(24): p. 5515-5522.

8. H. Sakoda, J. Fisher, S. Lu, F. Buchanan, The effect of accelerated aging on the wear of UHMWPE. J Mater Sci Mater Med, 2001. 12(10-12): p. 1043-1047.

9. C.J. Schwartz, S. Bahadur, The role of filler deformability, filler-polymer bonding, and counterface material on the tribological behavior of polyphenylene sulfide (PPS). Wear, 2001. 250: p. 1532-1540.

10. Q. Zhao, S. Bahadur, A study of the modification of the friction and wear behavior of polyphenylene sulfide by particulate Ag2S and PbTe fillers. Wear, 1998. 217(1): p. 62-72.

11. M. Palabiyik, S. Bahadur, Tribological studies of polyamide 6 and high-density polyethylene blends filled with PTFE and copper oxide and reinforced with short glass fibers. Wear, 2002. 253(3-4): p. 369-376.

12. J. Saida, M. Matsushita, A. Inoue, Nano icosahedral quasicrystals in Zr-based glassy alloys. Intermetallics, 2002. 10(11-12): p. 1089-1098.

13. X.Y. Yang, E.A. Rozhkova, D.J. Sordelet, Quasicrystal formation in gas-atomized Zr80Pt20 powders. Philos Mag, 2006. 86(3-5): p. 309-315.

14. X.Y. Zhou, P.Y. Li, J.M. Luo, S.Q. Qian, J.H. Tong, Sliding friction of Al-Cu-Fe-B quasicrystals. J Mater Sci Technol, 2004. 20(6): p. 709-713.

15. P.D. Bloom, K.G. Baikerikar, J.W. Anderegg, V.V. Sheares, Fabrication and wear resistance of Al-Cu-Fe quasicrystal-epoxy composite materials. Mat Sci Eng a-Struct, 2003. 360(1-2): p. 46-57.

16. B.C. Anderson, P.D. Bloom, K.G. Baikerikar, V.V. Sheares, S.K. Mallapragada, Al-Cu-Fe quasicrystal/ultra-high molecular weight polyethylene composites as biomaterials for acetabular cup prosthetics. Biomaterials, 2002. 23(8): p. 1761-1768.

17. G. Lewis, Properties of crosslinked ultra-high-molecular-weight polyethylene. Biomaterials, 2001. 22(4): p. 371-401.

18. C.J. Schwartz, S. Bahadur, Development and testing of a novel joint wear simulator and investigation of the viability of an elastomeric polyurethane for total-joint arthroplasty devices. Submitted to Wear, 2005.

19. S.A. Biggs, C.R. Bragdon, K. Garas, O.K. Muratoglu, P.J. Caruso, W.H. Harris. Qualitative analysis of polyethylene particles extracted from bovine serum used in a hip simulator. in 11th Conference of the European Society of Biomechanics. 1998. Toulouse, France.

20. G. Lewis, C. Rogers, H.H. Trieu, Dynamic thermomechanical properties and crystallinity of ultrahigh molecular weight polyethylene tibial inserts. J Biomed Mater Res, 1998. 43(3): p. 249-260.

21. D.A. Baker, A. Bellare, L. Pruitt, The effects of degree of crosslinking on the fatigue crack initiation and propagation resistance of orthopedic-grade polyethylene. J Biomed Mater Res A, 2003. 66(1): p. 146-154.

22. S. Ahmed, F.R. Jones, A Review of Particulate Reinforcement Theories for Polymer Composites. J Mater Sci, 1990. 25(12): p. 4933-4942.

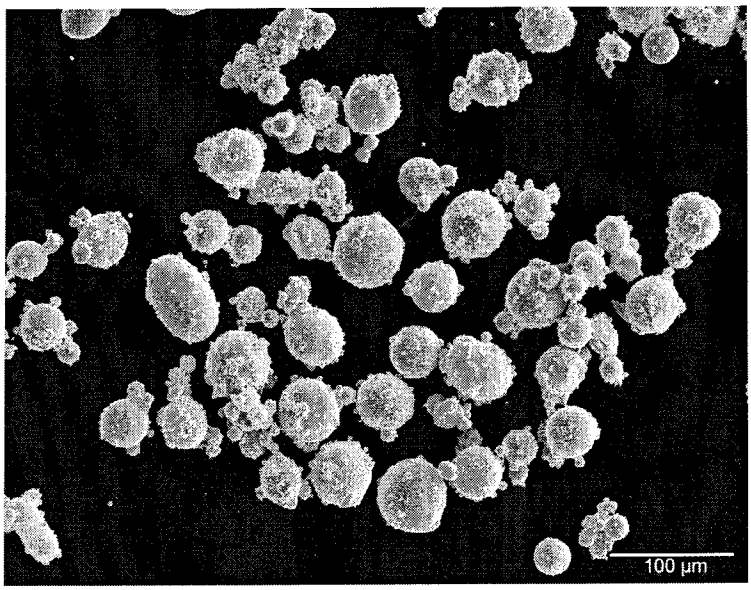

Figure 4.1 SEM image of Pt-Zr quasicrystals used as fillers in UHMWPE.

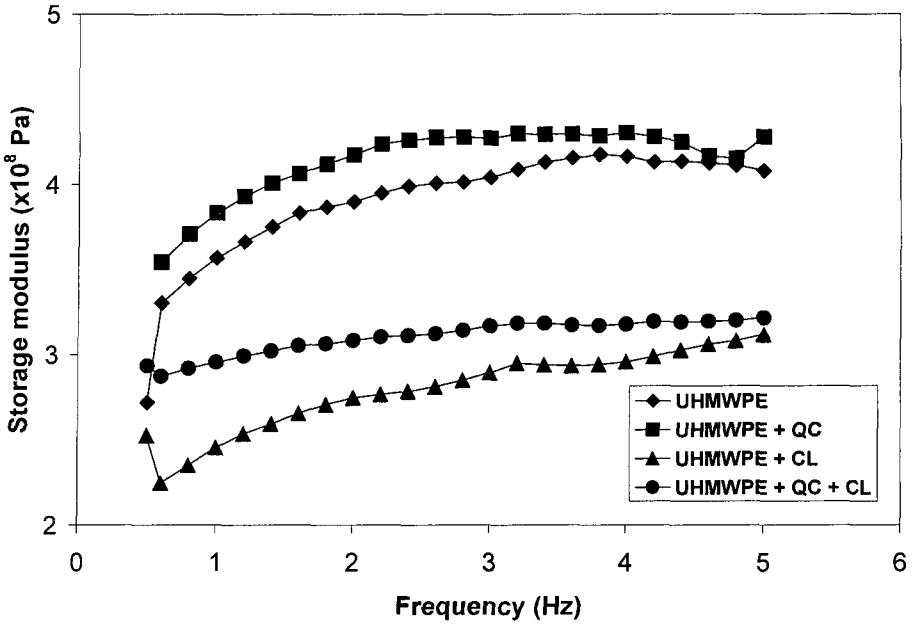

(a)

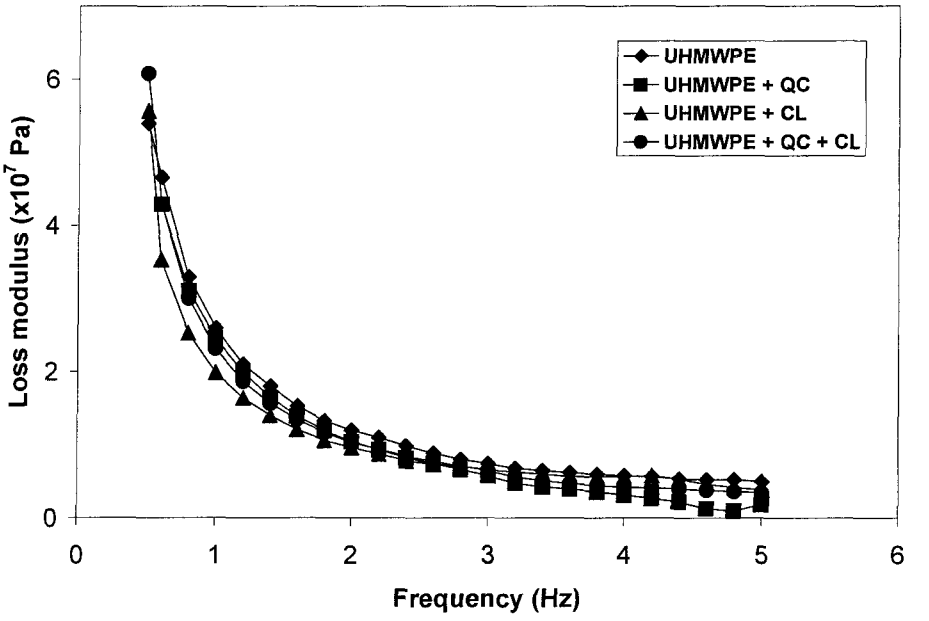

(b)

Figure 4.2 Variation of storage and loss modulus as a function of frequency for the four treatment groups. QC = filled with quasicrystals, CL = crosslinked

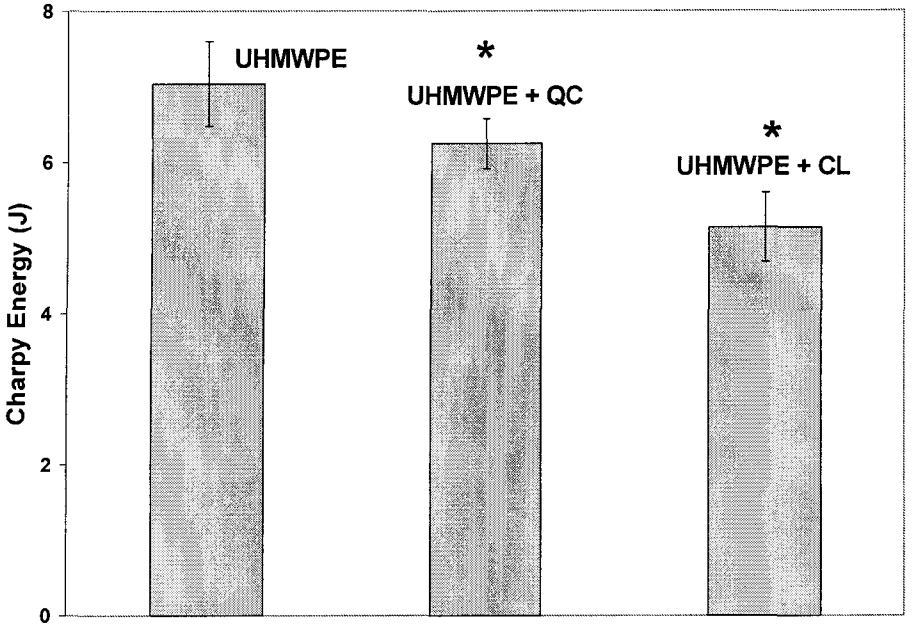

Figure 4.3 Charpy impact energy results for unmodified, QC-filled, and crosslinked UHMWPE. Bars represent one standard deviation on either side of the mean. An * denotes a statistically significant difference from unmodified UHMWPE.

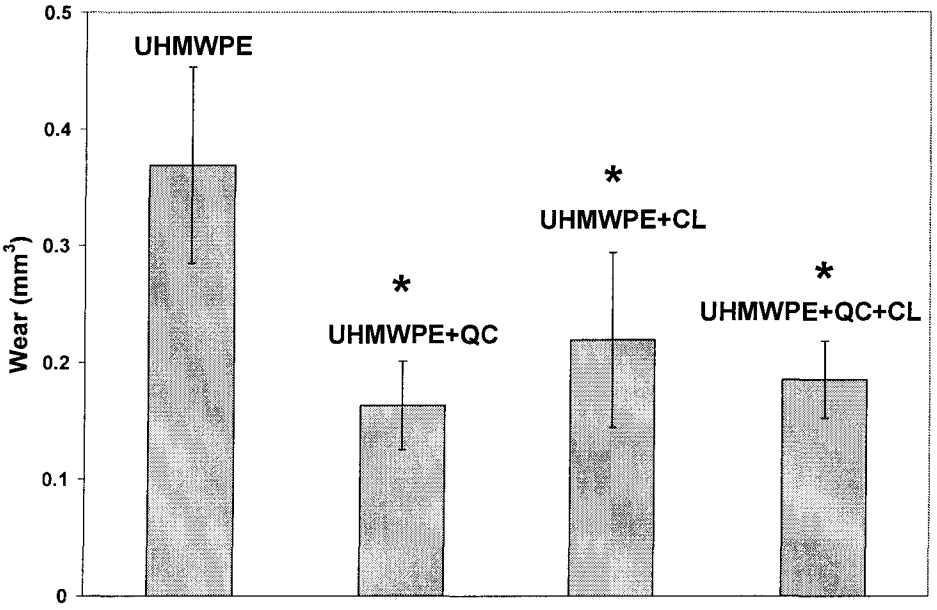

Figure 4.4 Comparison of the volumetric wear of UMHWPE modified by QC fillers, crosslinking, or both, as obtained from 250,000 cycle tests in the DAWS. Error bars represent one standard deviation on either side of the mean.

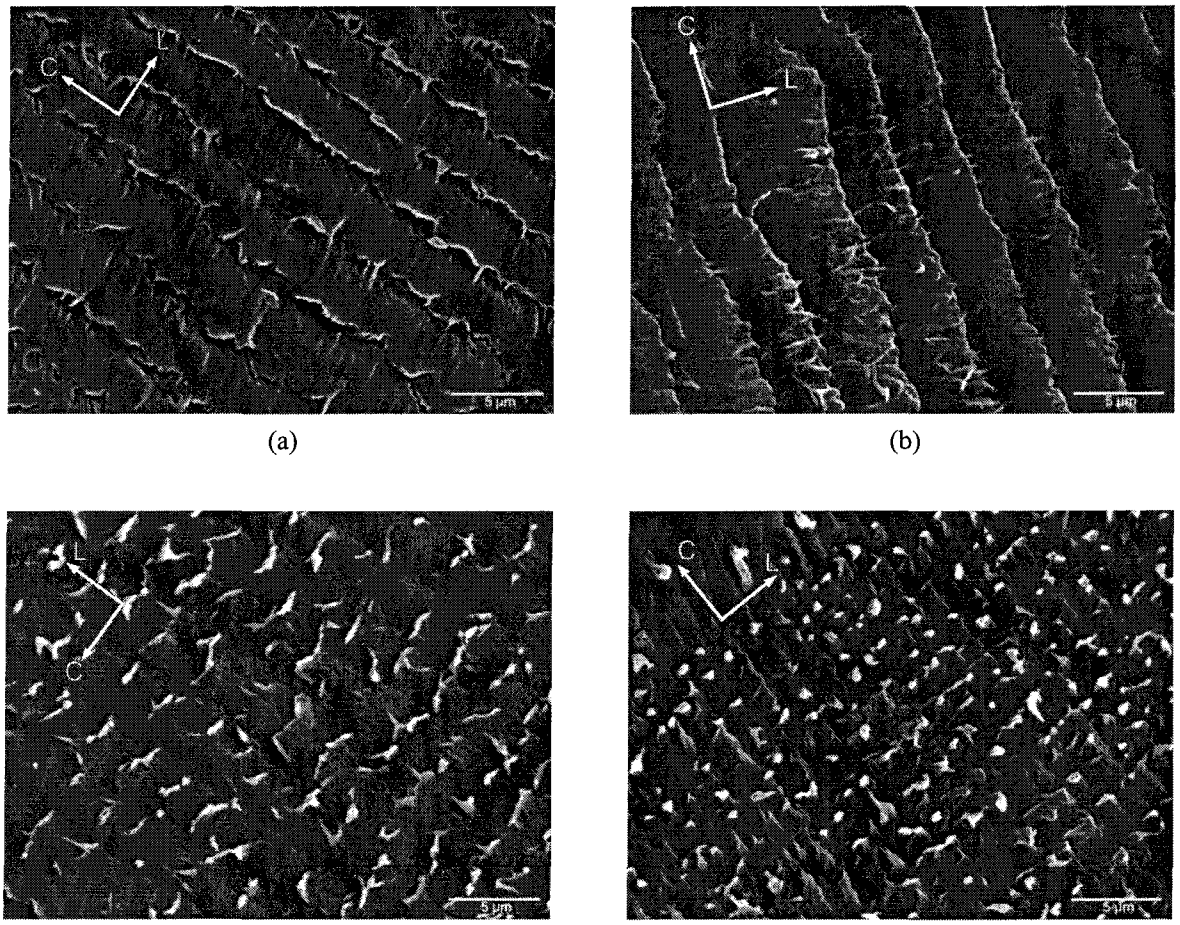

Figure 4.5 SEM micrographs of wear surfaces of: (a) UHMWPE; (b) UHMWPE+QC; (c) UHMWPE+CL; (d) UHMWPE+QC+CL. In the images, "L" indicates sliding direction parallel to the counterface shaft axis, while "C" indicates the perpendicular direction.

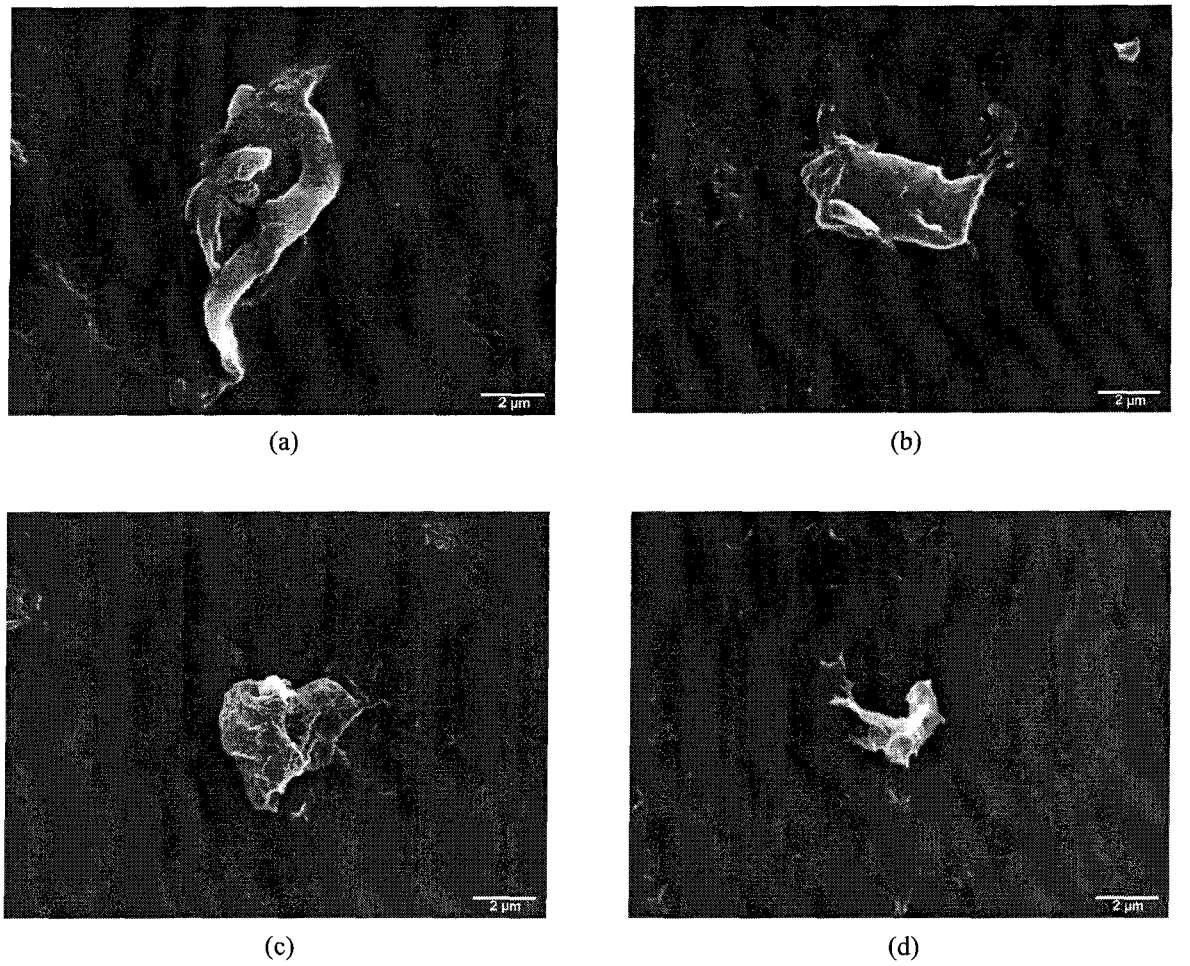

(a) (b)

(c) (d)

Figure 4.6 SEM micrographs of wear particles of: (a) UHMWPE; (b) UHMWPE+QC; (c) UHMWPE+CL; (d) UHMWPE+QC+CL.

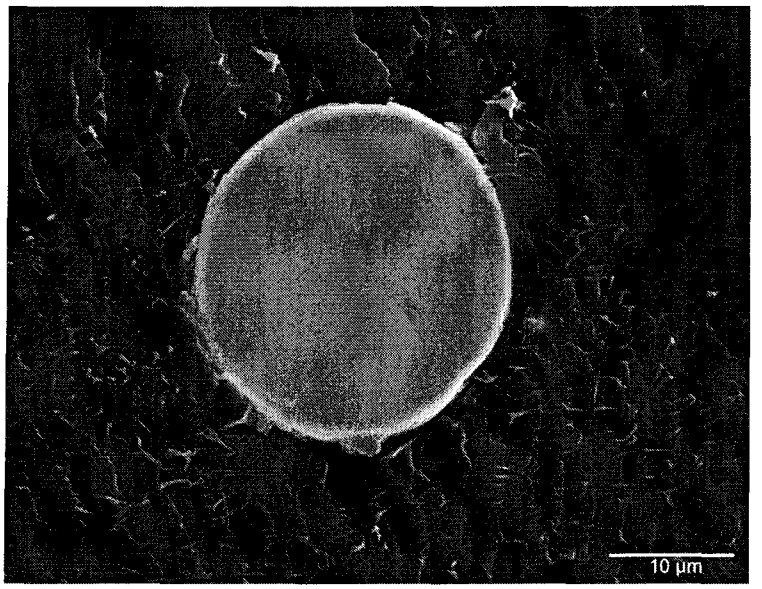

Figure 4.7 Micrograph of a Pt-Zr quasicrystal embedded in the worn surface of a QC-filled UHMWPE specimen. Stereomicroscopy was used to measure the difference in heights between the QC surface and the surrounding UHMWPE.

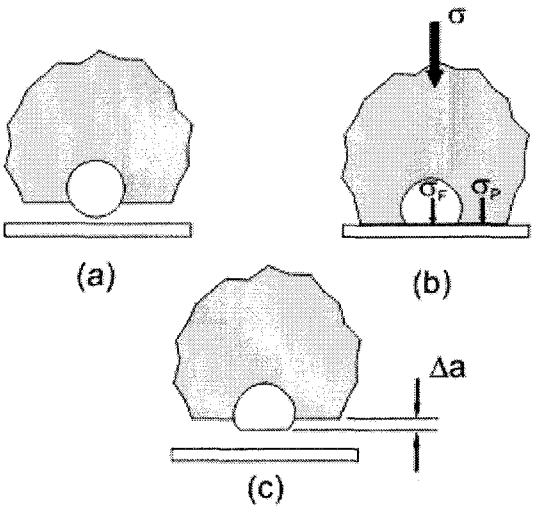

Figure 4.8 Illustration of the QC-filled UHMWPE surface in (a) before contact, (b) during loaded contact, and (c) after separation from the counterface. The sharing of load is shown in (b) where the normal stress $\sigma = \sigma_F + \sigma_P$. σ_F and σ_P are the stresses experienced by the filler and polymer, respectively.

CHAPTER 5
EFFECT OF MILD CROSSLINKING OF UHMWPE WITHOUT STABILIZATION ON DYNAMIC MECHANICAL PROPERTIES AND WEAR RESISTANCE

A paper to be submitted to *Biomaterials*

Christian J. Schwartz and Shyam Bahadur

5.1 Abstract

In order to produce UHMWPE with increased wear resistance for artificial joints, yet avoid degradation in stiffness and oxidation resistance, irradiation crosslinking of the polymer at doses lower than commonly used is proposed. Mild crosslinking eliminates the need for subsequent stabilization of free radicals. In this study, four groups of UHMWPE were investigated: a) compression-molded, non-crosslinked, b) crosslinked with 50 kGy electron-beam irradiation, thermally stabilized, c) crosslinked, non-stabilized, and d) crosslinked, non-stabilized, and exposed to accelerated oxidation to simulate years of storage or *in vivo* exposure. Dynamic mechanical analysis showed that crosslinking and subsequent thermal stabilization significantly reduced the elastic modulus of UHMWPE, while omission of the stabilization step yielded a more moderate reduction in elastic modulus. Differential scanning calorimetry and swell ratio measurements were used to investigate the reduction in storage modulus. Accelerated aging of UHMWPE was not found to decrease the storage modulus over that of non-stabilized, non-aged polymer. Fourier Transform Infrared spectroscopy showed that aging of non-stabilized UHMWPE increased the oxidation of the polymer, but much less than with higher amounts of crosslinking. Finally, the wear amounts resulting from the different treatments were compared by wear testing in the Dual-Axis Wear

Simulator (DAWS), a machine that subjects pin specimens to multidirectional sliding while immersed in a simulated joint fluid. Crosslinking of UHMWPE showed a significant increase in wear resistance. Aging of the non-stabilized polymer showed no adverse effects on wear. These results suggest that there may be great potential for the use of mild crosslinking in the treatment of UHMWPE in artificial joints because it imparts high wear resistance without the need for thermal stabilization.

5.2 Introduction

Artificial joints are widely used for the treatment of pain and degraded joint function due to injury or arthritic damage. These incorporate an ultra-high molecular weight polyethylene (UHMWPE) component articulating against a polished metallic member. This polymer-on-metal system is used in the hip, knee, and other synovial joints and the design of these devices has been refined for decades. However, even with all of the years of development and experience with these implants, their pain-free lifetime is significantly limited because of the osteolytic loss of bone around the devices due to the response of the body to UHMWPE wear particulate [1]. One approach used in the past several years to increase the wear resistance of the polymer has been crosslinking by means of either gamma-ray or electron-beam irradiation. Crosslinked UHMWPE resists wear due to the inhibition of polymer chain orientation during the multidirectional wear process that has been reported to occur in implanted joints [2]. This approach has shown tremendous benefits in terms of increased wear resistance of the polymer, however, there are serious tradeoffs that must be considered when crosslinking is used.

While the reduction in UHMWPE wear is achieved through crosslinking, there is a substantial reduction in mechanical properties including ultimate strength, elastic modulus, ductility, and fatigue strength [3]. These effects are caused because of the reduction in crystallinity and energy absorption capability of the polymer upon crosslinking. In addition to this, the crosslinked polymer develops increased susceptibility to oxidative degradation and embrittlement [4]. This phenomenon occurs because of the generation of residual free radicals during crosslinking and the vulnerability of these radicals to oxidation *in vivo*. In order to stave off this oxidative attack, the crosslinked polymer is typically exposed to temperatures at or near the melting point for a number of hours [5]. This procedure allows free radicals the mobility to recombine thus avoiding oxidative damage and thus stabilize the polymer. There are two main drawbacks to thermal stabilization, however. The first is that this thermal treatment removes the benefits of the polymer processing history due to the annealing effect and, as such, eliminates the possibility for using processing techniques to offset the property degradation encountered during crosslinking. The second drawback is that even with thermal stabilization UHMWPE components show signs of oxidative degradation and embrittlement after a number of years in storage [4]. Thus, it would be advantageous for the implant designer to identify a method that would allow for the increase in wear resistance through crosslinking while limiting oxidation of the crosslinked polymer over time, and having the potential of property improvement by processing.

It has been reported that the wear resistance of UHMWPE increases drastically with mild crosslinking and approaches an asymptotic maximum due to diffusion constraints of the polymer at higher radiation doses [6]. This suggests that mild crosslinking may be sufficient to achieve significant wear resistance. Furthermore, the use of lower doses to produce

limited crosslinking would likely produce fewer residual free radicals in the crosslinked polymer. With this lower potential for oxidative attack, the stabilization step might be shortened or eliminated entirely. This would allow for retention in the improvement of mechanical properties of UHMWPE by favorable processing technique such as the use of higher pressures to increase crystallinity [7].

There are some points that need to be considered if the thermal stabilization step is not used. One of these is whether a mildly crosslinked and non-stabilized UHMWPE component would have the requisite stiffness for an artificial joint along with sufficient damping to accommodate both static and dynamic loads. This involves understanding how crystallinity of the polymer is affected by crosslinking and the post-irradiation stabilization step. Another point is the extent of oxidation experienced by the crosslinked UHMWPE without stabilization. In terms of the acceptability of this approach, the requirements are enhanced wear resistance with negligible oxidation, as determined by simulative testing.

In this paper, the authors have investigated the viability of using a radiation dosage at the lower end of the dosage ranges reported in the literature [3, 8]. As mild crosslinking would result in lower risk of oxidation of the polymer, the possibility of eliminating the thermal stabilization step and its effect on various aspects of the performance of crosslinked UHMWPE in artificial joints is examined.

5.3 Materials and Methods

UHMWPE powder (Sigma-Aldirch, St. Louis, Missouri) was compression molded at a temperature of 200°C with an applied pressure of 250 MPa in a custom-made mold. This produced pins with a diameter of 6.4 mm and a length of 9.5 mm. Four groups of pins, with

four to six pins in each group, were produced based on treatments subsequent to compression molding. One group of UHMWPE pins was stored immediately after molding in a dark place to serve as non-crosslinked control specimens for this investigation. The three remaining groups of pins were sealed in vacuum packaging and electron-beam irradiated with a dose of 50 kGy in a linear accelerator facility in order to crosslink them. Immediately after irradiation, one of the groups was placed in an air-circulating oven at 120°C for 10 hours to thermally stabilize any residual free radicals present in the crosslinked pins. Of the two remaining groups of pins, one group was placed in a dark area for storage until use, and the other group was exposed to accelerated aging in a sealed chamber under an atmosphere of 506 kPa of pure oxygen for 8 days at a temperature of 80°C. This aging regimen was chosen based on what has been reported in the literature to simulate 3 to 5 years of shelf aging [9].

A sledge microtome was used to slice 240-μm thick sections from pins from each of the four groups. The slices were used to obtain thin beams with a width of 5 mm and a length of 9.5 mm. These were tested in a dynamic mechanical analyzer (DMA, Perkin Elmer 7e) with a three-point bend fixture having a span between support points of 5 mm. They were subjected to a sinusoidal load with a mean load of 110 mN and an alternating load of 100 mN and the storage and loss moduli were recorded as a function of frequency in the range of 0.5 to 5.0 Hz. The mean of the property values from three samples pertaining to each treatment group is shown in the plots.

The crosslink density of the control and crosslinked specimen groups was calculated by using the swell ratio of the polymers in a solvent [10]. Pins from each group were weighed on an analytical balance and placed in a closed jar with 50 mL xylenes (Fisher Scientific,

Fair Lawn, New Jersey). The jars were placed in an agitated oil bath at a temperature of 110°C for 24 hours in order to extract any non-crosslinked UHMWPE from the pins. The swollen pins were removed from the jars, gently blown with air, and placed in weighing bottles that had been previously weighed for tare purposes. The bottles containing the swollen pins were sealed and weighed on the analytical balance, and the mass of the swollen pins was calculated. This value included the total mass of crosslinked polymer left in the sample in addition to the mass of the absorbed solvent. Each weighing bottle was opened and placed in a vacuum oven at 100°C for 16 hours, until repeated weighing showed that all of the solvent had evaporated. The dried pins were removed from the bottles and weighed again to determine the amount of solvent that had been removed, and thus the mass of crosslinked polymer left in the sample. These values were used in accordance with the ASTM standard to calculate swell ratio and crosslink density.

To determine the crystallinity of the control and crosslinked samples, differential scanning calorimetry (DSC) was employed. The 240-μm thick slices of pins were cut into small pieces and sealed in appropriate sample cups for analysis. The calorimetric scan between the temperatures of 25 and 200°C was performed at a rate of 10°C per minute. The area under the endothermic melting peak from 60 to 155°C [6] was measured and divided by the latent heat of fusion of 100% crystalline UHMWPE to determine the crystalline percentage in the polymer. At least three separate samples from each of the treatment groups were used to calculate the mean value of crystallinity.

In order to determine the extent of oxidation in the non-stabilized pins between the aged and non-aged groups, Fourier Transform Infrared Spectroscopy (FTIR) was used in conjunction with a microscopy stage. A sledge microtome was used to cut 120-μm thick

disks with a diameter of 6.4 mm from each pin being analyzed. The disks were placed in the microscope and FTIR was performed at increasing depths from the circumferential surface of the disks. The index of oxidation was defined as the ratio of area under the carbonyl peak (1730 to 1760 cm^{-1}) to that of the methyl group stretching peak (near 1320 to 1380 cm^{-1}) from the IR fingerprint scan of the samples. Carbonyl groups are indicative of oxidation of the polymer, while methyl groups are used as a reference standard to normalize the FTIR data for UHMWPE [11]. In this way, oxidation index versus depth in the sample could be plotted to determine the extent and location of oxidation.

Wear tests were performed on the four groups of pins in the Dual Axis Wear Simulator (DAWS), a joint-wear simulating machine whose specific details are described elsewhere [12]. The 316L stainless steel cylindrical counterface of the DAWS was finished to a surface roughness of 0.10 μm Ra in the axial direction. The wear machine was programmed to expose the wear pins to a 6.4-mm by 6.4-mm square wear path under a load of 39 N. This produced a nominal contact pressure of approximately 3.1 MPa. Before testing the pins were cleaned and weighed to a precision of 10^{-5} g. The pins were then subjected to 250,000 wear cycles while immersed in a bovine serum solution at 37°C, traversing the square wear path (total distance 25.6 mm) every 1.22 seconds. Two stations on the DAWS subjected pins to loading but not sliding, in order to determine the amount of fluid uptake during the test. After the completion of wear tests, the pins were again cleaned, dried, and weighed to determine the loss of mass due to wear. This value was corrected based on the fluid uptake of the control pins, and the density of the pin material was used to calculate volumetric wear. Following wear testing, the worn surfaces of representative pins was removed and coated

with gold for examination with scanning electron microscopy (SEM) to determine the wear mechanisms.

5.4 Results and Discussion

5.4.1 Viscoelastic properties and morphological characteristics

The DMA results showing storage and loss moduli are presented in Figure 5.1. Because of the stringent mechanical requirements on an artificial joint, both the elastic stiffness and damping capability of candidate materials are of vital importance. During standing, the articulating surface of an artificial hip or knee must be stiff enough to support the static load without excessive deformation, however during stair climbing the material must be able to damp the effects of impact loading. The plots of storage moduli clearly show that the as-molded UHMWPE has the highest elastic stiffness. When the polymer is crosslinked, the storage modulus is reduced. The greatest reduction in modulus results from crosslinking followed by the thermal stabilization. In this case, a reduction of over 40% over that of as-molded UHMWPE is observed. Both the aged and non-aged, non-stabilized UHMWPE showed a reduction in storage modulus of less than 30% over the frequencies observed. When the loss moduli results are examined, it is clear that crosslinking, with or without thermal treatment, has little effect. All of the treatment groups have similar loss moduli over the range of frequencies, and thus show that this mild amount of crosslinking and subsequent stabilization or aging does not alter the damping capability of UHMWPE.

The DMA results are understood when morphological information is considered. Table 5.1 reports the crystallinity and crosslink density values obtained by measurement. A direct correlation between storage modulus and % crystallinity is observed. Higher values of

storage modulus follow higher percent crystallinity. During compression molding, the polymer chains have the mobility to crystallize to a high degree. This resulted in a crystallinity of 57.4% for the as-molded polymer, and a crosslink density that was too low to be measured accurately. The crosslinked polymers all showed lower crystallinity than the as-molded UHMWPE. This can be explained by the mechanisms of crosslinking and stabilization. Electron-beam irradiation exposed the polymer to a dose of high-energy particles that caused chain scission and the generation of free radicals. Most of these free radicals recombined and formed the crosslinked network. However, the crosslinks themselves served as obstacles to formation of crystalline order and thus the polymer emerged from irradiation with lower crystallinity than it previously had. In the case of these polymers, the % crystallinity after crosslinking was 48.4%. After the irradiation process, there were residual free radicals resulting from broken polymer chains that had not recombined. There were two possible fates for these radicals. Either they could eventually combine with neighboring radicals to further increase the crosslink density, or they could react with molecular oxygen and start a propagating oxidation reaction. During thermal stabilization at 120°C, the radicals had sufficient mobility to recombine and thus further the crosslinking process. This is shown by an increased crosslink density over the non-stabilized polymer, and a corresponding reduction in crystallinity (45.2%). On the other hand, the radicals in the UHMWPE that had been aged at 80°C in oxygen did not possess the mobility to further crosslink. This is evidenced by the fact that there was not a significant increase in crosslink density, nor a decrease in crystallinity (48.4%).

5.4.2 Oxidation of non-stabilized pins

Oxidation in UHMWPE has been shown to produce embrittlement of the polymer and higher wear rates [8]. After crosslinking, the residual free radicals in the polymer act as initiation sites for a self-propagating oxidation process. For use in a biomedical application, it is necessary to ensure that the polymer does not become susceptible to oxidative attack with crosslinking and stabilization. Figure 5.2 shows the FTIR spectrum for crosslinked UHMWPE in the non-stabilized and aged condition. The carbonyl and methyl peaks are indicated. Carbonyl groups in the polymer result from bonding of oxygen with carbon atoms in the chain backbone, and show infrared absorbance near 1740 cm^{-1}. Calculation of the area under this peak has been shown to be a good indicator for the extent of oxidation of UHMWPE. Due to the difficulty in producing FTIR scans with repeatable intensities, a reference peak must be used for normalization of different data sets. For this purpose, the vibration of the methyl groups at the end of the polymer chains was used, which has an absorbance peak near 1370 cm^{-1}. From the FTIR spectra, the area under these peaks was determined and the ratio of the carbonyl peak area to the methyl peak area gave the oxidation index. This procedure was used for all of the UHMWPE groups investigated.

Figure 5.3 is the plot of oxidation index for the non-aged and aged UHMWPE up to a radial depth of 2000 μm starting from the outside surface of the pin. It shows that the aged pins have a higher level of oxidation than the non-aged pins. This is to be expected considering the extreme aging conditions that the polymer had been subjected to. The maximum amount of oxidation was found on the outside surface of the pins, with indexes of 0.033 and 0.052 for the non-aged and aged samples, respectively. However, other investigators report oxidation indexes that are at least an order of magnitude greater than

those observed here. For instance, Oral *et al.* [8] have shown that stabilization with α-tocopherol doping leads to indexes greater than 0.4, while Kurtz *et al.* have reported values over 4.5 [11]. The difference in oxidation levels between these studies and the current investigation is primarily in the radiation dose used for crosslinking. In other words, mild crosslinking leads to very low levels of oxidative damage even after significant aging.

5.4.3 Wear results

Figure 5.4 shows the volumetric wear amounts for the four groups of UHMWPE pins. A Tukey's HSD test showed that the wear of the as-molded UHMWPE was statistically higher than that of the other three groups. Furthermore, there was no increase in wear observed in the non-stabilized pins after accelerated aging. This indicates that the slight difference in oxidation between the aged and non-aged samples did not affect the wear resistance adversely. Thus, skipping the stabilization step in the treatment of UHMWPE shows promise as a method of increasing the durability of UHMWPE, while minimizing the effects of oxidation in storage or *in vivo*.

An examination of the SEM micrographs of the worn pin surfaces in Figure 5.5 sheds light on the mechanism involved in these wear processes. In all cases, striated surfaces with a characteristic spacing are seen. In addition, it is seen that the greatest amount of surface damage occurred with the pin sliding in the direction parallel to the counterface cylinder axis. These features indicate that UHMWPE asperities were stretched along the direction of the motion vector during sliding. As the wear path changed direction, the stretching direction continually changed leading to an accumulation of deformation until the fracture strain of the polymer was reached. The presence of striations is the most distinctive feature of the worn surfaces, and thus their explanation may hold clues to the differences found among the wear

amounts of the groups of pins investigated. There are likely three underlying phenomena at work that caused these wear amounts and surface features.

The first factor to be considered is the mobility of polymer chains on the worn surface of the pins. Due to the shear loading that was encountered during the wear cycle, the chains were oriented in the direction of sliding, thereby strengthening the polymer in this direction but weakening the polymer in the transverse direction. The square wear path used in this investigation exposed the sliding pins to four changes of direction during each wear cycle, thus continually reorienting the polymer chains and rendering the surface in a weakened condition for the next step in the wear cycle.

A second factor that led to the surface features observed is the directionality of surface roughness of the counterface. To finish the counterface shaft to the desired surface roughness for wear tests, it was rotated about its axis during polishing. This likely led to a lower surface roughness in the circumferential direction versus the lateral direction. Therefore, the pins encountered a somewhat rougher surface as they moved in the lateral direction during the wear cycle.

The final factor that may have affected the character of the worn surfaces was the quality of lubrication during each stage of the wear cycle. The square wear path was accomplished by successive counterface rotation and lateral movement of the pins. During rotation of the counterface, lubricant fluid was likely drawn into the sliding interface and thus a favorable lubrication condition was possible. However during the lateral sliding stages of the wear cycle, lubrication was not that good because the counterface shaft was stationary. In this way, the pins experienced cycles of good and poor lubrication quality with every change in the direction of pin movement.

Examination of the figure shows some clear differences between the as-molded and crosslinked UHMWPE surfaces. The spacing between striations on the as-molded surface is approximately 5 μm, while in the crosslinked polymers it is nearer to 2 μm. The reason for this was the reduced deformation capability of the crosslinked polymer under loading. A significant loss in ductility of UHMWPE with crosslinking has been reported [3].

The treatment involving mild crosslinking with no stabilization, as opposed to higher crosslinking with thermal stabilization, appears to have considerable potential for use in artificial joints. This investigation has shown that this treatment results in smaller reduction of the storage modulus because of less reduction in crystallinity as compared to the use of thermal stabilization. Such mildly crosslinked specimens showed a very limited amount of oxidation even after aggressive aging. In view of these benefits along with the considerable increase in wear resistance, lightly crosslinked UHMWPE with no stabilization treatment has great potential for use in artificial joints.

5.5 Conclusions

The following conclusions have been made based on the results of this work:

1. Crosslinking by means of electron-beam irradiation with a dosage of 50 kGy reduced the elastic modulus of UHMWPE due to the reduction in crystallinity of the polymer. Thermal stabilization further reduced crystallinity and therefore degraded the stiffness of UHMWPE more than the non-stabilized samples.
2. Accelerated aging of non-stabilized, crosslinked UHMWPE in an oxidative atmosphere at elevated temperatures did not affect the elastic modulus.

3. Accelerated aging of non-stabilized, crosslinked UHMWPE led to a slight increase in oxidation index of the polymer over that of the non-aged samples. However, the levels of oxidation were far below those reported for UHMWPE that had been crosslinked to a greater extent.
4. The wear of non-stabilized, crosslinked UHMWPE was statistically identical to that of UHMWPE that had been crosslinked and thermally stabilized. Furthermore, accelerated aging of crosslinked, non-stabilized polymer showed no increase in wear amounts over crosslinked, non-aged UHMWPE.
5. The wear of as-molded and crosslinked UHMWPE was due to accumulated cyclic strain experienced during multidirectional sliding in the test machine.
6. Surface striations observed on the worn UHMWPE surfaces indicate the effects of polymer chain orientation, surface roughness orientation of the counterface, and depletion of lubricant during the wear cycle.
7. Crosslinking of UHMWPE reduces the deformation capability of the polymer and thus accounts for the distance between striations found on the wear surface.

5.6 References

1. D. Sacomen, R.L. Smith, Y. Song, V. Fornasier, S.B. Goodman, Effects of polyethylene particles on tissue surrounding knee arthroplasties in rabbits. J Biomed Mater Res, 1998. 43(2): p. 123-130.
2. M. Turell, A. Wang, A. Bellare, Quantification of the effect of cross-path motion on the wear rate of ultra-high molecular weight polyethylene. Wear, 2003. 255(2): p. 1034-1039.

3. G. Lewis, Properties of crosslinked ultra-high-molecular-weight polyethylene. Biomaterials, 2001. 22(4): p. 371-401.

4. S.-K. Young, T.-S. Keller, K.-W. Greer, Wear testing of UHMWPE tibial components: influence of oxidation. 2000.

5. R. Chiesa, M.C. Tanzi, S. Alfonsi, L. Paracchini, M. Moscatelli, A. Cigada, Enhanced wear performance of highly crosslinked UHMWPE for artificial joints. J Biomed Mater Res, 2000. 50(3): p. 381-387.

6. O.K. Muratoglu, C.R. Bragdon, D.O. O'Connor, M. Jasty, W.H. Harris, R. Gul, F. McGarry, Unified wear model for highly crosslinked ultra-high molecular weight polyethylenes (UHMWPE). Biomaterials, 1999. 20(16): p. 1463-1470.

7. N.C. Parasnis, K. Ramani, Analysis of the effect of pressure on compression moulding of UHMWPE. J Mater Sci Mater Med, 1998. 9(3): p. 165-172.

8. E. Oral, K.K. Wannomae, N. Hawkins, W.H. Harris, O.K. Muratoglu, Alpha-tocopherol-doped irradiated UHMWPE for high fatigue resistance and low wear. Biomaterials, 2004. 25(24): p. 5515-5522.

9. S. Lu, F.J. Buchanan, J.F. Orr, Analysis of variables influencing the accelerated ageing behaviour of ultra-high molecular weight polyethylene (UHMWPE). Polymer Testing, 2002. 21(6): p. 623-631.

10. ASTM D 2765-01, Standard Test Methods for Determination of Gel Content and Swell Ratio of Crosslinked Ethylene Plastics: ASTM International.

11. S.M. Kurtz, O.K. Muratoglu, R. Gsell, K. Greer, F.W. Shen, C. Cooper, F.J. Buchanan, S. Spiegelberg, S.S. Yau, A.A. Edidin, Interlaboratory validation of

oxidation-index measurement methods for UHMWPE after long-term shelf aging. J Biomed Mater Res, 2002. 63(1): p. 15-23.

12. C.J. Schwartz, S. Bahadur, Development and testing of a novel joint wear simulator and investigation of the viability of an elastomeric polyurethane for total-joint arthroplasty devices. Accepted for publication in Wear, 2006.

Table 5.1
Measured % crystallinity and crosslink density of the four UHMWPE treatment groups.

Material	% Crystallinity (mean ± SD)	Crosslink density (x 10^{-4} mol/dm^3)
UHMWPE, as molded	57.4 ± 0.4	Below measurement limits
Crosslinked, stabilized	45.2 ± 0.5	124.1
Crosslinked, non-stabilized	48.4 ± 0.5	120.0
Crosslinked, non-stabilized, aged	48.4 ± 0.4	121.8

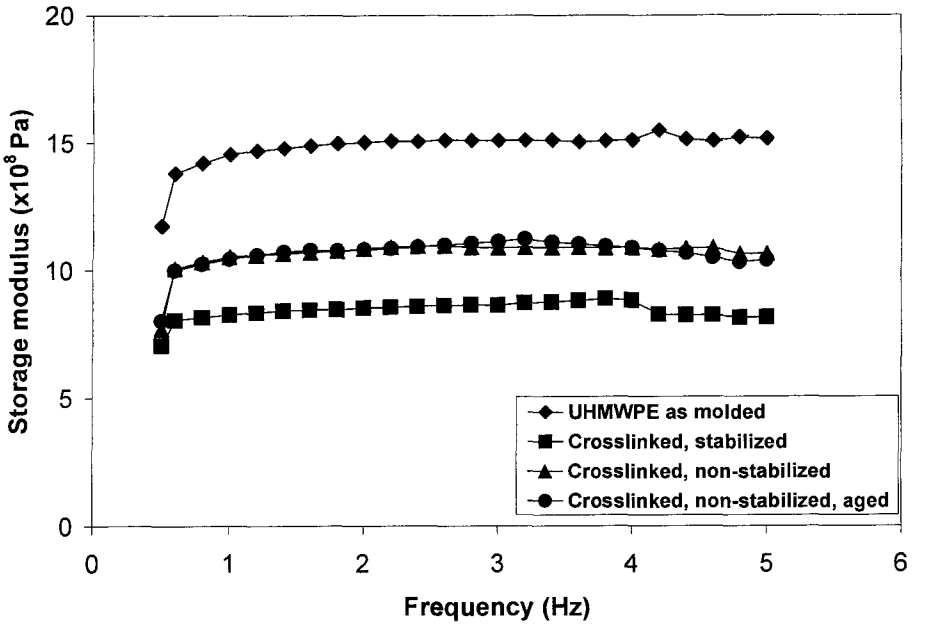

(a)

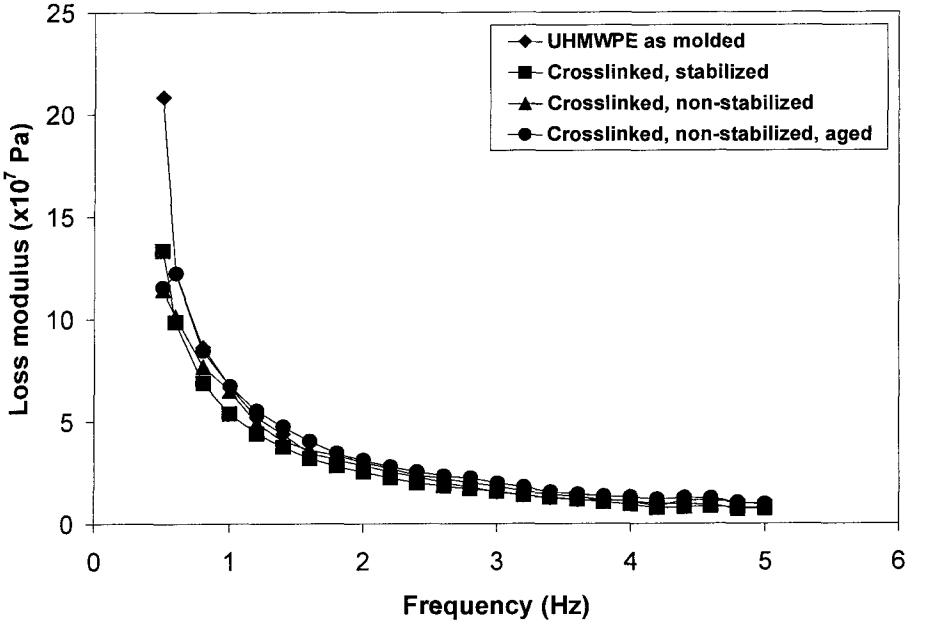

(b)

Figure 5.1 Variation of storage and loss moduli as a function of frequency.

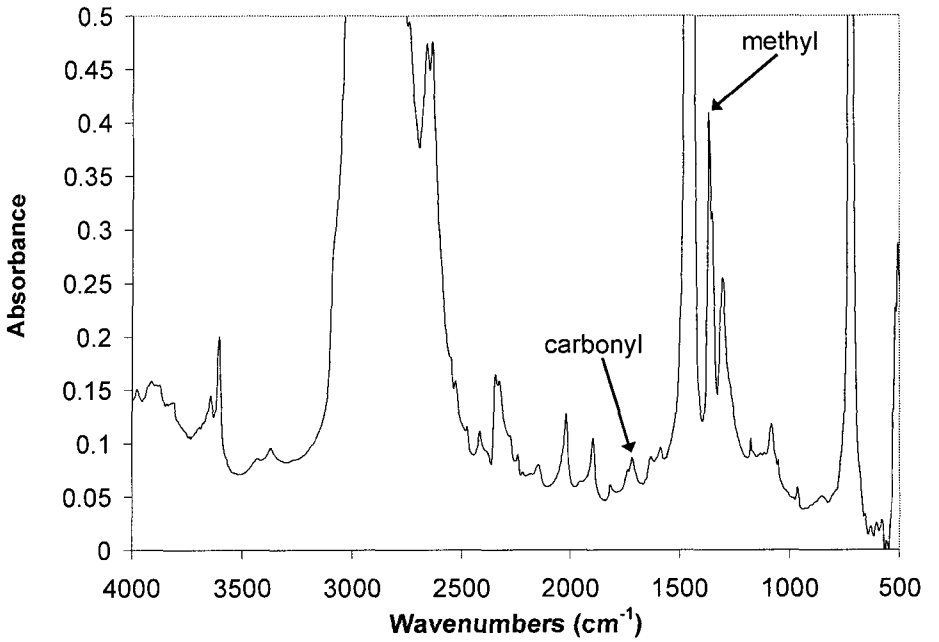

Figure 5.2 FTIR spectrum of UHMWPE pin in the crosslinked, non-stabilized, and aged condition. The arrows illustrate the carbonyl and methyl peaks used, respectively, to calculate the oxidation index.

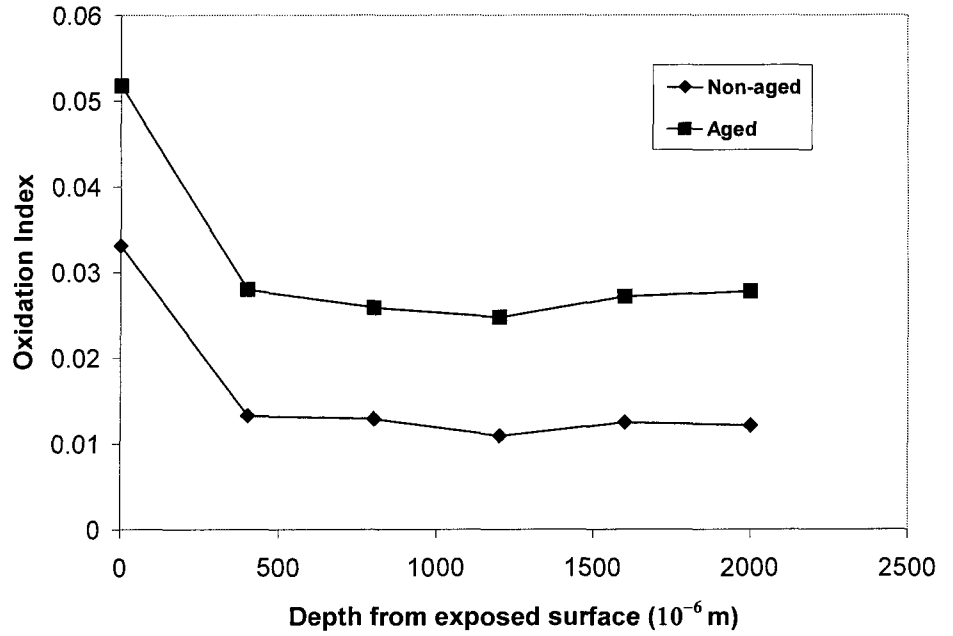

Figure 5.3 Comparison of oxidation index of non-stabilized UHMWPE in aged and non-aged conditions.

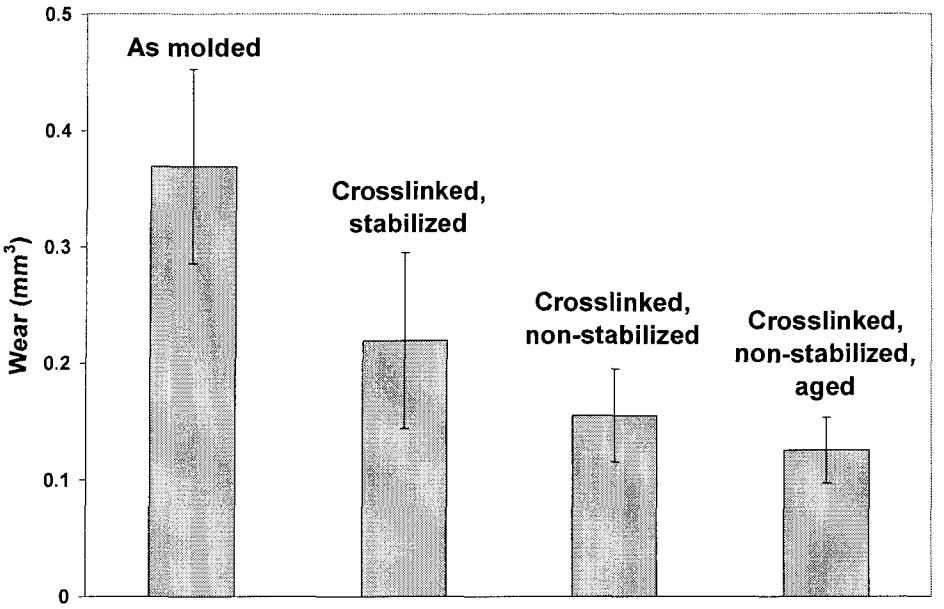

Figure 5.4 Volumetric wear loss of pins subjected to 250,000 cycles in the DAWS using a square wear path under 39 N loading. Bars are ± one standard deviation.

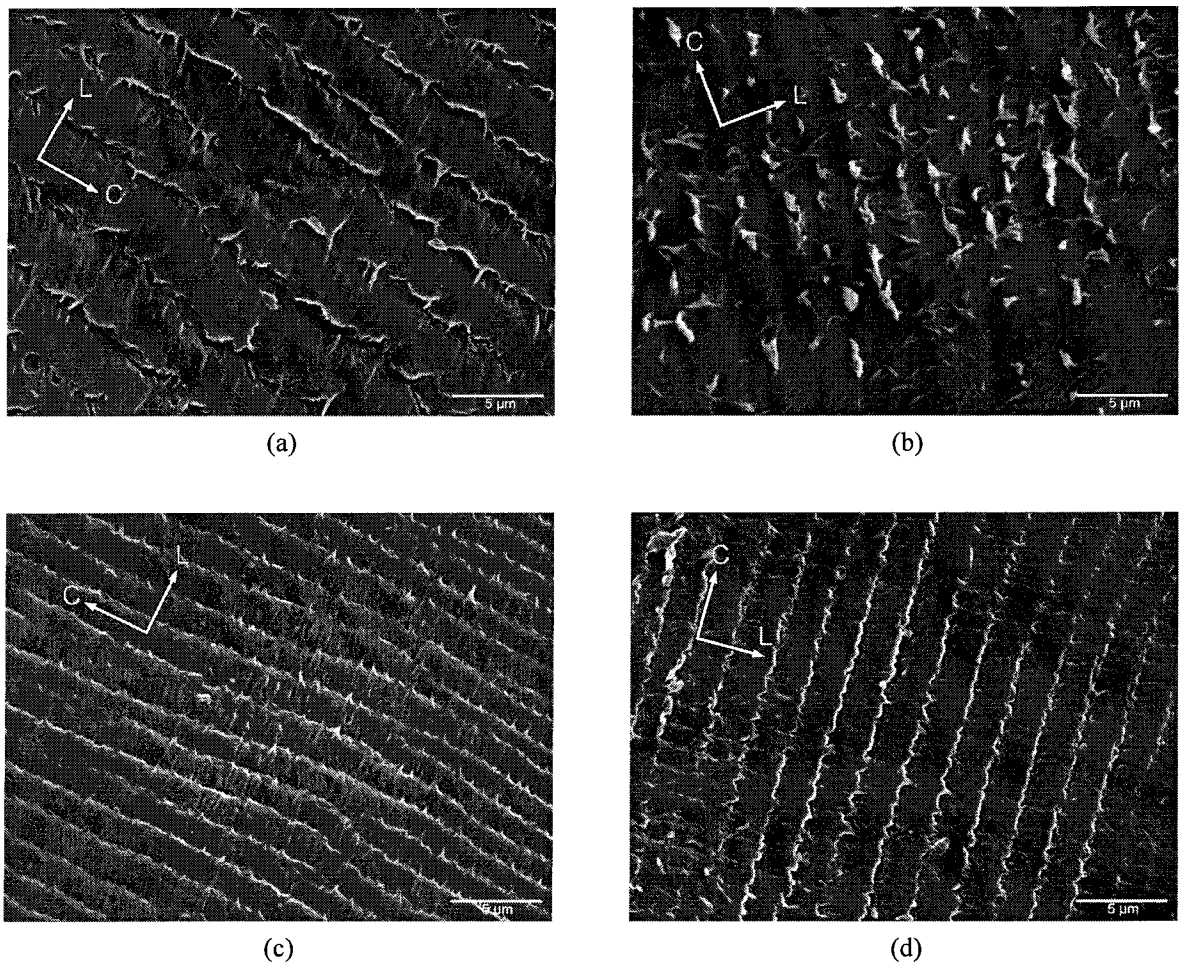

Figure 5.5 SEM micrographs of wear surfaces of UHMWPE in the following conditions: (a) As molded; (b) Crosslinked and thermally stabilized; (c) Crosslinked and non-stabilized; (d) Crosslinked, non-stabilzed, and aged. In the images, "L" indicates sliding direction parallel to the counterface shaft axis, while "C" indicates the perpendicular direction.

CHAPTER 6
INVESTIGATION OF THE MORPHOLOGY, VISCOELASTICITY, AND WEAR RESISTANCE OF POLYURETHANE-UHMWPE BLENDS FOR POTENTIAL USE IN ARTIFICIAL JOINTS

A paper to be submitted to *Wear*

Christian J. Schwartz and Shyam Bahadur

6.1 Abstract

As an alternative to ultra-high molecular weight polyethylene (UHMWPE), polyurethane (PUR) elastomer blends have been investigated for use as an articulating surface in artificial joints. While PUR has shown very low wear rates, the possibility of lowering wear amounts further by blending PUR with surface-activated UHMWPE particles is studied in this paper. For this purpose, PUR-UHMWPE blends were produced with 10 and 20% UHMWPE particles, by weight, in two different size ranges. Morphological examination of the blends was performed with scanning electron microscopy (SEM) which showed that while 10% proportions of UHMWPE led to a continuous PUR matrix, the use of 20% proportions produced an overabundance of particles which had poor adhesion with the matrix material. Dynamic mechanical analysis (DMA) of these blends showed a substantial increase in storage and loss moduli over pure PUR. It was also observed that smaller UHMWPE particles increased the storage modulus more than larger particles, however no size effect was observed with loss modulus. The blends were subjected to multi-directional sliding in a bovine serum solution in the Dual-Axis Wear Simulator (DAWS) for 250,000 cycles along a 6.4-mm square wear path under a load of 39 N. Unblended PUR produced wear amounts less than UHMWPE, while the 10% blends showed an even greater reduction in wear. The

20% blends exhibited extremely high wear rates, by comparison. The results of this work show that the PUR-UHMWPE blends have good wear resistance with increased elastic stiffness and damping, so long as the proportion of UHMWPE is not excessive.

6.2 Introduction

Total-joint arthroplasty (TJA) has been used by orthopedic surgeons for decades in the treatment of joint pain and lost function due to the loss of articular cartilage from arthritis or injury. The most common design of a TJA implant, such as for the hip or knee, includes a polished metallic surface articulating against a polymeric component made of ultra-high molecular weight polyethylene (UHMWPE). The latter has been chosen as a bearing material for these devices because it has an extremely low wear rate [1-3], and is fairly biocompatible as a bulk material. Efforts have continuously been made to reduce UHMWPE wear, because the particulates generated in wear are responsible for inciting an osteolytic response *in vivo*. It is this response which significantly limits the pain-free lifetime of the devices.

One of the properties of UHMWPE that has made it attractive as a bearing material is its stiffness. However, this rigidity precludes it from exploiting the advantageous lubrication conditions found in a healthy synovial joint. Articular cartilage, which is porous and more compliant than UHMWPE, supports hydrostatic and possibly hydrodynamic lubrication during the walking cycle [4]. UHMWPE functions in a sliding condition with little presence of a lubricating film layer [5]. In view of the compliant behavior of articular cartilage, investigators have looked at alternatives to UHMWPE. Both analytical and numerical studies of joints with compliant articulating surfaces have been undertaken [6-8]. In

addition, compliant polyurethanes (PUR) have been used in *in vitro* experiments as acetabular cups in artificial hips [9, 10]. In a further attempt to achieve the useful mix of properties of articular cartilage, layered polyurethanes have been studied [10]. The latter reflect the gradient of properties in articular cartilage that range from compliant on the outside articulating surface, to rigid on the interior surface that contacts the subchondral bone. Quigley *et al.* have gone so far as to propose a number of compliant polyurethanes that would perform optimally as UHMWPE alternatives based on their mechanical properties and biocompatibility [11]. The authors have worked with one of these materials, Pellethane 2363-80A™ (Dow Chemicals), and found that its wear was substantially lower than that of UHMWPE in a simulated joint environment [3]. The reduction in wear with compliant materials has been attributed to their ability to conform to the curvature of the counterface and thus produce lower contact stresses. Furthermore, as a group, polyurethane elastomers posses excellent shear strength and tear resistance.

In light of the benefits realized with compliant materials from the reduction in contact stresses, and the extremely low wear rates observed with UHMWPE, it was decided to capitalize on the combined benefits of these two materials. A potential addition to the list of candidate biomaterials for use as bearing surfaces in artificial joints might thus be a blend made with a compliant polyurethane matrix and UHMWPE particles. There are considerable concerns involving the use of a blended phase in a biomaterial, including the immune reaction to particulate that becomes dislodged during wear. However, it is possible that one might select a particle size that is large enough or adhered sufficiently so as not to be removed during the wear process.

The problem in blending these materials is that polyurethane is hydrophilic, while UHMWPE is non-polar and the two materials would not ordinarily mix well to produce an even dispersion of UHMWPE particles with good adhesion between phases. There are two ways to address this problem. The first is to use a compatibilizer, which is a compound with molecules of both polar and non-polar ends, much like a surfactant. A common compatibilizer used in polymer blending is polyethylene-grafted-maleic anhydride (PE-g-MAH) [12]. Blends of polar and non-polar polymers can be made by twin-screw extrusion of the polymers and compatibilizer [13]. This method can be impractical with UHMWPE because of its high melt viscosity. However, Yuan *et al.* have produced UHMWPE-rich blends with PUR using PE-g-MAH compatibilizer in a dual-roller mixer [12], and showed that some of these blends produced wear rates lower than pure UHMWPE in a flat-on-ring wear configuration. Their results were highly dependent on the amount of compatibilizer present. The second method to produce a blend of PUR and UHMWPE is to use polyethylene that has had its surface modified to contain polar groups [14]. Castable polyurethane elastomers can be produced either from raw materials or from commercially available products, and the surface-modified UHMWPE can be added during the curing stage. This provides excellent dispersion of the UHMWPE particles in the PUR matrix and eliminates the need for a separate-phase compatibilizer.

6.3 Materials and Methods

Two methods were attempted to produce blends of PUR and UHMWPE. In the first attempt, Pellethane resin was mechanically mixed with a chosen proportion of UHMWPE powder (Aldrich, St. Louis, Missouri) and 10% PE-g-MAH (Aldrich), by weight. The

mixture was fed into an intermeshing modular co-rotating twin extruder (American Leistritz, Somerville, New Jersey). While extruded material was produced with this method, it showed evidence of poor bonding of phases and was very brittle. The manipulation of temperature and screw-rotation rate did not produce a useful material and thus it was decided that another blending method was necessary.

The second attempt at blending the two polymers involved the use of castable PUR. Blends were prepared using a specially designed mold consisting of two halves that could be separated to remove cured specimens. The molded specimens were in the form of cylindrical bars with a diameter of 6.4 mm and a length of 19.0 mm. The polyurethane components used were Airthane® PET-80A prepolymer and Lonzacure® MCDEA-GS curative (both supplied by Air Products and Chemicals, Inc., Allentown, Pennsylvania). This is a toluene diisocyanate (TDI)-polyester-based polyurethane. It was chosen because it has a reported stiffness modulus very close to that of Pellethane 2363-80A. Unlike Pellethane, which is only available as course resin for injection molding, Airthane is prepared from liquid-phase materials thus allowing for the addition of another material in particulate form. The performance of this material is likely to be indicative of biomedical-grade polyurethanes that are based on diphenylmethane diisocyanate (MDI).

When unmodified UHMWPE powder is mixed into polar fluids such as water or the PUR prepolymer, it clumps together and therefore does not disperse well through the fluid. As a means of ensuring good dispersion and adhesion to the PUR matrix, UHMWPE particles were obtained that had been treated in an oxidizing atmosphere to produce active polar groups on their surface. These polar groups were expected to bond the two phases together much like a grafted compatibilizer would in extrusion-blended polymers. These surface-

activated UHMWPE particles (Aldrich) were obtained in two sizes: small particles ranging from 53 to 75 μm; and large particles with a reported average size of 180 μm. Figure 6.1 shows SEM micrographs of these particles illustrating their size range and shape. Two different particle sizes were chosen for this investigation because it has been reported that the reinforcing properties of filler particles increase as their size decreases [15]. This is due to the higher surface area to volume ratio of smaller particles. The PUR-UHMWPE blends were prepared by heating the prepolymer, curative, and mold separately to 100°C in an air-circulating oven. When the prepolymer was completely melted, it was removed from the oven and a drop of simethicone surfactant was added to reduce bubble formation during mixing. Surface-activated UHMWPE particles were then added in the chosen proportion. The materials were mixed well using a stirring tool before the mixture was placed in a sealed chamber under vacuum to degas at room temperature for approximately 10 minutes. The mixture was reheated in the oven to 100°C, the curative was added, and the polymer was again degassed under vacuum at room temperature. Finally, the liquid polymer was injected into the heated mold and allowed to cure for 20 minutes in the oven. After removal from the mold, the samples were placed back in the oven for 10 hours of post curing at 100°C. The blended samples were then placed in a desiccated chamber for storage until use.

As stated above, two UHMWPE particle sizes were used to make the blends. Two proportions of filler material were also investigated, 10 and 20%, by weight, thus leading to four different composite formulations. These included a PUR matrix with: a) 10% small filler (termed 10 S), b) 10% large filler (10 L), c) 20% small filler (20 S), and d) 20% large filler (20 L). These proportions were chosen based on past work with filled polymers that

showed optimal wear results when fillers were added in proportions between 10 and 20% [16-18]. Samples of pure PUR were also produced as a control material for the experiments.

The morphology of the blends was studied by SEM examination. For this purpose, cast bars were cooled in liquid nitrogen and then fractured. The fractured surfaces were rinsed in methanol and coated with gold for SEM examination. To investigate the extent to which the UHMWPE particles affected the structural integrity of the composites, bars of each composition were place in xylenes, a solvent for UHMWPE, for four hours to dissolve the filler. Observation of whether the bars remained intact or had crumbled indicated if the UHMWPE particles were in contact within the PUR matrix.

In order to determine the storage and loss moduli of the materials, DMA (Perkin Elmer DMA 7e) was performed on the cylindrical bars. A three-point bend fixture was placed in the DMA with a distance between supports of 10 mm. A sinusoidal load was applied with a mean force of 550 mN and an alternating force of 500 mN in the frequency range from 0.5 to 5.0 Hz. Deflection of the samples was recorded by a computer workstation connected to the DMA instrument.

Cylindrical pins, 6.4 mm in diameter and 9 mm long, were used in wear testing. The pins slid under a load of 39 N over a 6.4-mm square wear path (total distance 25.6 mm) in multi-directional sliding. Both pin and counterface were immersed in bovine serum lubricant solution maintained at 37°C. The test exposed the pins to plane-on-cylinder contact. The wear tests were performed in the Dual-Axis Wear Simulator (DAWS), reported elsewhere [3]. The machine was programmed to run 250,000 wear cycles during each wear test. The counterface was a 316L stainless steel cylinder polished to a surface roughness of 0.10 μm Ra.

Prior to testing, the pins were cleaned and dried for 8 hours at 80°C because of the very hygroscopic nature of PUR, to allow for an accurate measurement of their mass. Soak control specimens were used to compensate for absorption of fluid during the wear test that might affect the wear measurements. At the completion of wear testing, the pins were again cleaned and dried for 8 hours at 80°C, and then weighed. The worn surfaces of representative pins were removed and coated with gold to allow for examination of wear mechanisms in the SEM.

6.4 Results and Discussion

6.4.1 Morphology and its effects on properties

The morphological features of PUR and its blends made with UHMWPE are shown in Figure 6.2. The PUR surface morphology in (a) is smooth and almost featureless except for some small voids due to entrapped gas bubbles. The blends with 10% UHMWPE in (b) and (c) show a surface very similar to that of the PUR surface except for the dispersal of UHMWPE phases. Since in the blending process the temperature was well below the melting point of UHMWPE, the polyethylene phase retained the nearly round shape of the particles. Examination of the regions around UHMWPE particles indicates that there is a partial gap at the interface between the two phases. Thus, a perfectly intimate bond between the two phases was not achieved even though the UHMWPE particle surface had been activated. The micrographs in Figure 6.2 (d) and (e) show more features than in (b) and (c). The distribution of UHMWPE phases appears to be well dispersed and the bond between the phases of the two materials is good in some locations but poor in others. In some locations,

as shown in the circle in (e), UHMWPE particles are in direct contact indicating that the PUR matrix is not continuous everywhere. This would induce weakening in the blend.

The property ramifications of these morphological differences are seen in the storage and loss moduli shown in Figure 6.3. It is obvious that with the addition of UHMWPE to PUR, the elastic stiffness of the elastomer was increased considerably. In general, the storage modulus was increased by 44 to 52 % over that of pure PUR. The loss moduli of the filler materials were also higher than that of PUR. In our earlier work, the storage modulus of UHMWPE was found to vary from 1.17 to 1.52 GPa over the same range of frequencies, while loss modulus varied from 9.44 to 209 MPa [18].

Examination of the storage moduli data for the blends reveals two trends: a) smaller particles of UHMWPE produced higher moduli for a given percentage of it, and b) 10% UHMWPE blends had higher moduli than 20% blends for a given particle size. In regards to particle size, it has been reported that smaller particles lead to higher moduli due to the increase in surface area-to-volume ratio that governs the amount of bonding between the two materials. For example, carbon black nanoparticles in rubber have been reported to produce optimal reinforcement properties [19]. As for the properties of UHMWPE in PUR, the blends with 20% UHMWPE had a slight reduction in the storage modulus as compared to that of 10% because the flaws due to weak adhesion between the two phases negated the effect of higher proportion. This is demonstrated by the following relation, which is often used to determine the synergism between the polymers in a two-component blend:

$$P = P_1C_1 + P_2C_2 + IP_1P_2 \tag{6.1}$$

where P is the property of interest (storage modulus in this case), C is the proportion of polymer in the blend, and I is the synergy factor. Positive values of the synergy factor indicate that a particular property of the blend is greater than the weighted sum of its components, while negative values indicate a non-synergistic blend. Using the storage modulus data obtained in this study, the synergy factor can be determined for the PUR-UHMWPE blends. For the 10% blend with small UHMWPE particles, a storage modulus of 3.48 MPa was measured at 3 Hz. The modulus of pure PUR at this frequency was 2.33 MPa, while that of pure UHMWPE was 1.51 GPa. These values give the value of I equal to -4.3 x 10^{-8}. Howsoever small, the negative value indicates that the fabrication process used for these blends resulted in a non-synergistic blend which indicates poor bonding between the two phases.

The samples of blends were soaked in xylenes to discern the presence of an interconnecting network of UHMWPE particles in the blends. The blends with 10% UHMWPE were swollen but still intact after the solvent had dissolved the UHMWPE. However the 20% blends, when soaked in xylenes, crumbled and disintegrated into smaller fragments. This shows that there was not sufficient PUR within the UHMWPE particle network to maintain the integrity of the sample.

6.4.2 Wear results

The wear amounts for UHMWPE, PUR, and its blends are shown in Figure 6.4 for the conditions stated in the caption of the figure. The unfilled PUR had the mean volumetric wear of 0.343 mm^3. This value is somewhat lower than that found for non-crosslinked UHMWPE, and thus shows that a compliant material like PUR is as good or even better for TJA application from the point of wear provided other requirements such as stiffness and

compliance are satisfied. 10% UHMWPE blends had even lower wear than pure PUR. In contrast to this, 20% UHMWPE blends had fairly high wear. The data shows that particle size of UHMWPE used in the preparation of the blends had little effect on the wear amounts. The elastomeric PUR and its blends with UHMWPE were able to conform to the curvature of the counterface better than rigid UHMWPE and thus experienced lower contact pressures during sliding. This could explain why the wear of PUR and its blends with 10% UHMWPE were so low. The reason for the very high wear of 20% UHMWPE-PUR blends was the excessive number of locations with defects because of the poor bonding between the phases.

An examination of the wear surfaces in Figure 6.5 shows striking differences among the different blends investigated. Wear of pure PUR shown in (a) produced a smooth surface. At very high magnifications, regions on the surface were identified with material in the process of being gouged from the bulk. There is little evidence of plastic deformation or fibril formation, as has been reported for UHMWPE [3]. Rigid polymers, such as UHMWPE, undergo polymer chain orientation on the wear surface in response to the shear stresses encountered during sliding. This process can lead to high wear when the sliding direction becomes transverse to the direction of polymer chain orientation. Such orientation is temporary in the case of elastomeric polymers because it recovers as soon as the stress in that direction is relieved. Wear surfaces of the 10% UHMWPE blends in (b) and (c) show UHMWPE-phase regions embedded in the PUR matrix. The PUR surface is fairly smooth with no sign of wear, as opposed to that of UHMWPE which shows texture generated during the wear process. Contrast these with (d) and (e) for the 20% UHMWPE blends, which show the UHMWPE particles appearing to protrude from the surface. In addition, there is separation of UHMWPE particles from PUR matrix on the surface.

A better insight into the wear process on the surfaces of the component materials in the 10% UHMWPE blend is obtained by looking at Figure 6.6. This shows the wear on the PUR and UHMWPE phases side-by-side at higher magnification than Figure 6.5 (c). The UHMWPE phase is on the right side of the image and shows the presence of numerous fibrils of material that have been pulled out during sliding. The tearing of these fibrils resulting in detachment from the surface contributes to wear. As stated earlier, the compliant nature of PUR results in much lower stresses on the PUR phase and hence the phenomena like tearing and detachment are absent and so the wear on the PUR phase is much lower.

These results show that PUR-UHMWPE blends have promising potential for use in artificial joints. However, more work needs to be done to produce blends with superior adhesion between the phases of UHMWPE and PUR, where the results are expected to be better. Another advantage of the blends is that they can be tailored to suitable composition to meet the variable demands in terms of the mechanical and tribological properties of different kinds of joints.

6.5 Conclusions

The following conclusions were made based on the results of this investigation:

1. The combination of elastomeric PUR and surface-modified UHMWPE produced blends of good integrity with an UHMWPE proportion of 10% by weight. With a 20% proportion of UHMWPE in PUR, blends had a weak structure because of poor adhesion between the materials.

2. The addition of UHMWPE particles to elastomeric PUR considerably increased its storage and loss moduli, so long as the proportion of UHMWPE in the blend was not excessive.
3. Smaller UHMWPE particles increased the storage modulus more than the larger particles. However, no difference was observed for loss modulus with regards to particle size.
4. The volumetric wear of the 10% UHMWPE-PUR blends was less than that of pure PUR and that of UHMWPE. This was due to its ability to conform to the curvature of the counterface and thus reduce contact stresses. 20% UHMWPE-PUR blends had higher wear amounts due to adhesion problems between the PUR and UHMWPE phases.
5. No differences were found in wear behavior between the blends made with small filler particles versus large filler particles.

6.6 References

1. O.K. Muratoglu, C.R. Bragdon, D.O. O'Connor, M. Jasty, W.H. Harris, R. Gul, F. McGarry, Unified wear model for highly crosslinked ultra-high molecular weight polyethylenes (UHMWPE). Biomaterials, 1999. 20(16): p. 1463-1470.
2. G. Lewis, Properties of crosslinked ultra-high-molecular-weight polyethylene. Biomaterials, 2001. 22(4): p. 371-401.
3. C.J. Schwartz, S. Bahadur, Development and testing of a novel joint wear simulator and investigation of the viability of an elastomeric polyurethane for total-joint arthroplasty devices. Accepted for publication in Wear, 2006.

4. R. Krishnan, M. Kopacz, G.A. Ateshian, Experimental verification of the role of interstitial fluid pressurization in cartilage lubrication. J Orthop Res, 2004. 22(3): p. 565-570.

5. J. Blamey, S. Rajan, A. Unsworth, R. Dawber, Soft layered prostheses for arthritic hip joints: a study of materials degradation. J Biomed Eng, 1991. 13(3): p. 180-184.

6. T. Stewart, Z.M. Jin, J. Fisher, Analysis of contact mechanics for composite cushion knee joint replacements. Proc Inst Mech Eng [H], 1998. 212(1): p. 1-10.

7. A.N. Suciu, T. Iwatsubo, M. Matsuda, Theoretical investigation of an artificial joint with micro-pocket-covered component and biphasic cartilage on the opposite articulating surface. J Biomech Eng, 2003. 125(4): p. 425-433.

8. M.T. Raimondi, C. Santambrogio, R. Pietrabissa, F. Raffelini, L. Molfetta, Improved mathematical model of the wear of the cup articular surface in hip joint prostheses and comparison with retrieved components. Proc Inst Mech Eng [H], 2001. 215(4): p. 377-391.

9. S.L. Smith, H.E. Ash, A. Unsworth, A tribological study of UHMWPE acetabular cups and polyurethane compliant layer acetabular cups. J Biomed Mater Res, 2000. 53(6): p. 710-716.

10. T. Stewart, Z.M. Jin, J. Fisher, Friction of composite cushion bearings for total knee joint replacements under adverse lubrication conditions. Proc Inst Mech Eng [H], 1997. 211(6): p. 451-465.

11. F.P. Quigley, M. Buggy, C. Birkinshaw, Selection of elastomeric materials for compliant-layered total hip arthroplasty. Proc Inst Mech Eng [H], 2002. 216(1): p. 77-83.

12. H. Yuan, P. Hu, Study of a compatibilized ultra-high-molecular-weight polyethylene and polyurethane blend. Journal of Applied Polymer Science, 2001. 81(13): p. 3290-3295.

13. M. Palabiyik, S. Bahadur, Tribological studies of polyamide 6 and high-density polyethylene blends filled with PTFE and copper oxide and reinforced with short glass fibers. Wear, 2002. 253(3-4): p. 369-376.

14. D.H. Yang, G.H. Yoon, S.H. Kim, J.M. Rhee, Y.S. Kim, G. Khang, Surface and chemical properties of surface-modified UHMWPE powder and mechanical and thermal properties of it impregnated PMMA bone cement, III: effect of various ratios of initiator/inhibitor on the surface modification of UHMWPE powder. J Biomater Sci Polym Ed, 2005. 16(9): p. 1121-1138.

15. L. Bokobza, Elastomeric composites. I. Silicone composites. Journal of Applied Polymer Science, 2004. 93(5): p. 2095-2104.

16. C.J. Schwartz, S. Bahadur, The role of filler deformability, filler-polymer bonding, and counterface material on the tribological behavior of polyphenylene sulfide (PPS). Wear, 2001. 250: p. 1532-1540.

17. M.H. Cho, S. Bahadur, Study of the tribological synergistic effects in nano CuO-filled and fiber-reinforced polyphenylene sulfide composites. Wear, 2005. 258(5-6): p. 835-845.

18. C.J. Schwartz, S. Bahadur, S. Mallapragada, Effect of crosslinking and Pt-Zr quasicrystal fillers on the mechanical properties and wear resistance of UHMWPE for use in artificial joints. undergoing submission, 2006.

19. G. Kraus, Reinforcement of elastomers. Polymer engineering and technology. 1965, New York,: Interscience Publishers. xv, 611 p.

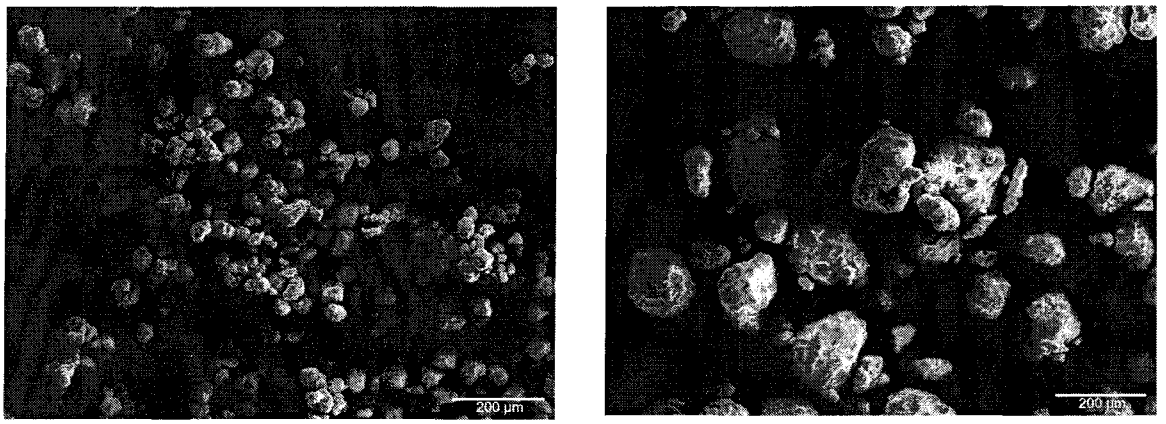

(a) (b)

Figure 6.1 SEM micrographs of the a) small, and b) large surface-modified UHMWPE particles used as fillers.

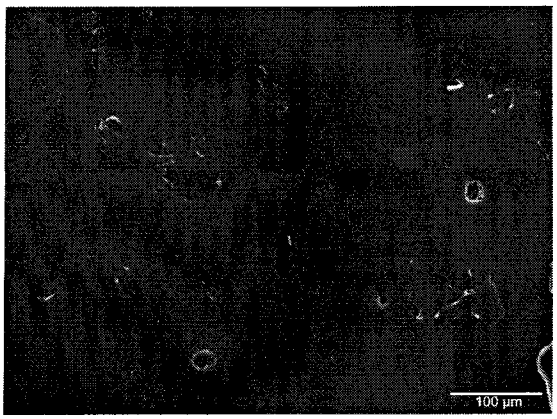

(a)

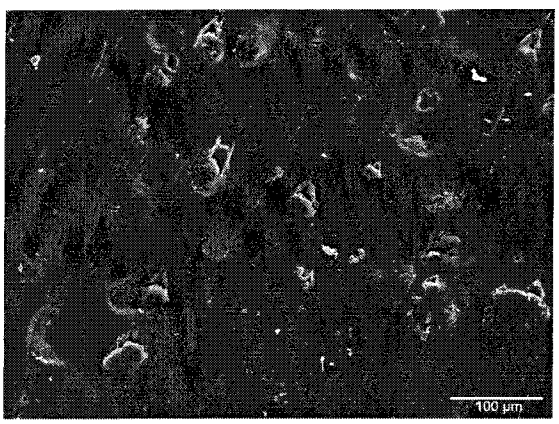

(b)

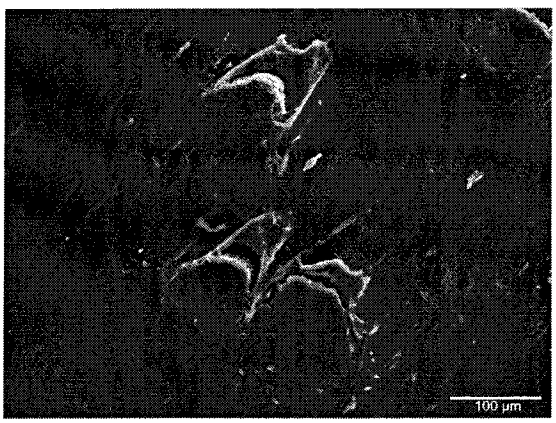

(c)

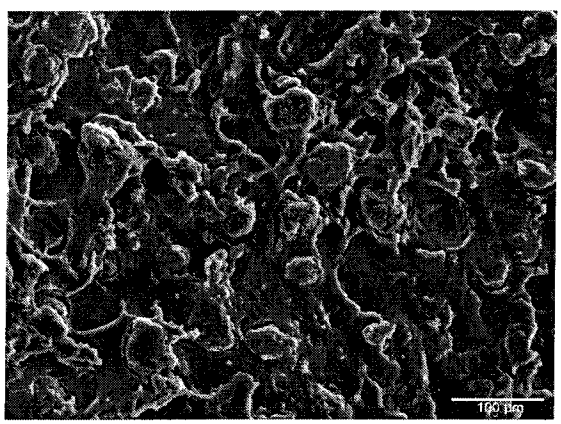

(d)

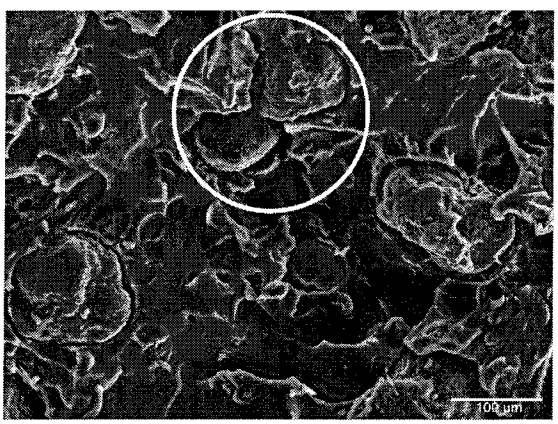

(e)

Figure 6.2 SEM micrographs showing the morphology of PUR and its blends: a) pure PUR, b) PUR with 10% UHMWPE in small particles, c) PUR with 10% UHMWPE in large particles, d) PUR with 20% UHMWPE in small particles, and e) PUR with 20% UHMWPE in large particles. Circle in e) shows UHMWPE particles in contact.

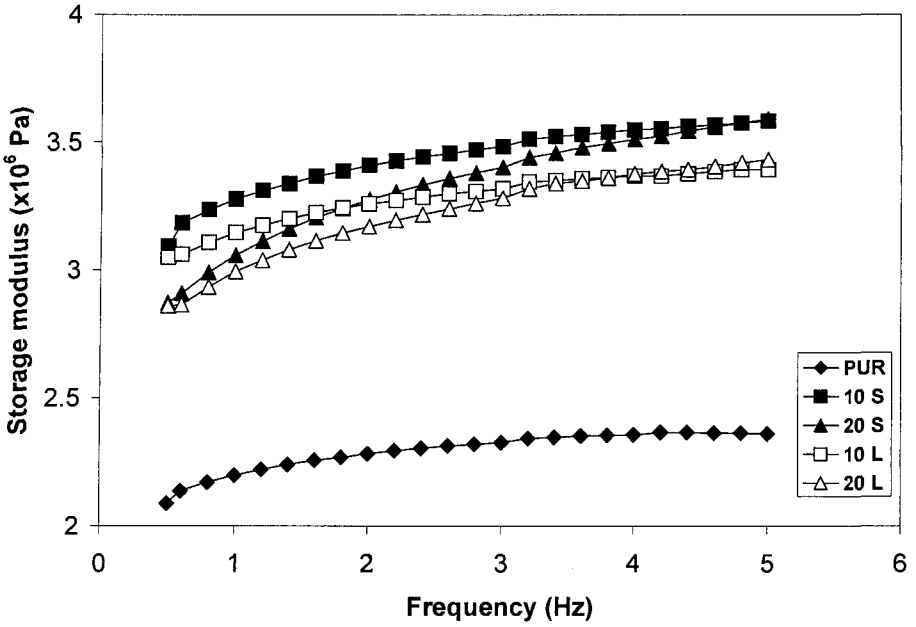

(a)

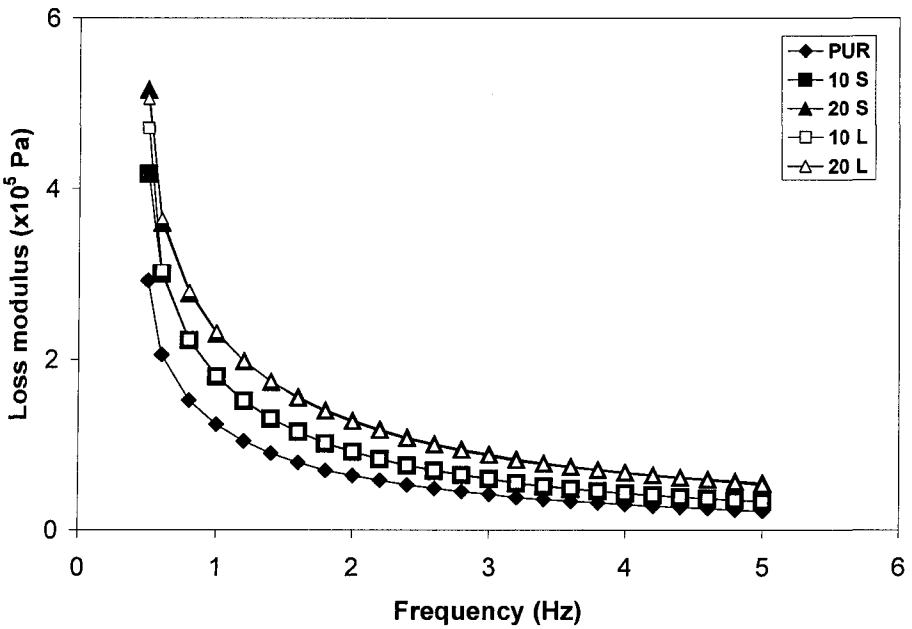

(b)

Figure 6.3 Variation of storage and loss moduli as a function of frequency for PUR-UHMWPE blends. The numbers indicate UHMWPE percentages by weight, while the letters "S" and "L" denote small and large UHMPWE particle sizes, respectively. Note that the two 10% UHMWPE blends have overlapping data points, as well as the 20% blends.

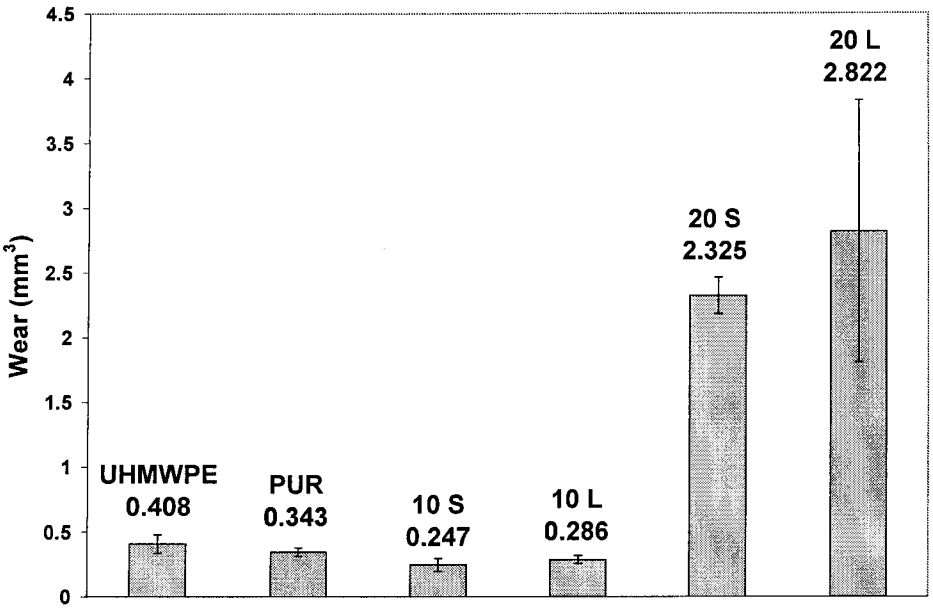

Figure 6.4 Volumetric wear amounts of UHMWPE, unfilled PUR, and the blends after testing in the DAWS for 250,000 cycles over a 6.4-mm square wear path and 39 N loading while immersed in bovine serum solution at 37°C. Bars indicate ± one standard deviation. "S" and "L" denote the small and large filler particles, respectively, used in the preparation of the blends.

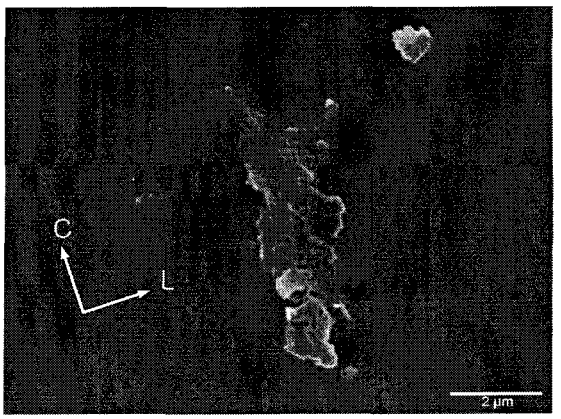

(a)

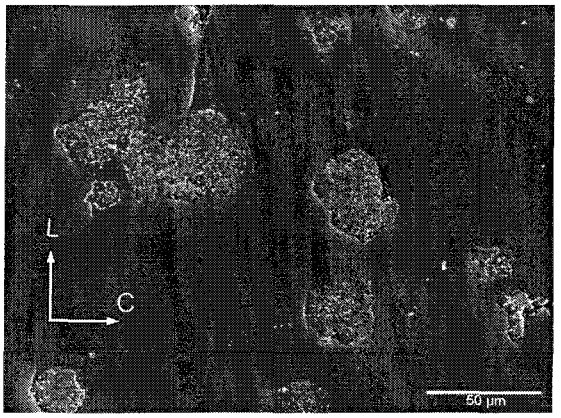

(b)

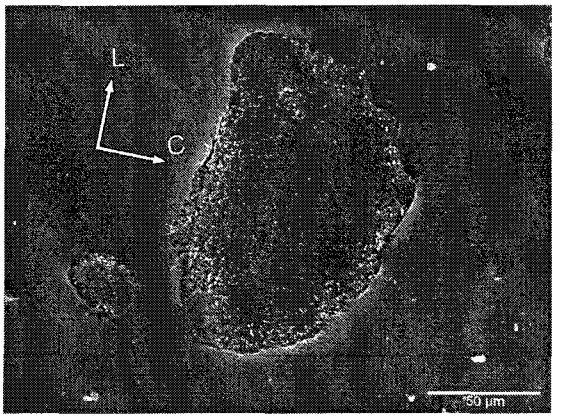

(c)

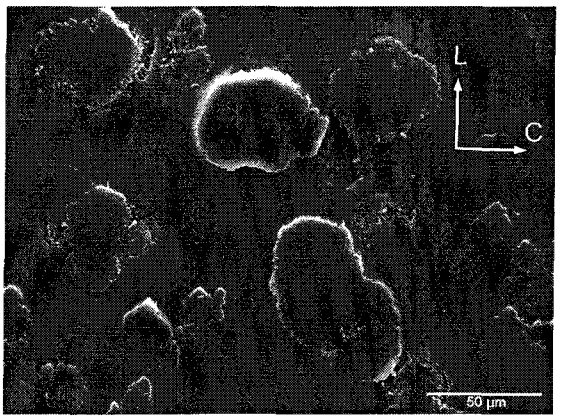

(d)

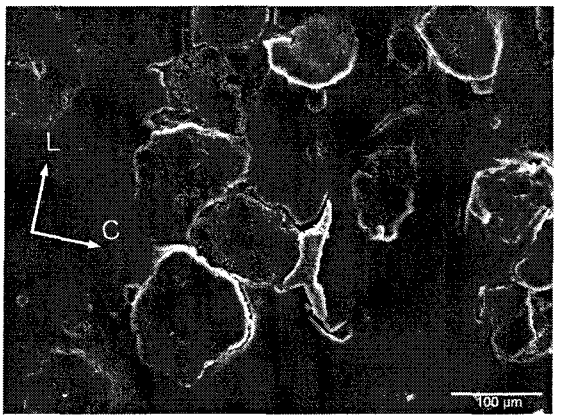

(e)

Figure 6.5 SEM micrographs of the worn surface of PUR and its blends: a) pure PUR, b) 10% UHMWPE in small particle size, c) 10% UHMWPE in large particle size, d) 20% UHMWPE in small particle size, and e) 20% UHMWPE in large particle size. In the images, "L" indicates sliding direction parallel to the counterface shaft axis, while "C" indicates the perpendicular direction. Also, a) is at much higher magnification than the others.

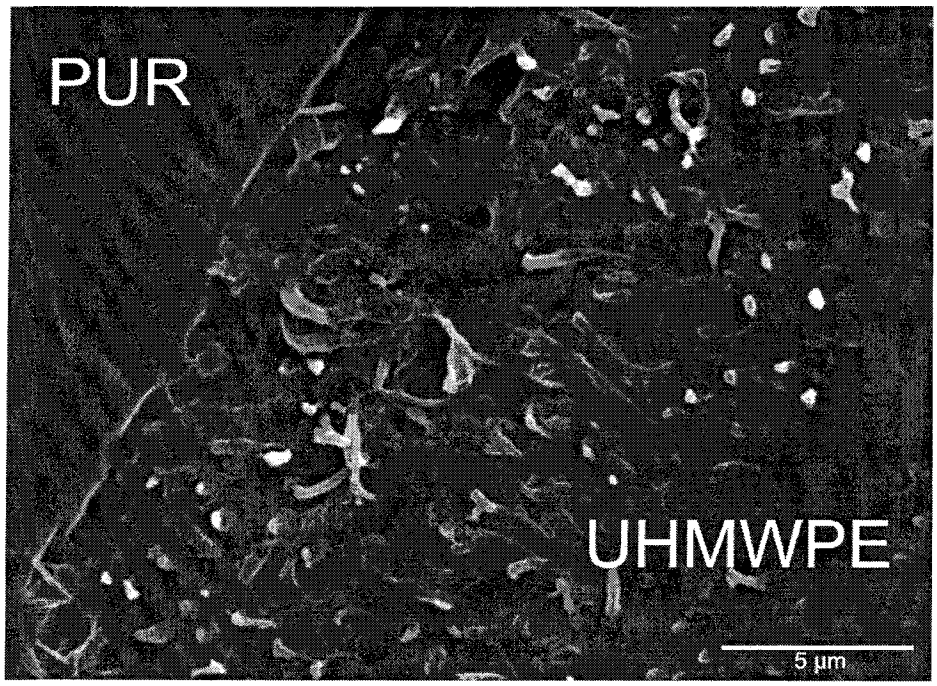

Figure 6.6 Micrograph showing wear on both the PUR and UHMWPE phases side-by-side for the 10% UHMWPE blend with large particles.

CHAPTER 7
GENERAL CONCLUSIONS

This work has shown that improvements can be made in the durability of artificial joints, based on proper materials selection, and proper treatments to these materials. The results indicate that progress has been made in addressing the two fundamental aspects governing the pain-free lifetime of artificial joints: the wear or UHMPWE, and the use of alternative materials that may be less osteolytic than UHMWPE. Furthermore, it was shown that simulative testing with a very simple machine can produce realistic results for screening of candidate biomaterials for joint applications. The following conclusions were draws from this work:

1. The Dual-Axis Wear Simulator (DAWS) has the capability to expose biomaterials to multidirectional sliding while immersed in bovine serum solution to produce realistic wear mechanisms and wear amounts. A 6.4-mm square wear path, a cycle frequency of 0.81 Hz, under a load of 39 N produced results that were most similar to those reported in the literature for more complex testing machines and implants retrieved after *in vivo* use.
2. The ratio of length to width of the wear path played an important role in the amount and mechanism of wear of biomaterials. With UHMWPE, a square wear path (ratio = 1) produced the highest wear, while linear paths (ratio = ∞) produced extremely low wear rates.
3. Wear of non-crosslinked polymers such as UHMWPE was due to three factors: a) the orientation of polymer chains on the wear surface during sliding, b) the directionality

of surface roughness on the DAWS counterface, and c) the depletion of lubricant during portions of the wear path.

4. Materials with very low shear strength, such as PTFE, produced extremely high wear amounts.
5. Pellethane 2363-80A, with a very low elastic modulus, showed wear amounts significantly lower than non-crosslinked UHMWPE. This was due to the fact that its compliance allowed the material to conform to the counterface during wear, and thus lowering contact pressure.
6. Increasing the compliance of the counterface significantly reduced wear in the case of bovine articular cartilage.
7. Bovine articular cartilage exhibits a substantial amount of viscoelasticity, thus enabling it to support static loads without excessive deformation while dissipating impact loads during the walking cycle.
8. Crosslinking of UHMWPE significantly reduced its wear by inhibiting the ability of the polymer chains on the pin surface to orient themselves during sliding. This prevented directional weakening of the polymer when the sliding direction became transverse to the chain orientation direction.
9. Crosslinking reduced the elastic modulus of UHMWPE due to a reduction in crystallinity. Impact toughness of crosslinked UHMWPE was also less than that of the as-molded polymer. Crosslinking also reduced the ability of UHMWPE to plastically deform before fracture.
10. The wear surface of UHMWPE after multi-directional sliding showed the presence of periodic ridges of raised and separated material. These ridges were a result of the

stretching of the wear surface in response to shear stress during the wear process. The spacing of the ridges was dependent on the extent of plastic deformation that the material could support before fracture. Thus the distance between striations in crosslinked UHMWPE was less than that of the as-molded polymer.

11. Filling UHMWPE with 20% Pt-Zr quasicrystals (QC), by weight, provided a reduction in wear as great as 50 kGy irradiation crosslinking did. Wear was reduced by the ability of the filler particles to partially shield the surrounding UHMWPE matrix from shear stresses during sliding.
12. The use of Pt-Zr quasicrystals increased the elastic modulus of UHMWPE, while not causing as much of a reduction in impact toughness as did crosslinking.
13. QC-filled UHMWPE shows considerable potential for use in artificial joints based on it combination of high wear resistance and improved elastic modulus over that of unfilled, non-crosslinked UHMWPE.
14. Thermal stabilization further reduced the crystallinity of crosslinked UHMWPE by allowing residual free radicals the mobility to combine and produce further crosslinking.
15. With mild amounts of crosslinking, such as with 50 kGy irradiation, there was very little oxidation of UHMWPE after accelerated aging for 8 days at 80°C in a highly oxidative atmosphere.
16. The wear resistance of aged, non-stabilized UHMWPE that had been crosslinked was statistically similar to that of thermally stabilized polymer. Furthermore, crosslinked UHMWPE that had not been thermally stabilized had higher stiffness than the stabilized polymer. This stiffness was retained even after accelerated aging.

17. The addition of surface-activated UHMWPE particles in a 10% proportion, by weight, to elastomeric PUR considerably increased its storage and loss moduli. 20% proportions led to a weakened blend with poor adhesion between phases.
18. Smaller UHMWPE particles increased the storage modulus more than the larger particles. However, no difference was observed for loss modulus with regards to particle size.
19. Because of its ability to conform to the geometry of the counterface and thus reduce contact pressures, the wear or 10% UHMWPE-PUR blends was less than that of non-crosslinked UHMWPE.

ACKNOWLEDGMENTS

I have received a tremendous amount of support with my research to prepare this dissertation. The National Science Foundation's Graduate Research Fellowship Program provided the financial support to do this work, while numerous Iowa State University faculty and staff provided the guidance, advice, and motivation to complete it. Among these people deserving special thanks are Mr. Larry Couture and Mr. Gaylord Scandrett, for their advice and assistance in fabrication of equipment. Additionally, I want to thank Dr. Surya Mallapragada for her guidance with much of the biological and biomedical issues involved in this work, and for the generous use of her laboratory facilities. Furthermore, I am thankful to the rest of my Program of Study Committee for their guidance and advice in pursuing this research.

I owe thanks to my faculty advisor, Dr. Shyam Bahadur, not only for advice concerning the research aspects of this work, but also for guidance concerning the societal impacts of this type of research and the ethical responsibilities of the investigator. His attention to detail and quality is a model that I have used in my career.

I am most grateful to my wife, Marie, and my daughter, Victoria, who were willing to take this journey with me and shared in the sacrifices that were made in order for me to complete this work. I am especially lucky to have such a loving, wonderful and understanding family that has enabled me to pursue my dream of an academic career.